Università degli Studi di Padova

Department of Industrial Engineering

Final dissertation for the degree of

Doctor of Philosophy of Industrial Engineering

Curriculum Materials Engineering

Series XXXII

Direct Ink Writing of Geopolymers

Supervisor: Ch.mo Prof. **Paolo Colombo**

Ph.D. candidate: **Paolo Scanferla**

UNIVERSITÀ
DEGLI STUDI
DI PADOVA

Head Office: Università degli Studi di Padova

Department of Industrial Engineering

Ph.D. COURSE IN: Industrial Engineering
CURRICULUM: Materials Engineering
SERIES XXXII

DIRECT INK WRITING OF GEOPOLYMERS

Thesis written with the financial contribution of ITT ITALIA S.R.L.

Supervisor: Ch.mo Prof. Paolo Colombo

Ph.D. student: Paolo Scanferla

To my parents,

I love you

Acknowledgements

When it's time to remind all the people involved in my work, I just simply cannot fail to thank from the bottom of my heart my supervisor Prof. Paolo Colombo for having given me the possibility to experience such a great group, for his humanity, for all his time dedicated to my research and for his kindness. It has been a great time being one of your disciples, starting this path more than 4 years ago with all the insecurities and doubts. You've been such an inspiring figure and a mentor for me, thanks for all the advice, knowledge and support you gave me.

All this would not have been possible if ITT, especially in the person of Dr. Agusti Sin, had not believed in my abilities. Thanks for having trusted me and for this PhD period I'm about to finish.

Part of the work presented in this thesis, especially the rheology characterization of GPP ink, is a result of a collaboration between the University of Padua and the Saint-Gobain Research Provence in the frame of the European project called AMITIE, Additive Manufacturing Initiative for Transnational Innovation in Europe. I want to thank all the people involved in this collaboration, especially Dr. Caroline Tardivat, Stéphane Richaud and Zoé Rhodes, who gave me the possibility to work on my research and kindly answered all my questions and doubts, your collaboration was precious and essential to reach these results.

Thanks to Prof. Enrico Bernardo for all the hints and help during this tough PhD.

I would like to thank all my past and new colleagues of the Advance Ceramics groups, with an honorable mention for Giorgia Franchin and Alberto Conte to have guided my path throughout my research work, I don't think all of this would have been possible without your help and time. Thanks also to Hamada Elsayed, Renata Fuss Botti, Johanna Schmidt, Chengyin Bai, Filippo Gobbin, Karine Oliveira, Useche Inchauspe, Giulio Giometti and Anna De Marzi. Working with you sweetens the everyday routine of a (probably not) working 3D-printing.

Thanks to all the guys in the DII labs group: Marco Sturaro, Marco Angiola, Marco Bersani, Andrea Paduano, Gianmarco Giordano, Elena Colusso, Angeloclaudio Nale and all the others, sorry if I forgot to mention. The shared moments of infinite coffee breaks and lunches were the relief to everyday work and the possibility to solve simple problems in (not so) simple ways.

Thinking about the period spent in SGRP, what I remember most is the time with all the SG crew: Mangesh, Sidhanth, Hassan, Zane, Deborah, Benjamin, Lucas, Usha, Laura, Theo, Maxime,

Baptiste, Helene, Julien and Andrea. Thanks for having accepted me as one of your most close friends. I won't forget the kindness and the friendship you showed me. Hope to see you again and again.

Thanks also to every friend I met during the conferences: Elena, Gianmarco, Andrea, Daniele, Nicoletta.

Thanks to all my friends and the people who always believed in me, especially Lorenzo, thank you for your time spent chatting and doing nerdy things, as we were used to do during our childhood.

I want to thank two groups of friends, we love to call ourselves JADS and SaB. Thank you for helping me relieving the everyday heaviness with friendship and laugh.

It’s with sincere heart that I would like to thank Marzia for having sweetened all these 3 years of PhD with love, complicity and joy. The weight of this work is lighter when there’s someone who believes in you, no matter what you are doing. Thanks also to your family, Matteo, Mirena and the little Minou, for having accepted me as part of the family. I will never forget you.

I want to say thank you to all my relatives, especially to zia Berica, Milva and Giovanna, for sharing thoughts, pain and joy. Your support is the precious thing that keeps me fighting for a better future. A special thought goes to zio Luciano, you passed away when all this began, may your spirit guide us all.

Thanks for the first supporter and the best friend for life, my brother Carlo, your story is always a source of inspiration for my life.

And, finally, thank you, dear mum and dad, Antonella and Renato, for the everyday support, the love, the happiness and the never-ending trust in me. What I’ve become is only thanks to you, I will never be grateful enough to repay all the efforts and sacrifices that you’ve made for giving me the best opportunities of all.

Abstract

Geopolymers are materials that were studied for the first time in the '70s by J. Davidovits as an alternative to Portland cement. Some aspects about production and some physical proprieties aren't completely understood yet. Recently attention is focused on the realization of geopolymer matrix composites, thanks to the lower fabrication costs compared to the mostly used ceramics composites, for the availability of the raw materials and for their lower environmental impact.

Additive Manufacturing (AM) processes are recent technologies, that starting from early ‘90s begun to gain more and more interest between industrial companies and scientific communities, because they allow fast custom-made production, impossible to obtain with traditional production processes. 3D-printed objects find their application in a wide variety of fields, spacing from military, to aerospace, from automotive, to sports and even to biomedical.

Direct Ink Writing (DIW) is part of direct AM technologies and is based on a layer-by-layer continuous deposition of an extruded filament. This technology was first called “robocasting” by Cesarano in his patent (2001). It is mostly used for the production of porous ceramic structures as tissue repairing lattices and catalyst carriers. Not all materials can be used as ink in DIW, the ideal behavior is that of a Bingham fluid, which can be extruded at low pressure and rapidly recover its viscosity to maintain the shape desired.

Subject of this thesis is the implementation of a geopolymeric slurry in a DIW process for the production of porous structures. To attain this score, a deep rheological optimization was needed, and thanks to the use of rheology agents and different kind of fillers was possible to obtain geopolymeric inks and geopolymeric composite inks with enhanced printability features. Further to this work, it was possible to understand the evolution of compressive strength through the temperature in order to choose the best ratio between performance gained and time of treatment. Density, microstructural, XRD and chemical analysis were involved to clarify how temperature affects the overall samples characteristics.

Finally, the addition of short fibers, especially carbon fibers, gave the possibility to print lattices with enhanced fracture toughness, as observed in SEM micrographs of fracture surfaces, where the strengthening mechanisms (debonding, delamination and pull-out) have been identified.

Table of contents

Research motivation

It is widely known that the capacity of being able to control materials microstructure allows to modify and tune physical properties. The high mechanical characteristics of steels are due to insoluble secondary phases dispersion, therefore non coalescent, on the metal matrix, like the dispersion of very fine particles (with a diameter below 0.5 μm) of refractory oxides (of Al, Mg, Ti, Th, etc.) in a metallic solution. This brings to immobilization of dislocations, which are linear defects present on a metallic material crystalline reticule, characterized by a high distortive energy, derived from the field of tensions that is generated in the surrounding reticule. Dislocations movement determines a plastic deformation and it is necessary to minimize the reticule tensional state and then decrease its energy state [1].

The microstructure control can be obtained in two ways: through thermal treatments, as for metallic and glass ceramic materials, or with the addition of fillers like fibers, which are utilized as reinforce on a matrix with poor mechanical performance.

Fiber reinforced polymeric plastic matrix composite materials are the most successful composites [2]. Despite plastics poor mechanical resistance, fiber reinforcement can lead to modify and develop new features, so as to make plastic matrix composite materials competitors of metals. A clear example is the automotive field, where composites are trying to replace metal materials having similar mechanical performance, but a much lower weight that allows significant savings in fuel consumption.

In applications that require resistance to temperatures over 200°C, the vast majority of polymeric matrix composites cannot be used. For this kind of applications, ceramic matrix composite materials have been developed for more than thirty years [3].

Ceramic materials are well known for their high thermal stability, high thermal-shock resistance, high elastic modulus, high hardness, high corrosion resistance and low density. Nevertheless, they are brittle materials offering low resistance to crack propagation [4].

Fracture resistance of these materials is increased by dispersing a secondary phase within the matrix, chosen to act as barrier to the crack propagation. Fiber reinforced ceramic matrix composites behavior is called quasi-ductile, and is given by toughening mechanisms, such as matrix/fiber interfaces rupture (debonding), fibers sliding through the matrix (delamination) and fibers extraction from their seats (pull-out). This result is possible when fibers and matrix are of the same nature, both

ceramic, but fibers possess greater mechanical proprieties than matrix, for example while using carbon fibers. In this case, the interface between matrix and fiber has to be low, thus crack energy is absorbed and dissipated in fibers/matrix friction. This results in fracture resistance that can exceed 20 MPa/m^2 [2]. If fiber creates a strong bond with matrix, the crack can propagate trough the fiber and the toughening mechanisms possible are deflection and plastic deformation of the fiber, as it happens when using a ductile reinforce, like steel fibers.

Over the past 25 years, many projects have been carried out on the development of new ceramic composite materials, with increasing diffusion in aerospace applications, for propulsion, vehicles and land transportations, as well as in the nuclear and chemical industries [5]. However, to produce most of ceramic/ceramic composites, which consist on ceramic matrix and ceramic filler, specific conditions are needed, increasing drastically their final cost [4,6]. For example, C/C composite is produced by pyrolysis of an organic matrix or by CVI, both technologies require high processing temperatures (over 1000°C) in inert atmospheres (Ar or N) [2].

Geopolymers are inorganic materials suitable for use in the manufacture of ceramic composites at low temperature. Geopolymers production occurs at room temperature, without expensive machines or controlled environments, by mixing an aluminum silicate in powder in an alkaline solution containing a silicate. Moreover, current interest in environmental issues, brings attention to geopolymers, because their realization allows a reduction of carbon dioxide emissions, lower than those generated for the production of cement, thus reducing the waste of resources [3]. These materials were first produced in late 1970's [3] as alternatives to thermoset organic polymers and ordinary Portland cement [7,8,9].

Additive Manufacturing (AM) technologies are quite recent and starting from early '90s gained more and more interest among scientific communities and industrial companies. It is based on a layer-wise build-up of a tridimensional solid object starting from a digital form. Nowadays, 3D-printed objects find their application in a wide variety of fields, spacing from aerospace, to automotive, sports and even biomedic [10]. The term Additive Manufacturing contains lots of different printing technologies, which differ mainly from the way the final object is produced: direct printing, in which the material printed is actually the material of the final object, and indirect printing, when the material printed acts as binder for a second material and the union between the two materials constitutes the final object.

Direct ink writing (DIW), also called Robocasting [11], is the most used additive manufacturing process to produce 3D-printed ceramic objects [10]. It is based on the continuous deposition of an

extruded infinite filament in a layer-wise form. The intrinsic properties of geopolymers allow them to be used as pastes in a DIW process, although, this research path is still under investigation.

The demand of high performance, cheap and environmentally sustainable ceramic composites can be met by geopolymer matrix composites printed via DIW, in order to satisfy all industrial needs in terms of shapes and ease of production.

Aim of the study

This project proposes the development of a method to produce porous 3D-printed ceramic composites with geopolymeric matrix. What drives the production of these kind of ceramic composites based on geopolymers is the opportunity to reduce costs, compared to other ceramic composites such as carbon based or silicon based, and to have lower environmental impact, compared to same purposes ceramics like cements. Geopolymers came to the attention of scientific communities starting from late ‘70s, but there are already extensive studies on their mechanical, physical and chemical properties. However, their production method is still based on conventional traditional ceramic routes, such as casting. Additive manufacturing is a recent technology spreading among industrial companies form the ‘90s, which can be declined to a large variety of applications: from automotive, to aerospace, from military to sport and biomedical.

The challenge of the present work is to create new kind of ceramic composites via an innovative additive production method, Direct Ink Writing.

This work can be divided into three parts: the rheological optimization, the mechanical optimization and the experimentation with printable geopolymeric composites. The first part investigates the use of different rheological agents and fillers within the geopolymeric slurry to obtain a printable paste; the second concerns the use of different kind of fillers and thermal treatments to achieve the best mechanical performances; and the last one is an analysis of the production of 3D-printed geopolymeric composites added with different kind of fibers that enhances the overall mechanical properties, which make the composite worth of production. For the first part a deep rheological characterization was needed, for second and third parts mechanical, morphological, chemical and thermal characterization was done.

3D-printing of geopolymeric inks can be applied on the production of filters for catalysis or water purification, with tailored geometries and enhanced ionic interexchange if added with active fillers. Fast prototyping of fine pottery with unique design, not easily reproducible with classic methods of ceramic forming, is also a suitable field in which the combination of DIW with geopolymers can be used. Moreover, this technology and the material used are ideal to a scaled-up process of 3D-printing of shelters/small houses, drastically reducing the human labor cost.

Thesis organization

State-of-the-art and present development on Additive Manufacturing of geopolymers are presented in Background, with focus on the production of geopolymer matrix ceramic composites and direct ink writing of ceramics. Geopolymer characteristics, reaction mechanism and applications are described.

Chapter 1 reports on a short description of material used, the motivation behind their use and the methods of production and characterization of 3D-printed geopolymer lattices.

In Chapter 2 the results of experimental data collected during the research activities with methods seen in chapter 1 are presented and discussed. This chapter is subdivided into three paragraphs: rheological optimization, which is subdivided into two sub-paragraphs for the optimization of GP 13 PEG and GPP inks, mechanical optimization and printing of geopolymer composite inks. At the end of each paragraph case studies are presented, that show printing possibilities with geopolymer inks and examples of inks that have to be further optimized.

Chapter 3 is focused on the discussion of final conclusion and on possible future works.

In the Appendices are reported side-topic not necessarily linked to the main one:

- The possibility of producing ternary/quaternary composites made of 3D-printed geopolymeric composites impregnated with silicones is showed in Appendix A;
- The research activities carried out during the AMITIE Secondment in Saint-Gobain Research Provence are discussed in Appendix B.

Background

I. Geopolymers

The term "geopolymer" was first adopted by J. Davidovits around the 1970s [3] and applied to a mineral material class obtained from the reaction of an aluminosilicate and an alkaline solution. These materials were originally developed as a fire-resistant alternative to thermosetting polymers [7]. A geopolymer is universally known as a sodium aluminosilicate mineral, solid and stable formed from a hydroxide or an alkaline silicate which activates a solid powder containing the aluminosilicate.

The silica (SiO_2) and alumina (Al_2O_3) contained in the geopolymer is derived from an alumino-silicate in powder, usually a kaolinitic clay such as metakaolin, or fly-ashes, which are carbon combustion wastes, reacting in an activating solution, generally alkaline. A continuous tridimensional structure is formed, made stable through oxygen atoms sharing (figure I.1). These covalent bonds determine the structure name according to the Si:Al ratio: sialate Si-O-Al-O, sialate-siloxo Si-O-Al-O-Si-O or sialate-disiloxo Si-O-Al-O-Si-O-Si-O, also called poly(sialate), where the term sialate is an abbreviation for aluminosilicate (table I.1).

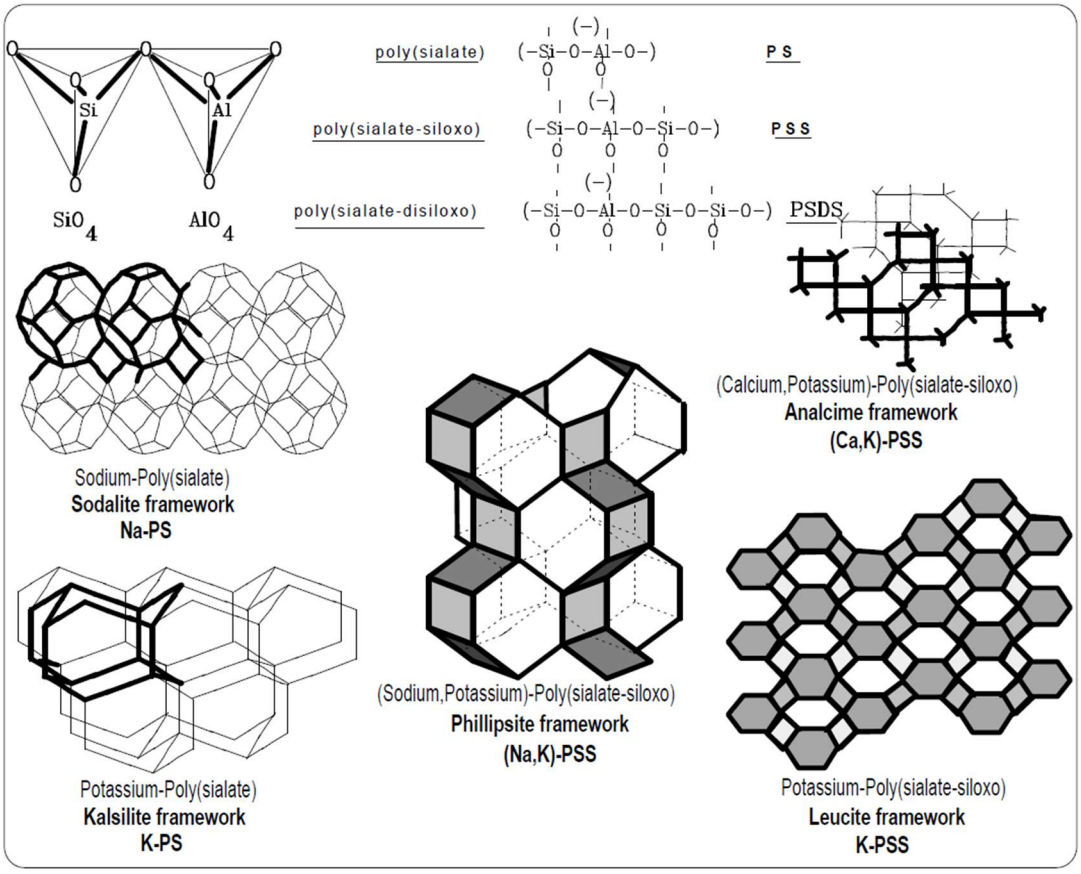

Figure I.1: Schematic representation of tridimensional geopolymer structures [12].

Table I.1: Geopolymers classification and typical application fields.

Si:Al ratio	Nomenclature	Applications
0	Siloxo	Bricks, ceramics, fire protection
1	Sialate	Cements and concretes, radioactive waste encapsulation
2	Sialate-siloxo	Foundry equipment, tools for Ti processing, fire protection fiber glass composites (resistance < 1000°C)
3	Sialate-disiloxo	Sealants for industry (< 600°C), tools for Al SPF
> 3	Sialate link	Fire and heat resistant fiber reinforced composites

However, geopolymerization can take place also in acid conditions, mainly in a solution with phosphoric acid, leading to the formation of poly(phosphor-siloxo) and poly(alumino-phosphor) geopolymeric chains.

The nomenclature based on the notion of sialate was coined by J. Davidovits [13], where the term sialate corresponds to a silicon-oxygen-aluminum bond, and siloxo to a silicon-oxygen-silicon bond.

Geopolymers may be considered amorphous and semi-crystalline synthetic zeolites equivalents. The polymerization reaction can be classified as an inorganic polycondensation and compared with zeolite formation: most of zeolites syntheses proceed in basic conditions using the hydroxyl group (OH^-) as mineralizing agent, that is as promoter of the dissolution of inorganic metallic species forming. The presence of some metallic species is needed to complete the silicon and alumina dissolution, and also to catalyze the condensation reaction. Geopolymers are formed by the individual co-polymerization of aluminium and silicate species, which in turn are formed from the dissolution of silica and alumina part of high pH materials in presence of soluble silicates [8].

The geopolymerization, which is the reaction that brought to the formation of a geopolymer, is an exothermic process which proceeds through the formation of oligomers (dimers and trimers) which are the unities that form the macromolecular tridimensional structure. One of the various formation mechanism involves the reaction of aluminosilicatic oxides with alkalis and the breaking of the alkalic polysilicates Si-O-Al bonds with a formula $(Si_2O_5, Al_2O_2)_n$. This is done by the calcination of aluminosilicate hydroxides (Si2O5, Al2(OH)4) through the reaction:

$$2\ (Si_2O_5, Al_2(OH)_4) \rightarrow {}_2\ (SiO_5, Al_2O_2)_n + 4\ H_2O \quad (1)$$

Or from the SiO and Al_2O vapors condensation as follows:

$$4\ SiO_{(vap)} + 2\ Al_2O_{(vap)} + 4\ O_2 \rightarrow (Si_2O_5, Al_2O_2)_n \quad (2)$$

which produces also silica fume and corundum ($2SiO + O_2 \rightarrow 2\ SiO_2$ and $Al_2O + O_2 \rightarrow Al_2O_3$).

Geopolymerization steps (figure I.2) include [15]:

1. the dissolution of a solid aluminosilicatic oxide in an alkaline solution of M-silicate, where M is an alkaline metal;
2. the diffusion of aluminium and silicon which are dissolved on the particles surface through the inter-particular spaces;
3. the formation of two gel phases, resulting from the polymerization between the activating solution containing the silicates and aluminium and silicon compounds;
4. finally, the gel phase consolidation.

The distinction between geopolymers occurs, besides the aluminosilicate source (kaolin, metakaolin or fly-ash) and the Si/Al ratio, also through the activating solution composition, which is an aqueous solution containing a metal, necessary for the tridimensional structure formation. It can be sodium (Na), potassium (K), phosphorous (P) or calcium (Ca) based.

Metakaolin or fly-ash alkali activated materials are a unique new group of materials with properties raging from those of cements, ceramics and zeolites, depending on their formulation, like for example quick mechanical characteristics development, fire resistance, dimensional stability, chemical attack resistance, great compatibility with aggregates and reinforces, etc. Moreover, the production of geopolymer can happen at low temperature, even room temperature, reducing production costs of about 10-30% than ordinary Portland cement [16].

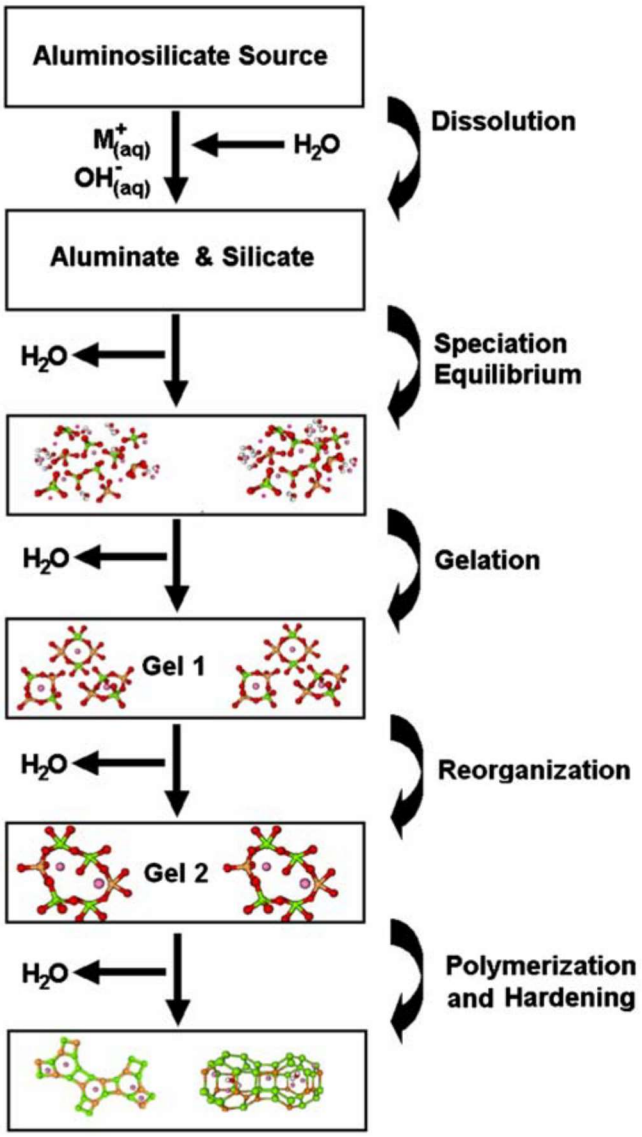

Figure I.2: Schematic model for geopolymerization steps [16].

Here are some examples of applications [12]:

- Geopolymeric binders and cements: Geopolymeric binders have been successfully introduced on the market. Geopolymeric cements are greener alternatives to OPC, as their process involves low-CO_2 emissions. Binders and cements geopolymer-based are useful for the realization of tools, cast molds for art objects, ceramics and structural construction materials;

- Production of low-cost ceramics: Geopolymers can enhance the traditional ceramics production minimizing costs and times of production. In fact, once the geopolymer is formed,

it can be treated at high temperatures (1000-1200°C) to crystalize the structure, which allows the realization of high-quality ceramics (figure I.3);

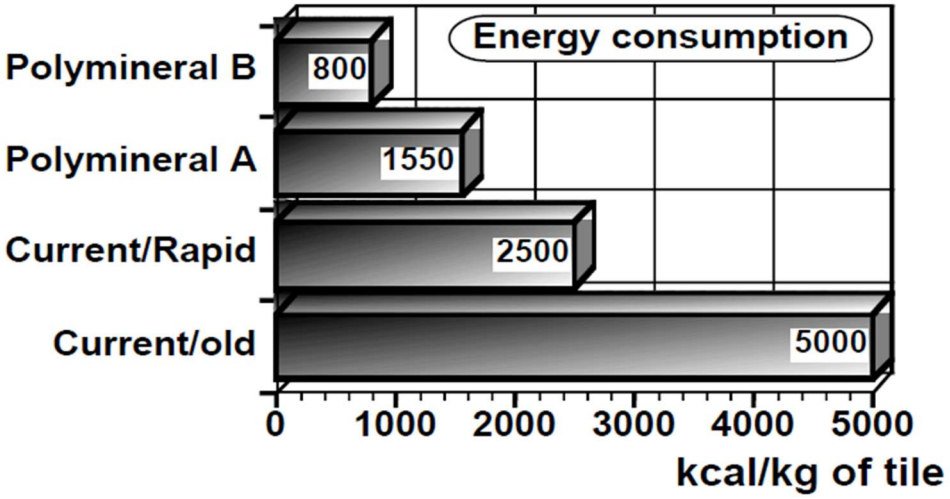

Figure I.3: Energy consumption for ceramic tile fabrication.

- Toxic wastes encapsulation: Zeolites are well known for their chemical adsorption characteristic. Geopolymers behave similarly to zeolitic and feldspathoid materials, immobilizing hazardous elements present in toxic wastes into the polymer matrix, and can also act as binders to transform semi-solid wastes into solid adhesives. Therefore, toxic elements contained in wastes mixed with geopolymer result "locked" inside the tridimensional structure of geopolymeric matrix (figure I.4). Furthermore, greek and roman ancient cement materials still endure on present days, sign of their exceptional durability and long-term stability;

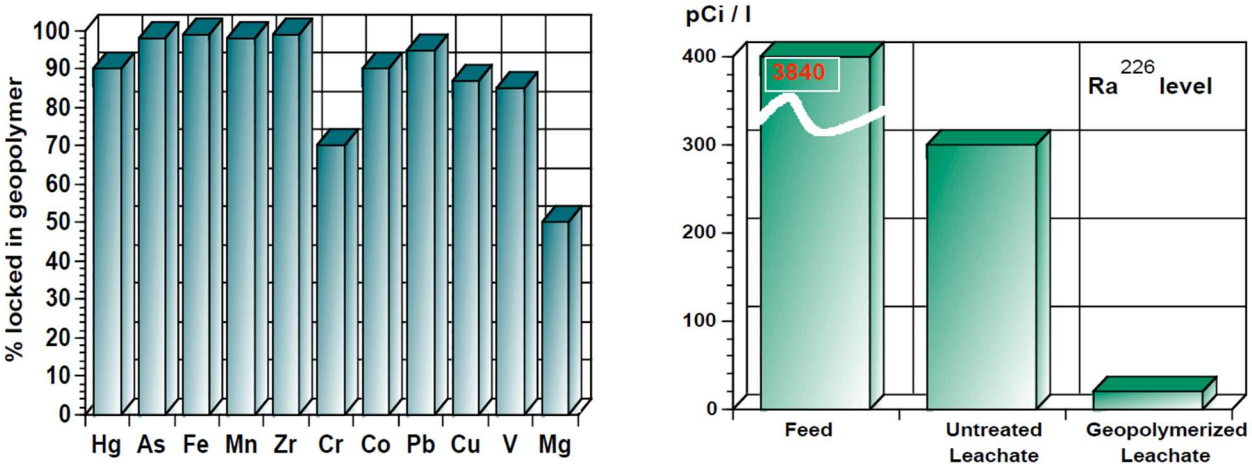

Figure I.4: (left): encapsulated elements in geopolymeric matrix;
(right): uranium leaching between geopolymerized and untreated uranium, as mined.

- Ceramic matrix for composites: High ease of production, low costs and the possibility of crystallization if heated at high temperatures make the geopolymer a good material to be suited on the production of ceramic matrix composites with fibers reinforcement. Given the composite proprieties, the main applications can be the same of polymeric matrix composites, but with non-toxicity characteristics, non-flammability [17] without fumes production, without the expensive production process needed for the realization of ordinary plastic and ceramic composites.

II. Geopolymer composites

Ceramic matrix composites find their application in various scenarios, where heat resistance, high mechanical strength and fracture toughness are required properties. Their production cost limits their use to niche products, applied only in high value-added fields, such as aerospace and military, where their performance justifies the disbursement necessary to obtain them. All ceramic composites produced for such applications are realized at high temperature in protected environments (i.e. over 1000°C in N_2 atmosphere) in order to not degrading the fiber reinforcement [2].

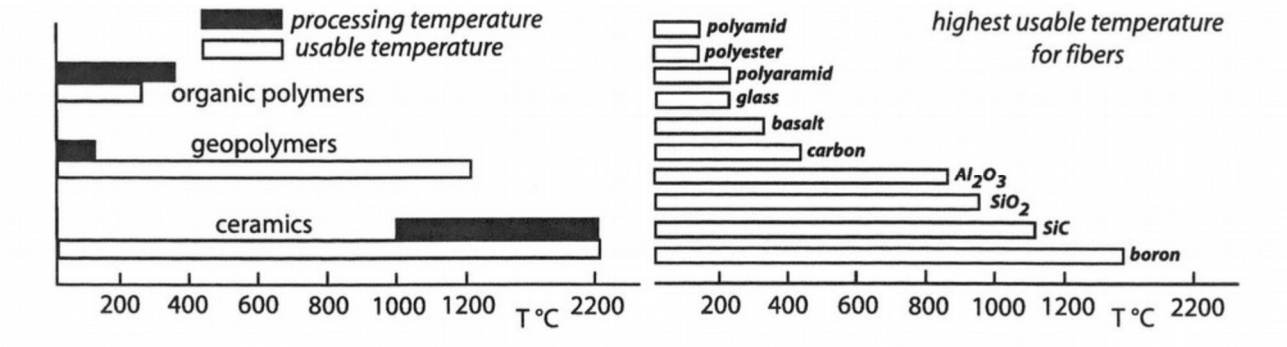

Figure I.5: (left): processing and usable temperatures for organic, ceramic and geopolymeric composites; (right): temperatures of usability for different kind of fibers [3].

As diagram on the left in figure I.5 shows, process temperatures for the production of a geopolymeric matrix composite are much lower than in ordinary composite production process. The positive aspects of using a geopolymeric matrix are multiple. In fact, a geopolymer can be used as amorphous matrix for the realization at room temperature of composite materials, or it can be understood as a pre-ceramic precursor, that, when heated at high temperature (around 1000°C) for a very limited period of time, undergoes crystallization forming a glass-ceramic matrix.

The interest around geopolymeric composites is relatively recent (1972) [3] and growing, thanks to their good properties, such as excellent fire resistance [17], low curing temperatures, low air and water permeability, weather condition resistance and low production costs. Geopolymers can be processed at temperatures from 20°C to 180°C with the same technology used for the fabrication of organic plastics, and the presence of high-performance ceramic fibers confer to the composite excellent mechanical properties in addition to a high temperature range of use (figure I.5).

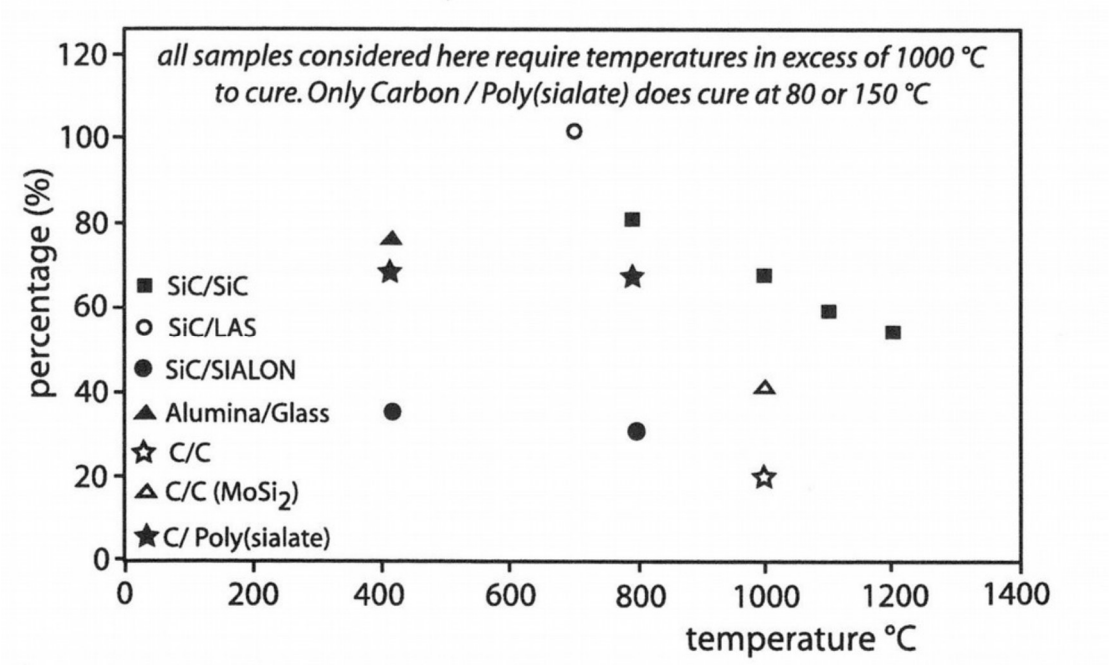

Figure I.6: Percentages of mechanical properties conservation over temperature for different ceramic composites [18].

2005 work by C. G. Papakostantinou et al. [18] showed the difference between a carbon fiber reinforced geopolymer composite, named here C/Poly(sialate), and other ceramic composites, such as C/C or SiC/SiC, in terms of mechanical properties retention after being exposed to high temperatures (figure I.6). The SiC/SiC composite (silicon carbide matrix, silicon carbide reinforcement) preserves up to 80% of its initial stress resistance after heating at 800°C, with a linear decrease to 1200°C, for which the residual strength is 55% the initial. SiC/LAS composite (Lithium-Alumina-Silicon glass matrix, silicon carbide fibers) shows at 600°C a strength slightly above those at room temperature (20°C). Alumina/Glass composite conserves good propriety up to 400°C (~75%) but starting from 600°C the glass matrix begins to soften. The C/C composite (carbon matrix, carbon fibers) does not lose strength only if when subjected to high temperatures the atmosphere conditions are not oxidizing, in these controlled environments it could be used while exposed up to 3000°C. Vice versa, if subjected to a non-controlled atmosphere, the mechanical performance of C/C composites rapidly decreases from 400°C, because of rapid oxidation and consequently combustion. If an anti-

oxidation additive is added to the C/C composite, as in the case of molybdenum silicide ($MoSi_2$), the conserved resistance increases up to 40% at 1000°C.

C/Poly(sialate) composite with geopolymeric matrix and carbon fibers, which should lose much of their resistance if exposed to high temperatures, conserves about 65% at 800°C of its original mechanical strength. This result is obtained thanks to the matrix structure, which protects the fibers against oxidation: However, this protection cannot last for long periods of time, but mostly only for few hours at maximum; if the application requires exposure to high temperatures for longer time, such as in aerospace field, then a partial or even total substitution of carbon with SiC fibers is needed.

First studies on the realization of a ceramic composite with geopolymeric matrix were carried out by Davidovits and Davidovics [19] from the first half of 1980s, using as matrix a potassium based geopolymer K-PSS (Potassium-Poly sialate-siloxo), used also by Jia et al. [20] and Zhao et al. [21], differing by the Si/Al molar ratio. More recent studies on geopolymer composite mechanics, show the implementation of different kind of geopolymers, for example the works of Li el al. [22] and Natali et al. [23] are focused on a sodium based geopolymer, as well as on the Kong et al. [24] study, but in this case the geopolymer is fly-ash based.

First fiber reinforcements added to geopolymer slurries were glass, carbon and silicon carbide fibers [19]:

- Glass E fibers: When in close contact with geopolymeric matrix, glass E fibers undergo two different kind of weakening: a chemical attack, that dissolves the fibers, given by the geopolymer pH, which is extremely basic, and a physic damage resulting from the difference in thermal expansion between fibers that expand if heated and geopolymer that shrinks because of the geopolymerization reaction. The adhesion to the matrix is excellent, if fact, when heated, fibers can be broken (figure I.7). This phenomenon is similar to glass fiber weakening in Portland cement composite subjected to ageing.

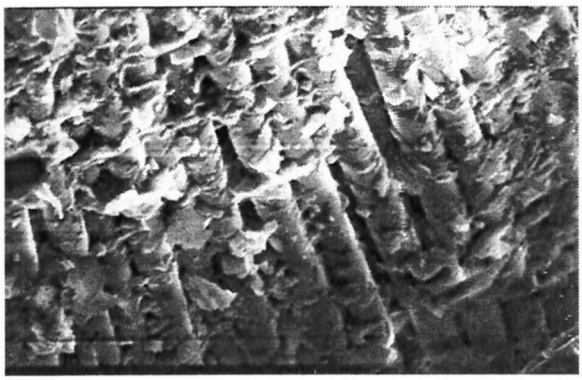

Figure I.7: SEM micrography of glass E fibers K-PSS geopolymeric matrix composite, detail of fibers nearly completely covered by matrix.

- Carbon fibers: Low wettability between fibers and matrix, fibers seem smooth with low or even none adherence with matrix (figure I.8).

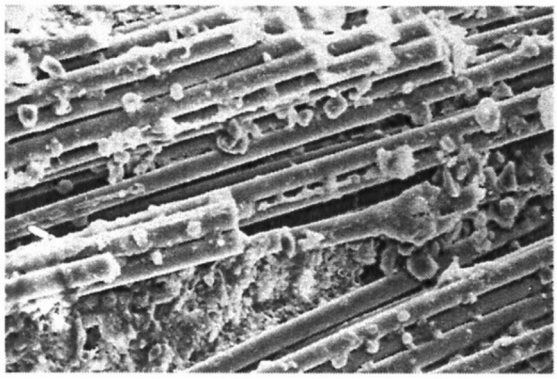

Figure I.8: SEM micrography of carbon fibers K-PSS geopolymeric matrix composite, detail of fibers with low adherence to the matrix.

- SiC fibers: Silicon carbide fibers show a medium adherence to the matrix (figure I.9) and a high flexural resistance for a wide range of temperatures that gives more than 100 MPa at 700°C (figure 6).

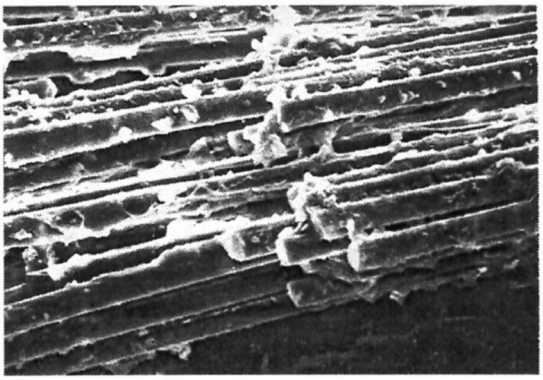

Figure I.9: SEM micrography of SiC fibers K-PSS geopolymeric matrix composite, detail of fibers each of those covered by matrix.

Natali et al. [23], focused their attention to the comparison in flexural behavior between different composites made with different type of fibers added to the same sodium-based geopolymeric matrix, such as carbon, glass E, PVA and PVC fibers. The matrix/fibers adhesion is satisfactory for all the composites, but best results are achieved with PVA fibers. The work brings to the attention an enhancement in ductility compared to unfilled geopolymer thanks to PVA fibers addition, PVC fibers composite, instead, show the highest fracture energy absorption capacity (figure I.10). However, these results are obtained with only 1% of fibers volumetric ratio.

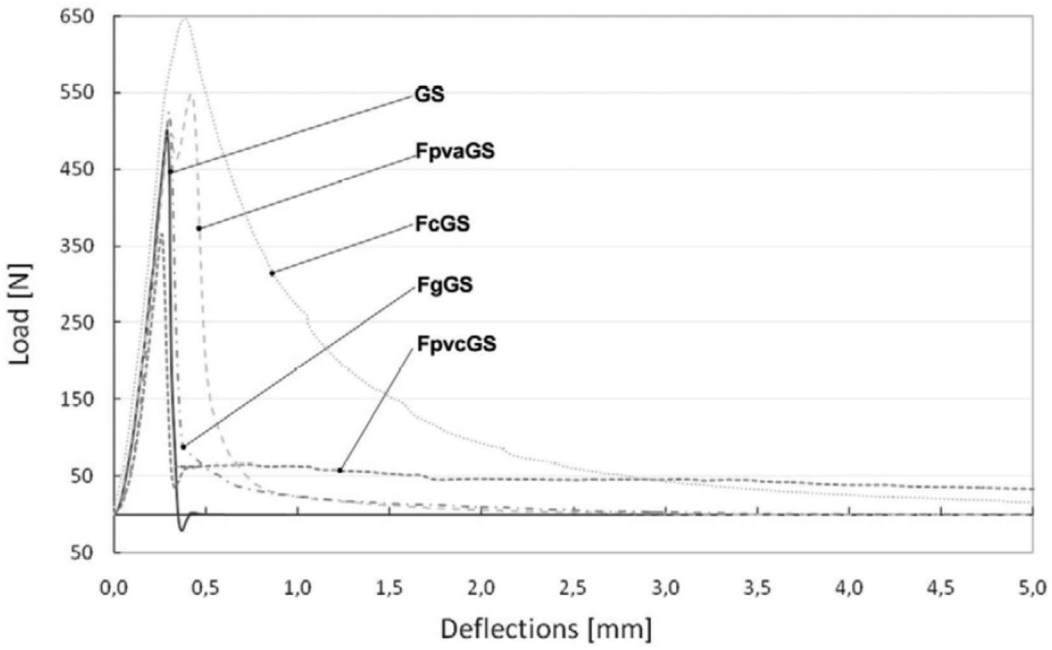

Figure I.10: Flexural strength obtained with 3-point bending tests on samples: GS (unfilled geopolymer), FcGS (carbon fibers reinforced geopolymer), FgGS (glass E fibers reinforced geopolymer), FpvaGS (PVA fibers reinforced geopolymer), FpvcGS (PVC fibers reinforced geopolymer) [23].

III. Additive manufacturing of ceramics

Additive Manufacturing (AM) process are based on Solid Freeform Fabrication (SFF) technologies, which allow the production of 3D solid objects starting from a digital design model, giving the possibility to eliminate industrial costs, such as tooling and production waste management, and to increase manufacturing flexibility and production rates. AM makes the realization of complex shapes, impossible to produce with traditional technologies (i.e. casting, forging, etc.), easy and fast prototyping possible. The American Society for Testing and Materials (ASTM) defines AM as a "process of joining materials to make objects from 3D model data, usually layer upon layer, opposed to subtractive manufacturing methods such as traditional machining" [25]. Subtractive manufacturing consists on the realization of a solid object via material removal from a large piece, most of these are machining processes like milling, grinding, etc.

The materials used, such as powder, liquid, slurry, filament or sheet [10], and the build-up way of final object realization distinguishes the AM technologies into two main categories:

- Direct AM: the material is deposited only where the object is;
- Indirect AM: the final object material results on the deposition of a binder, that can be a liquid/slurry or energy (UV, heat, etc.), on a second material.

In the indirect AM case excess of material has to be removed to free the printed structure, but, at the same time, it provides support to the realization of complex geometries and large spanning

overhangs, which require sacrificial structures if produced via direct AM processes. Indirect AM technologies can have production rates higher than direct AM, because the cross-section can be inscribed over the entire layer surface allowing the simultaneous production of more objects in one print. On the other hand, it's difficult to produce objects with closed porosity via indirect AM, because the removal of unreacted material inside the pores require the destruction of the part where the pore is located, even in the case of small open pores [10].

AM technologies part of the two groups are divided by ASTM into seven different categories (figure I.11) [25]: material extrusion, material jetting and direct energy deposition are part of direct AM; sheet lamination, VAT photopolymerization, powder-bed fusion and binder jetting are part of indirect AM.

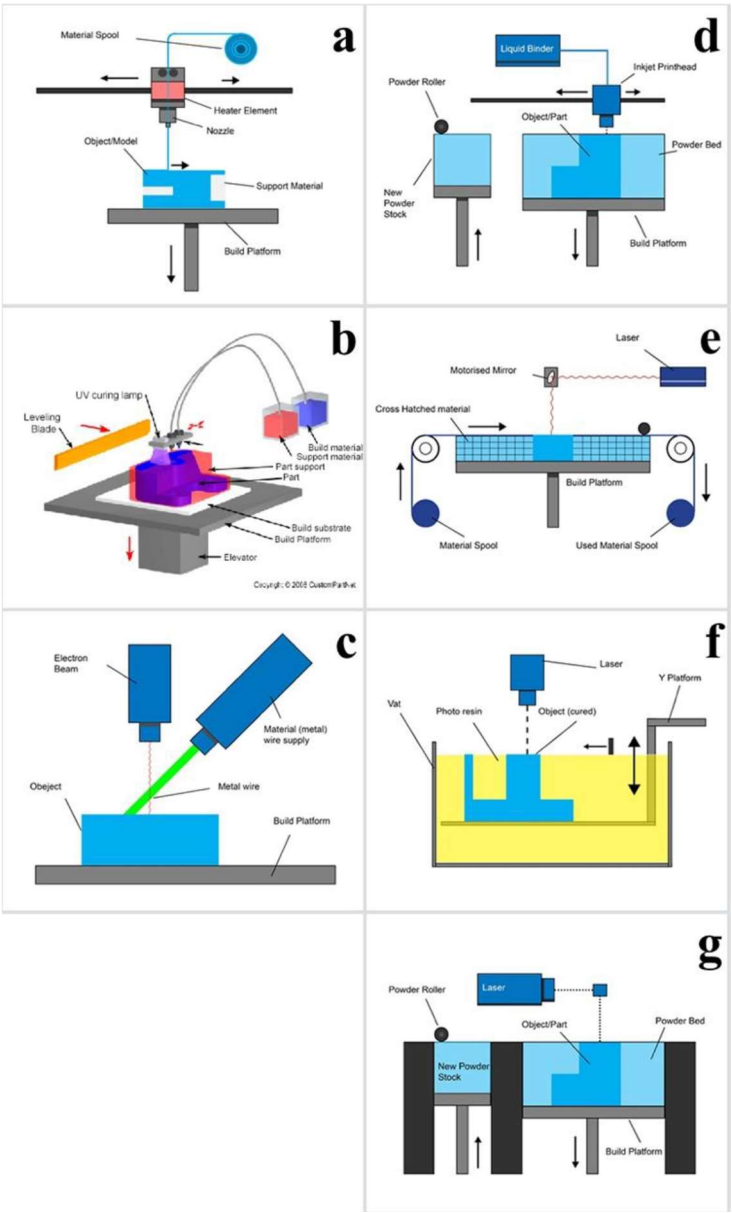

Figure I.11: Schematization of AM technologies: (a) Material extrusion, (b) Material jetting, (c) Direct energy deposition, (d) Binder jetting, (e) sheet lamination, (f) VAT photopolymerization, (g) Powder-bed fusion [25].

The most successful AM technologies are based on polymeric and metal materials. Multi-material structures obtained with materials with different functionalities and compositions can be implemented in 3D-printing process as well [26, 27]. In this point of view, direct AM seems the keenest technology to be combined with multi-material systems, including ceramics. On the other hand, indirect AM show more difficulties, for example the addition of metals to enhance conductivity in ceramic based AM is possible, but only for small concentrations [28].

The applications of ceramics via AM is shifting from design and fast prototyping to the production of objects with specific properties, that meet the market needs. But, in order to achieve satisfactory results, there are still some technological issues that are to be taken into consideration. Applications already discovered for this kind of processes are focused on the production of porous structures, foams, biocompatible scaffolds for tissue repairing, filters and catalyst carriers [29, 10]. The production of lattices with controlled amount, orientation and shape of pores is gaining more and more interest among AM research communities, because it is the only way that can be produced without expensive tooling. Therefore, AM can be seen as an aid to open up new research horizons, rather than competing with existing traditional technologies. However, AM processes are not well suitable to the production of fully dense, monolithic ceramics, which show greater mechanical properties than porous structures, making these technologies less competitive to replace industrial processes.

The need of technology deep understanding, expertise and post-production processes, which are required as usually objects printed are green body that have to be thermally treated, limit the user field to people already familiar with ceramics production or research.

IV. Direct Ink Writing of geopolymers

Direct Ink Writing (DIW), also called Robocasting by J. Cesarano et al. [11] in patent US 6027326 in 2000, is described as a "rapid prototyping system for forming parts of a predetermined material by depositing a bead of slurry onto a surface, the surface moving in a predetermined pattern with respect to the bead, and the slurry consisting of a mixture of a volatile solvent, particles of the predetermined material which are insoluble in the solvent, and a small amount of non-volatile organic binder and/or dispersant" [11]. This technique is based on an extruded filament layer by layer deposition forming a 3D solid object with a predetermined geometry. Not all materials are suitable to DIW, in fact, inks, thus called materials printed with this kind of process, must be extrudable in form of a filament and rapidly recover their viscosity once extruded, to maintain the geometry given by the

printing. Rheology proprieties are therefore a principal issue when it comes to decide if an ink is printable or not. In the same patent, Cesarano [11] explained what the requirements for ceramic slurries are in order to be printed, it has to be pseudoplastic. The ideal is an ink which shows typical Bingham pseudoplasticity, which is a fluid with initial yield stress, that when is overtaken the slurry can flow, and with viscosity that increases with the increasing shear rate. With these features, the ink can be easily extruded at low pressure, by a piston or an infinite screw, and it is able to quick recover its viscosity once extruded, in order to maintain the shape even in the case of suspended structures. Materials that show this behavior are generally addressed as reversible gel and ceramic suspensions can achieve it in different ways, including flocculation of the suspended particles for example by altering the pH, or adding organic binders and plasticizers [30]. Using polyelectrolytes to adjust suspension pH is difficult and requires fine tuning for each suspension to make them printable because the presence of ions in solution could interfere with ceramic particles, for example, changing pH of bioglass involves dissolution and leaching of ions in water [31]. Blending the suspension with an organic additive like a binder or a plasticizer is less difficult, and don't depend of what type of ceramic is used, but needs a further step, after the printing, in order to eliminate the additive. This method seems to not generate defects in final object [32]. Another option to form a reversible gel phase is to add gelling additives, which can be used in lesser amounts, making their elimination unnecessary [33]. A positive aspect of the last method is that it is not affected by nozzle clogging, so the diameter of the tip from where the slurry is extruded can be shrunk to 100 μm [34, 35], while the other methods require diameter not above 0.5 mm, and is possible to easily produce filament cross-sections different from cylindrical, such as squared, hexagonal, etc. or even hollow [36].

The most important limit to the DIW production technology is the possibility of printing massive monolithic objects, because filament surfaces generated during the process are typically rough and they tend to form voids at the interface between another filament (figure I.12). The presence of binder or organic additives can lead to the formation of porosity during their elimination step. Therefore, mechanical properties of these objects are affected by this kind of defects, meaning lower properties where the defects occur, mainly along the vertical direction. On the other hand, the production of porous structures via DIW is the most successful, leading to a large number of works concerning the production of lattices for tissue repairing applications. Miranda et al. [37] printed hydroxyapatite (HA) lattices with porosity of 39% and a compressive strength of around 50 MPa, which was nearly doubled after being immersed for two weeks in simulated body fluid [38].

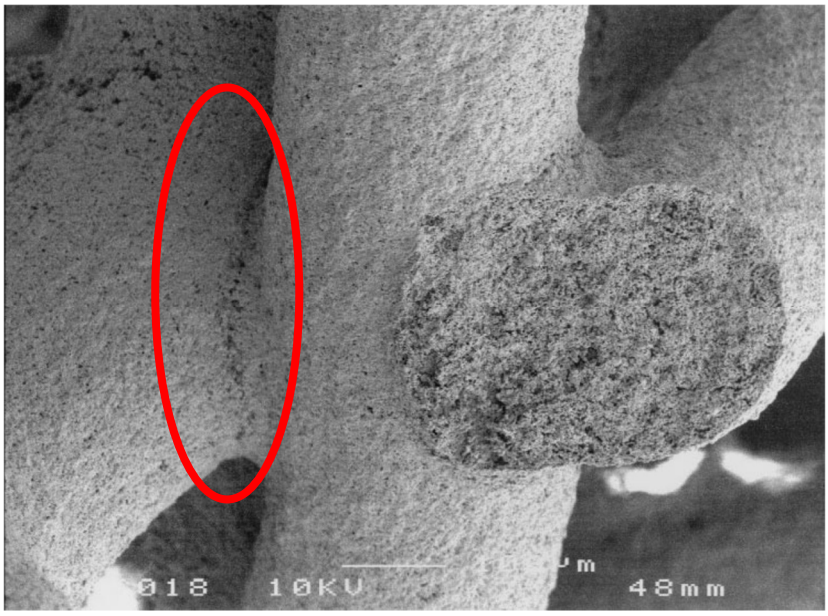

Figure I.12: SEM micrography of a sintered lattice made by DIW of Hydroxyapatite, in red detail of interface porosity [32].

Good results were achieved also in non bio-related fields, Stuecker et al. [39] were able to print mullite scaffolds with pore sizes of 100 to 1000 µm. Smay et al. [40] printed radial structures with strut size of 200 to 400 µm with increasing spanning distances between subsequent struts, and piezoelectric components for ultrasonic sensors [41] with the same ink.

Geopolymers have a gel-like structure and their intrinsic pseudo plasticity make them usable in a DIW process. Although, they are subjected to an ongoing reaction of polycondensation which makes the paste rheology time-dependent, in what can be seen as a 4D-printing process, where the fourth dimension is time. The time was exploited to produce 3D-printed structures with the possibility of changing properties or configuration if subjected to an external input [42, 43]. Materials used in 4D printing process are named as "smart materials" [44, 45], geopolymers can be good candidates to be implemented in DIW process as smart materials once their reaction is controlled.

Previous works on geopolymeric inks [46] mentioned the possibility of 3D-printing geopolymers through inverse replica of PLA sacrificial templates. More recent publication of Zhong et al. [47], reported the use of geopolymer slurry added with nanoscale graphene oxide powder, which allowed them to achieve a rheologic behavior good enough to be printed. This study is also set as the first example of a 3D-printed geopolymeric nanocomposite.

Recent publications [48, 49, 50, 51, 52] are focused on the printing of geopolymer and geopolymer-based concrete as construction material, but in these cases the printing technique is comparable to concrete beam extrusion, as printing nozzles are wide enough to produce large filaments, with

sections over 2.00 x 2.00 cm^2. Geopolymers in these studies are not the main material extruded, but they are used as filler or are so heavily added with fine aggregates or properties modifiers that they cannot be recognized as geopolymers anymore, but instead they can be called alkali-activated materials [53] or geopolymer cements.

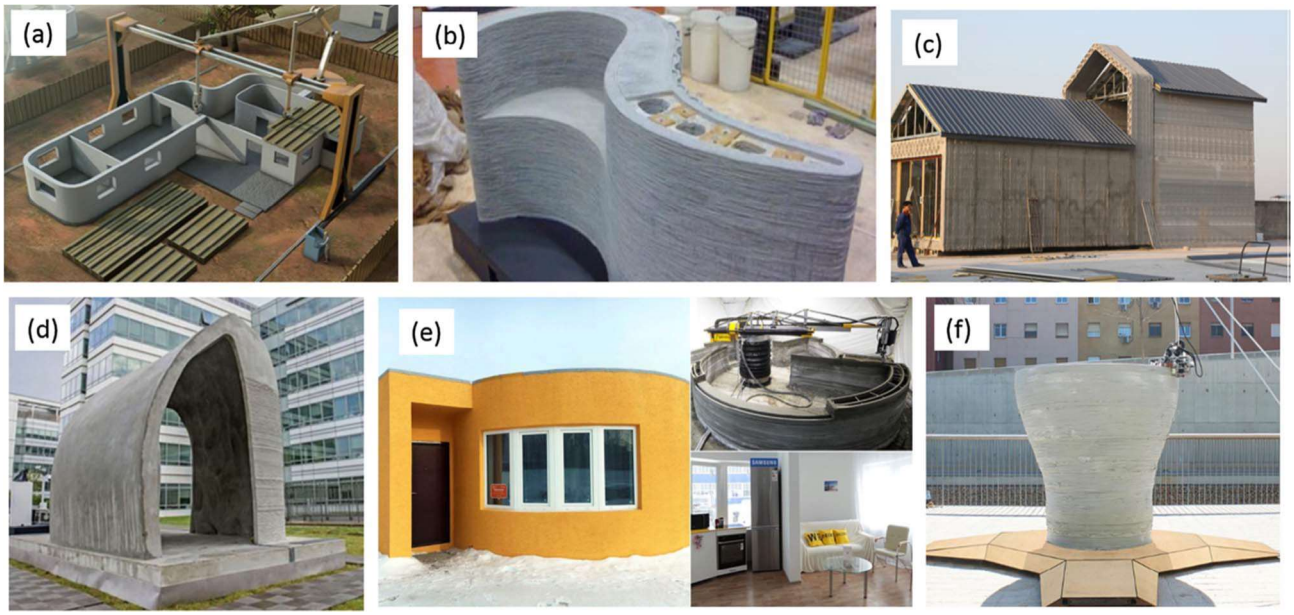

Figure I.13: Examples of large-scale 3D-printed objects made of geopolymeric cements: (a) Counter crafting, USA; (b) University of Loughborough, UK; (c) Winsun, China; (d) Xtree, France; (e) Apis-cor, USA; (f) Mini-builder, Spain [51].

Few companies and institutions started to experiment large scale 3D-printing of standard cement and concrete and they are trying to pass to geopolymer based ones. The most successful example is the realization of a full house structure of about 50 m^2 in only 24 hours (figure I.13 (e)) by Apis cor [54]. Little work has been done so far on DIW of geopolymers, so, the work presented in this thesis is set as an initial point in developing geopolymeric and geopolymeric composite inks printable via DIW, that could lead to further research to expand production possibilities.

Materials and Methods

1.1 Geopolymers

Geopolymers are inorganic aluminosilicates which are usually synthezised starting from an aluminosilicate in powder, that can be a kaolinitic clay, in an alkaline solution containing the alkaline metal that is part of the structure.

1.1.1 Requirements

The fundamental properties of a geopolymer are high mechanical strength and high thermal resistance, as well as rheological properties that make it usable in a direct ink writing process:

Mechanical strength: this parameter was studied by Duxson et al. [55], about the Si/Al ratio. The geopolymers chemical composition varies with the alkaline metal quantity, with a nominal chemical composition $Na_yK_{y-1}(SiO_2)_zAlO_2 \cdot 5.5H_2O$, in which y can be 0.00/0.25/0.50/0.75 and z 1.15/1.40/1.65/1.90 and 2.15. From the graph in figure 1.1, samples are labeled as Na, Na75, Na50, Na25 and K, i.e. without Na, and they represent five molar ratios respectively Na/[Na+K] = 1.00/0.75/0.50/0.25 and 0.00. As graph shows, the compression strength rises with the Si/Al ratio from 1.15 to 1.90, regardless of the ratios between the alkalis, to then decreases, just for a little, over 1.90. Samples show a similar strength to a fixed Si/Al ratio, with different alkalis ratios though, suggesting that the mechanical proprieties differences are around 10-20% to different ratios between alkalis, which is a typical phenomenon on the proprieties of chemically similar glasses.

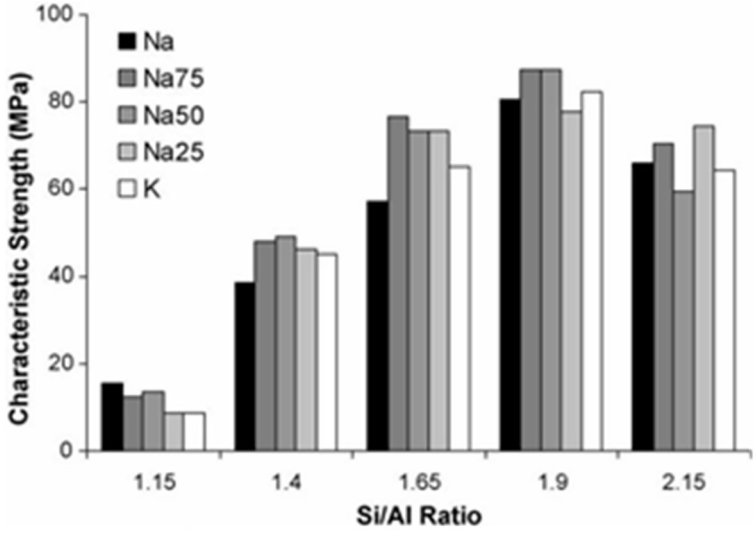

Figure 1.1: Compressive strength of geopolymer compared to Si/Al ratios specimens recorded at 7 days after preparation [56].

In the same work, the elastic modulus is taken into consideration (figure 1.2). Also, in this case, the modulus increases with the increasing Si/Al ratio, with a similar trend on samples with different alkalis ratio. The elastic modulus decreases when the Si/Al ratio is over 1.90, but such decrease is less relevant compared to the one in the mechanical strength.

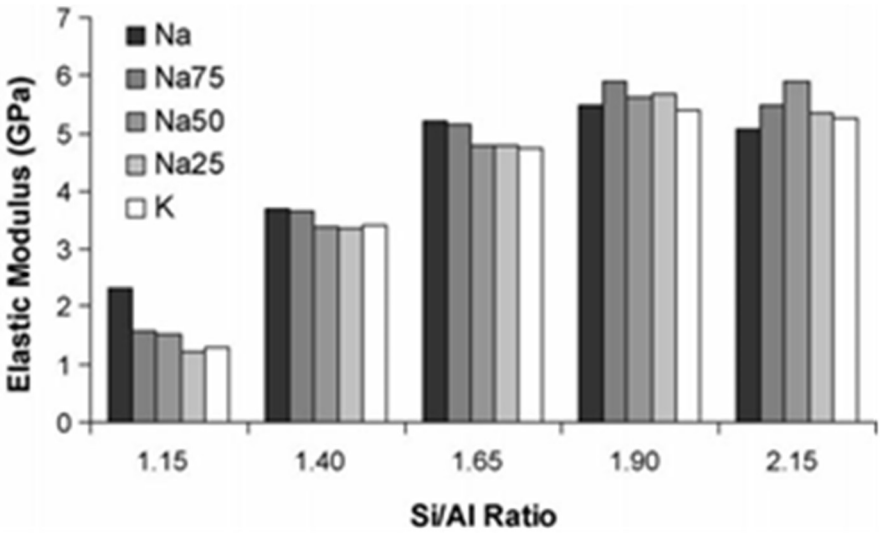

Figure 1.2: Elastic moduli of geopolymer specimens recorded 7 days after preparation [56].

Temperature resistance: a very important characteristic of all ceramic materials is the refractoriness at high temperatures, for which a ceramic can withstand high temperatures, even the exposition to flames, maintaining its chemical and physical properties [3]. In figure 1.3 are shown the comparatives between geopolymers with different compositions with their density and softening temperature.

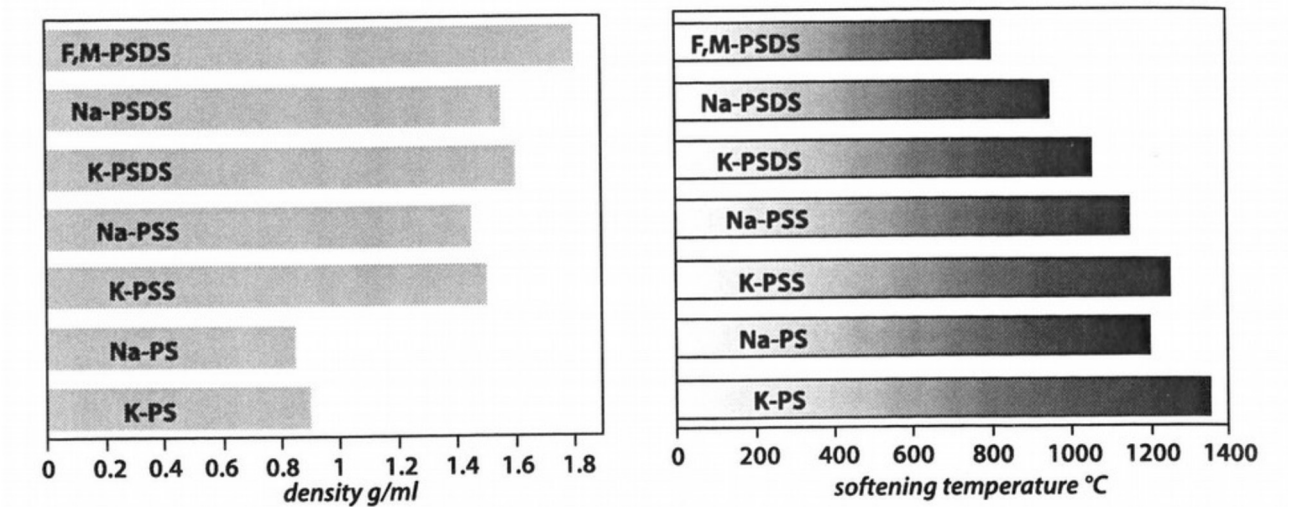

Figure 1.3: Apparent density (left) and softening temperature (right) for poly(sialate) (PS), poly(sialate-siloxo) (PSS) and poly(sialate-disiloxo) (PSDS) geopolymers. F geopolymer is made from fly-ash [3].

It is possible to understand the inverse correlation between density and softening temperature of geopolymers. Best results are obtained by the K-PS geopolymer, poly(sialate) potassium based, Si/Al ratio = 1.0, with a softening temperature of around 1350°C, to be compared with the melting point of the equivalent mineral, kalsilite $KSiAlO_4$, 1735°C. The second-best result is shown by Na-PS geopolymer, poly(sialate) sodium based, same Si/Al ratio of 1.0, and a softening temperature of around 1200°C, to be compared with the mineral equivalent, nepheline $NaAlSiO_4$, of around 1526°C.

Rheology: It is well known by literature [57, 58, 59] that freshly made geopolymeric slurries behave as a non-Newtonian fluid. They show a shear-thinning behavior with initial yield stress, i. e. Bingham pseudoplasticity [60], which is needed for a material that has to be extruded. The yield stress gives the possibility to the paste to not flow without pressure during the production, and high values of the storage modulus (G') over the loss modulus (G") indicate a strong tendency to keep the shape given by the nozzle once extruded. So, a typical geopolymeric paste can be potentially used in 3D-printing, however a fine tuning of the rheological aspects has to be done in order to have a printable ink. To do this kind of optimization, rheological agents must be added to the freshly made slurries.

1.1.2 Sodium-based geopolymer

A sodium-based geopolymer was chosen after the previous discussion based on the work carried out by Duxson et al. [55] and on the patent n° 4,472,199 deposited by Davidovits [74] with a poly(sialate) structure, Si/Al ratio of 2.0, once crystalized it shows nepheline as the main structure. Molar ratios are the following:

- SiO_2/Al_2O_3 = 3.8
- Na_2O/SiO_2 = 0.263
- H_2O/Al_2O_3 = 13.0
- Na_2O/Al_2O_3 = 1.0

The only variable ratio of this kind of geopolymer is the one correlate to water. The water content influences the overall mechanical properties, because it is responsible of the material's porosity percentage, then a lower amount of water corresponds to a structure with lower porosity, so a higher mechanical strength. However, the reaction of geopolymerization with a low amount of water is so quick that is impossible to use it on the production technology of the 3D-printing, because, once mixed, the slurry seems already solid. The gepolymer water ratio was chosen as a good compromise between reaction rate and fluidity of the slurry. In fact, previous works [61] on this same compound set the lowest possible water ratio with the same raw materials as 11.0.

1.1.3 Rheology Agents

As previously said, geopolymers undergo to a continuous reaction of polycondensation, which constantly changes their rheology over time. So, on one hand these materials can possibly be used as pastes in 3D-printing because of their intrinsic properties, on the other hand the evolution of their rheology over time has to be finely tuned, in order to achieve a more constant behavior during the production. Based on literature, two different organic additives were studied to choose the one which gives better printability to the slurry: PAA, poly acrylic acid and PEG, polyethylene glycol. The amount of additives added to the mixture is set as the lowest possible in order to have the right properties but to not influence reaction kinetics or chemical properties. PAA is added as a 7% of the total weight of the geopolymer's raw materials, PEG as a 5%. PAA is frequently used as a thickening agent in aqueous based systems as it creates an entanglement of polymer chains imparting a shear thinning behavior to the ink [62, 63]. Previous works show that PEG can be used to stabilize colloidal suspensions and to enhance the plastic behavior of a slurry [64, 65, 66, 67], and it has been already used as a gelling agent in the three dimensional printing of glass powder, as reported by A. M. Deliormanli et al. [68].

1.1.4 Fillers

To further increase the yield stress of the gopolymeric slurry, fillers are added. First, natural siliceous sand is used, sieved to have particles size below 300 μm, that is because the extrusion nozzle of the DIW equipment is set at 840 μm and clogging effects must be avoided. The rheology of sand-filled geopolymer is analyzed and compared with previous results. Previously made geopolymer powder is added to the mixture in place of sand. In this case, geopolymer is previously prepared, ground and sieved below 300 μm and finally added to the slurry with the same chemical composition. This lowers the formation of cracks after heat treatment.

1.1.5 Fibers

Fibers for the composites production are chosen after literature [20, 21, 22, 23, 24] and following a fundamental requirement, that is the resistance to alkaline environments. This because of the activating solution that makes the geopolymeric slurry highly basic, with a pH ≈ 14; therefore, uncoated glass, basalt or polymeric fibers would be dissolved during the production. For this reason, two different type of fibers normally used in alkaline environments were chosen: carbon and mineral

fibers. The volumetric percentage of fibers introduced into the matrix is set as the upper limit after which is no longer possible to produce the paste.

Ceramic fibers: The phenomenon that drives the composite fracture [4] depends on the bonding strength between matrix and fiber. If the fiber surface does not interact with the matrix, the strength of fiber-matrix interface is weak, the crack present in the matrix grows around the fibers and the interface is broken (debonding) before the fiber itself is damaged. Then, the crack stops at the interface with a fiber and has to spend energy to continue its propagation, this results in a graceful failure. Moreover, fibers form bridges through fracture surfaces and tend to maintain the geometry while the crack is propagating (delamination). However, once fibers are damaged, there is a substantial absorption of crack energy while fibers are pulled from the matrix fracture surfaces. This phenomenon is called pull-out and can be observed in stress-deformation diagram (figure 1.4) as a long tail right after the matrix failure, which is the sign of residual stresses that are beared only by the fibers until the sample finally breaks.

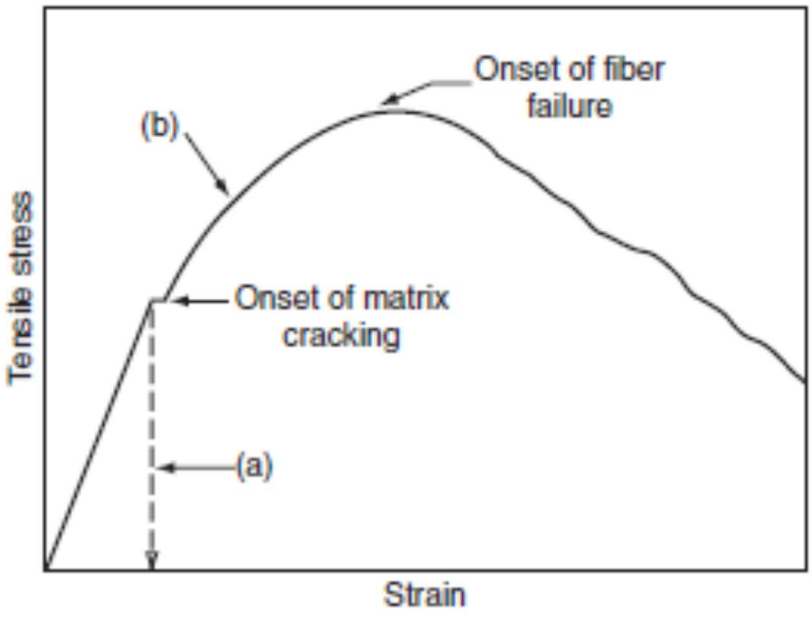

Figure 1.4: Typical diagram of a traction test of a ceramic composite: (a) the matrix is still intact; (b) the matrix is broken.

Debonding, delamination and pull-out are phenomena which give tenacity to a ceramic matrix composite. The energy of the propagating crack is absorbed to the extraction work of fiber from the matrix, mainly for three reasons:

1. Matrix recession, matrix recesses and fibers are on a compressive state, they are “caged” by the matrix;
2. Variability of fibers diameter, fibers have got a diameter which is the one declared by producer on average, but locally they are not uniform, they appear “rough” at high magnifications;
3. Weak chemical bonds, between matrix and fiber low energy bonds are formed, like van der Waal or hydrogen bridges, which they easily reform also when the fiber is being pulled.

1.2 Methods of Production

1.2.1 Geopolymeric inks

The reagents needed for the synthesis of the geopolymers composition in this work are alkaline sodium silicate activating solution, metakaolin and rheology agents, their composition given by manufacturers are listed in tables 1 and 2.

Table 1: Composition of sodium silicate solution as provided by manufacturer, R is the weight ratio: SiO_2/Na_2O [69].

INGESSIL SS 2942	
R	2.9
SiO_2 (%)	28.35
Na_2O (%)	9.77
Conc. (%)	38.12

Table 2: Composition of metakaolin powder as provided by manufacturer [70].

Argical M 1200 S	
SiO_2 (%)	55
Al_2O_3 (%)	39
$K_2O + Na_2O$ (%)	1
Fe_2O_3 (%)	1.8
TiO_2 (%)	1.5
CaO + MgO (%)	0.6

Sodium silicate solution: Prepared following the molar ratios between the species present in the final material (seen in par. 1.1.2) using distilled water, a concentrate sodium silicate solution (Ingessil SS 2942, Montorio, IT) and sodium hydroxide in pellets (NaOH, Sigma-Aldrich, St. Luis, MO, USA). The elements are poured in a bottle, sealed, agitated and when the sodium hydroxide looks to be completely dissolved, the bottle is store in a fridge at a temperature around 3/4°C, to counteract heat formed during the reaction between sodium hydroxide and water and gives the possibility to completely dissolve NaOH. The solution is kept at low temperature, since an increase of temperature corresponds to a quicker reactivity of the geopolymer mixture, as the geopolymerization proceeds with water elimination [3]. The preparation of the activating solution is done at least 1 day previous its use, after that period NaOH is completely dissolved and the solution is fully homogenized.

Metakaolin: The source of aluminosilicate used to produce geopolymers is a kaolinitic clay powder treated at 750°C for the time needed to fully evaporate all the water. Its commercial name is Argical M 1200 S (Imerys S.A., Paris, FR).

Rheology agents: Poly (acrylic acid) sodium salt with an average molecular weight of 5100 g/mol (PAA, Sigma-Aldrich, St. Luis, MO, USA) and poly(ethilenglycol) with an average molecular weight of 1000 g/mol (PEG 1000, Sigma-Aldrich, St. Luis, MO, USA) are used as rheology agents.

Geopolymer slurries are produced by mixing the different elements in a specific order. First, the rheology agent has to be dissolved into the solution, then metakaolin powder is poured and mixed. An overhead stirrer is used with the possibility to finely tune the rotational speed. The tool has a four-blade propeller geometry with a 50 mm diameter, made of inox steel AISI 316L, alkaline resistant (figure 1.5).

The mixing conditions chosen are:

- Rotational speed of 1000 rpm;
- Time of mixing: 10 minutes for each step, for the first one the time is only indicative, as the rheology agent must be fully dissolved into the solution before moving to next step.

Figure1. 5: Overhead stirrer (left) and rod (right) used for the production of geopolymers.

Once the mixing is over, the printing syringes are filled with the slurry and they are ready to be used in the printing process.

1.2.2 Filled geopolymeric inks

These inks are made starting from normal geopolymer inks adding different fillers in form of powder: sand and geopolymer.

Sand: Natural siliceous sand (figure 1.6) sieved below 300 μm, 20% vol.

Geopolymer powder: Already made geopolymer, produced as a normal geopolymer ink, but without rheology agent, cured at 80°C for at least one day, to fully evaporate water, crushed and sieved below 300 μm, 20% vol.

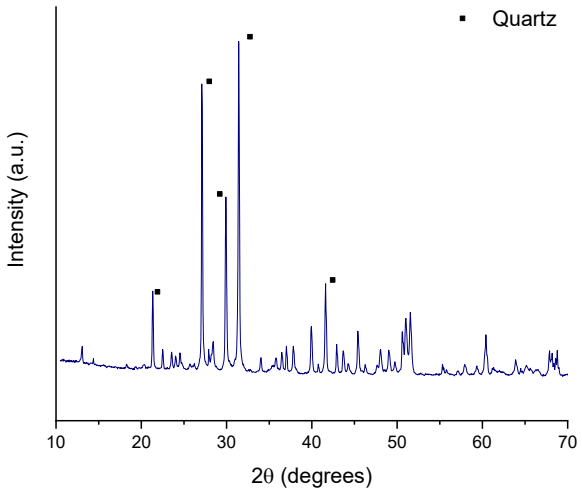

Figure 1.6: Diffractogram of natural siliceous sand used as filler.

The production of filled geopolymeric inks is the same as seen previously, but in this case filler powder is poured in the mixing solution right after the dissolution of PEG. To produce these kinds of inks, it is needed lot more energy for the mixing because of a higher viscosity, which results in higher rotational speed of the blade or the use of a spatula to better homogenize the slurry while mixing. Moreover, the increased solid to solution ratio gives a more solid behavior to the slurry, to keep the slurry less viscous mixing in an ice bath is needed. As a side effect, the evaporation of the water is lowered, so it is the reaction rate, giving more time to the geopolymer to be printed. After mixing, the filled syringes are stored in a refrigerator for about 30 minutes, this helps to achieve a more uniform paste with filler more homogenized inside the geopolymer. Finally, the ink is ready to be printed.

1.2.3 Composite geopolymer inks

As seen for the filled geopolymer inks, these ones are made starting from geopolymer ink and added with different kind of fibers. Compositions and properties of fibers used are presented in tables 3, 4 and 5.

Carbon fibers: Ferrari Carbon RCF MF100, not coated, average length 100 μm, 20% vol.

Table 3: Carbon fiber characteristics given by manufacturer [71].

RCF MF100	
Carbon content (%)	100
Fiber diameter (avg. μm)	7.5
Fiber length (avg. mm)	100
Fiber density (g/cm^3)	1.8
Tensile strength (MPa)	3500
Elastic modulus (GPa)	230
Elongation at break (%)	1.5
Coating (%)	0
Apparent density (bulk Kg/dm^3)	0.50

Mineral fibers: Lapinus Rockblade RB215 – Roxul 1000, not coated, average length 150 ± 25 μm, 20% vol.

Table 4: Mineral fiber composition given by manufacturer [72].

Chemical Analysis		
	Min. (% wt.)	**Max. (% wt.)**
SiO_2	38	43
Al_2O_3	18	23
CaO + MgO	23	28
FeO	4.5	8
$K_2O + Na_2O$	-	4.5
Others	-	6

Table 5: Mineral fiber characteristics given by manufacturer [72].

Parameter	**Average / Tolerance**	
Non-fibrous material	Norm.	Max.
	N > 125 μm	0.08%wt.	0.2%wt.
Fiber length	150 ± 25 micron	
Ignition loss	Max. 0.3%wt.	
Moisture content	Max. 0.1%wt.	
Fiber diameter (mass. wt. avg.)	Approx. 9.0 micron	
Fiber diameter (num. avg.)	Approx. 5.5 micron	
Specific surface area	Approx. 0.20 m^2/g	
Hardness	6 Moh	
Melting point	> 1000°C	
Specific density	2.73 ± 0.15 g/cm^3	
Colour	Grey/Green	

The method of preparation is the same as of filled geopolymer inks, but with fibers instead of fillers.

1.3 Direct Ink Writing of geopolymeric inks

Geopolymer pastes have an intrinsic pseudo-plasticity which make them usable in 3D-printing. Their rheology is non-Newtonian, they are thickening materials with initial yield stress, as they can be referred as Bingham fluids. The technology involved is a direct ink writing (DIW) process based on the deposition of an infinite extruded filament in a layer wise form, so it is very important to have an ink with initial yield stress high enough to maintain the desired shape and to sustain the weight of subsequent layers.

1.3.1 Equipment

The equipment used are two different 3D-printers (figure 1.7), both originally working as fused deposition modelling printer for polymeric material, but equipped with syringes for paste extrusion:

- Cartesian printer: Powerwasp Evo FDM, Wasproject, Massa Lombarda, IT, lateral resolution of 120 μm, Z resolution of 4 μm, the extrusion of the paste is possible by a mechanical piston actioned by a stepper motor;
- Delta printer: Powerwasp Delta 2040 Turbo, Wasproject, Massa Lombarda, IT, layer resolution of 50 μm, the extrusion is made by an infinite screw that pushes the paste provided by a pressurized vessel containing the material.

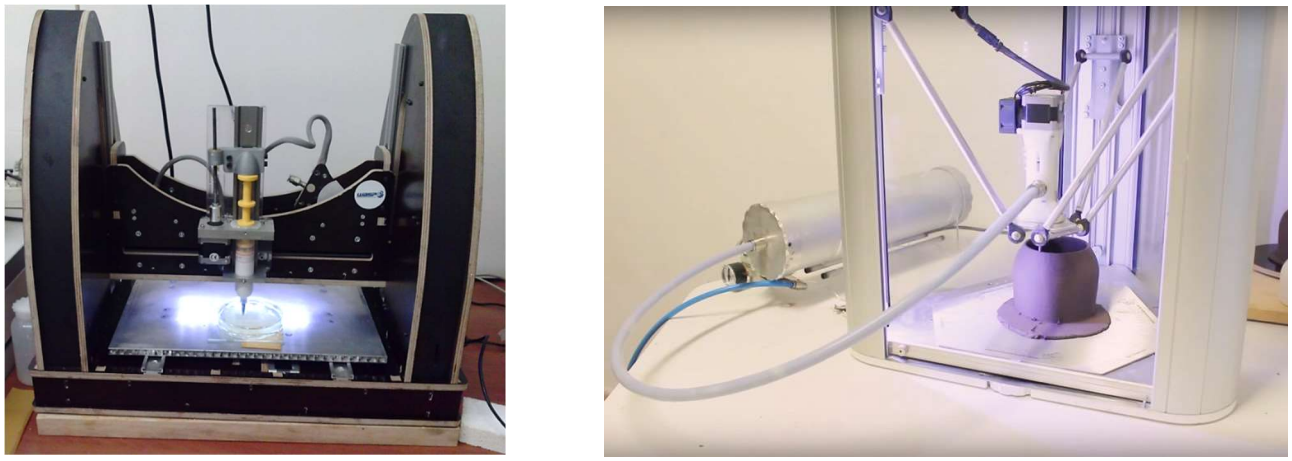

Figure 1.7: Printers used to produce samples: (left) cartesian; (right) delta.

The extrusion conical nozzles (Nordson Italia S.p.a., Segrate, IT) chosen have diameter of 840 μm, made of polypropylene, and are mounted on the end of the syringe, in the case of the first printer,

or at the end of the extrusion chamber, for the latter one. It should be noted that, even if the Evo printer is listed as a part of the equipment, it is used only for the production of pure geopolymer samples and to first evaluate the amount of rheological agent needed to be added to the slurry. This because of the high viscosity reached by adding PEG and PAA, pressure only driven extrusion is no more efficient, as at higher pressure geopolymer tends to separate from water, extruding mostly all the water first and then the dried geopolymer, greatly reducing the possible production time. Moreover, the stepper motor, which has to push the piston, cannot generate pressure high enough, resulting in extreme overheating. That is the reason why the process changed from the Evo to the Delta printer. The screw driven extrusion is more efficient in term of profile pressure, the filament undergoes the same pressure through its section, pressure value, greater than that obtainable with Evo printer, and uniformity of the paste, which is mixed inside the extrusion chamber by the screw spinning. This is particularly suitable for using inks with added fillers, such as fine aggregates or fibers (i.e. composite inks).

1.3.2 Samples geometry

The geometry of the samples design changes based on the mechanical test needed. Two structures are printed for compression and 3-point bending tests, both trabecular:

- For compression tests: 20.00 x 20.00 x 7.20 mm^3 lattices, 12 layers (figure 1.8);

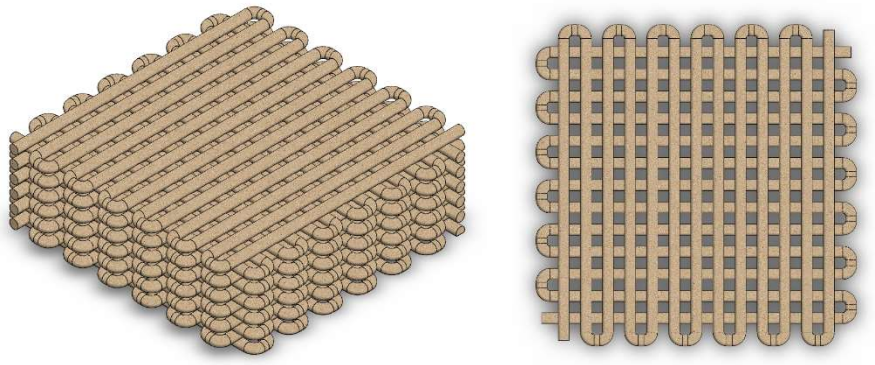

Figure 1.8: Digital model of samples used in compression test.

- For 3-point bending tests: 8.00 x 6.00 x 90.00 mm^3 lattices, 10 layers (figure 1.9), based on the fixed designation ASTM C1161 – 18 “standard test method for flexural strength of advance ceramics at ambient temperature”.

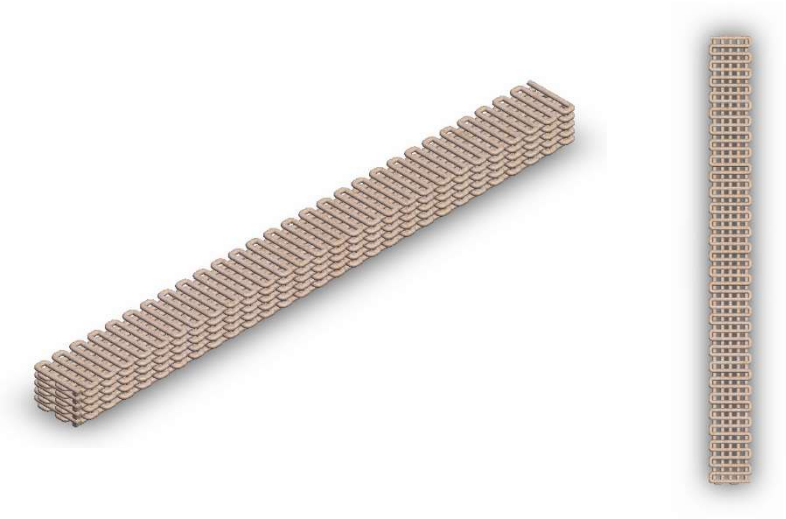

Figure 1.9: Digital model of samples used in 3-point bending test.

Filaments diameter is set as the nozzle's one at 840 μm, every layer is 600 μm height, to provide a small overlap causing a better adhesion with subsequent struts. The filaments alignment is 0-90°, with gaps set at 1600 μm. This is a simple geometry but gives the possibility to the operator to understand inks behavior while printing, so it is possible to quickly change printer parameters to produce better samples. Moreover, it is possible to understand if a paste is suitable to this kind of production, otherwise its composition could be tunable.

1.3.3 Printing Parameters

It should be noted that, as geopolymers are subjected to an ongoing reaction of polycondensation, i.e. geopolymerization, their rheology changes with time, in what can be seen as a 4D-printing process, where the fourth dimension is the time of reaction. As results will show, viscosity increases as the sample is produced. One of the solutions to minimize the problem is to optimize the rheological behavior over time. But, still, the paste, even if very slowly, continues to react anyways. This can be an obstacle to a successful printing, that could lead to differences onto final samples, such as weight, geometry and defects distributions. That's why, during the printing process, the presence of an operator is necessary in order to change the printing parameters, when required:

- Feeder pressure: the pressure used to force the paste into the extrusion chamber;

- Screw rotational speed: the rotation speed of the infinite screw that pushes the ink towards the nozzle;
- Filament deposition speed: the printhead movement speed.

Usually, the time of production for each sample ranges from 3 to 4 minutes, depending on the geometry. After the production, samples are sprayed with an alcoholic solution, to prevent high evaporation rate, sealed in boxes and treated thermally.

1.4 Thermal treatments

Like all cementitious materials, geopolymers also need time to set and to develop all the mechanical characteristics. A common geopolymer develops its maximum mechanical strength after setting for about a month at room temperature, as the same as cements. Previous studies [73] state that by varying the curing conditions, in terms of temperature and duration, it is possible to obtain a better mechanical resistance than that which would occur at room temperature.

A geopolymer at room temperature shows an amorphous structure. The process of crystallization allows nucleation and growth of crystalline domains and so the possible conversion from a preceramic to a ceramic material.

1.4.1 Curing

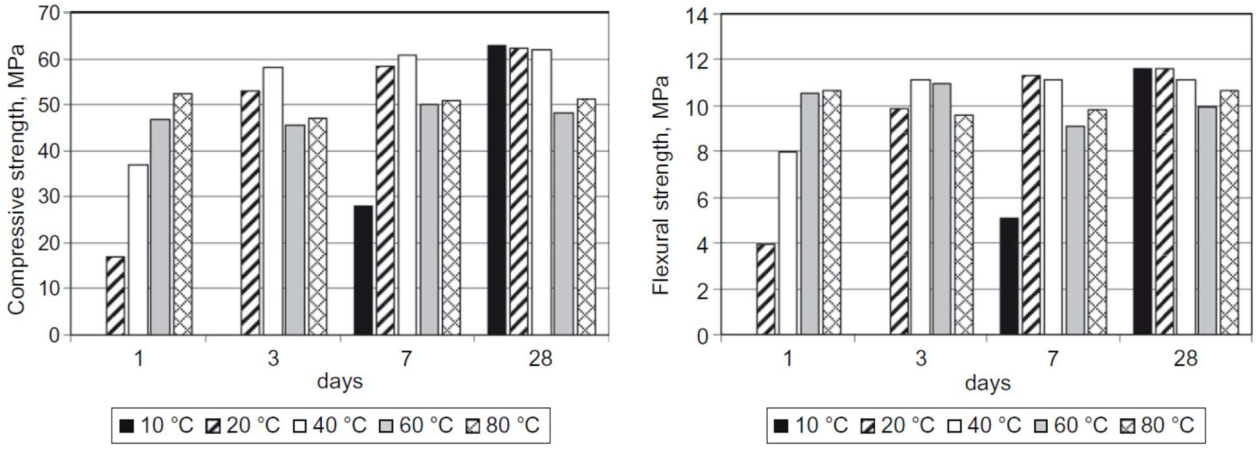

Figure 1.10: Development of compressive and flexural strength cured at 10, 20, 40, 60 and 80°C over different times 1,3,7 and 28 days [73].

The final object of curing heat treatment is the development of the highest mechanical resistance trough sustained heating at a given temperature for the needed time. Figure 1.10 shows that

varying temperature and time of treatment means having noticeable differences in term of mechanical performance, as showed there is nearly a 20% of difference between samples cured at 20°C (i.e. room temperature) and the ones treated at 80°C, for a period of one week [73].

To maximize the mechanical properties, two different temperatures of curing are chosen after literature, 40 and 80°C with a baseline comparison at room temperature, i.e. 25°C, for two different period of time, 1 day and 7 days. After the production, samples are sealed and stored in a furnace, already at the targeted temperature, to undergo the curing heat treatment.

1.4.2 Firing

Firing is called the second heat treatment with temperatures higher than curing. Samples are previously cured at 80°C for 1 day in order to make them manipulable and stable. This treatment is done to investigate how mechanical properties change with increasing temperatures, as geopolymers are completely amorphous at room temperature, but they crystalize at high temperature. As previously said, the structure reference for the geopolymer used in this work is nepheline, but it's not pure, it has some different ratios on the composition and impurities that could affect its behavior over temperature.

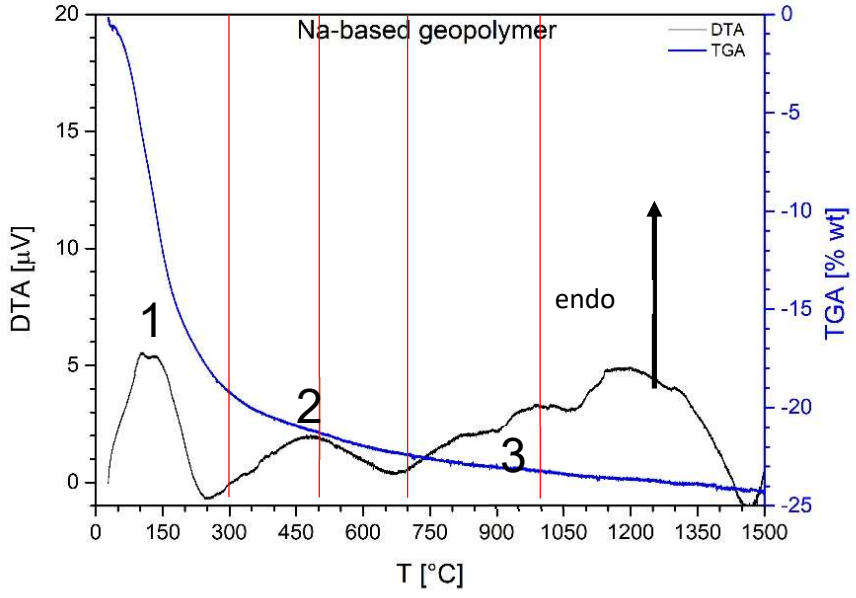

Figure 1.11: Thermal analysis of GP 13 geopolymer; the 3 major peaks are listed; red lines highlight treatment temperatures.

Firing heat treatment temperatures are chosen after the DTA analysis on the pure geopolymer (figure 1.11). As can be seen, the diagram has 3 different peaks, 2 of those endothermic and the last one exothermic:

1. First endothermic peak at around 150°C, that is the loss of physical water, that is the water released during the formation of the geopolymeric network structure, the so called physiosorbed water;
2. Second endothermic peak at around 450°C, the elimination of crystalline water, that is part of the structure and is chemisorbed by the condensation of -OH groups;
3. Last peak, exothermic, at around 900-1000°C, corresponds to the crystallization of the structure, in this range of temperatures nepheline crystals begin to nucleate and grow.

It is possible to see another endothermic peak after 1000°C, in fact at 1200°C the sample melts, hypothesis also supported by a fast treatment that was performed on the geopolymer at 1500°C. Once the treatment was over, the material appeared melted.

So, based on these considerations, 4 different temperatures are chosen:

- 300°C;
- 500°C
- 700°C;
- 1000°C.

The heating program is set as follows (figure 1.12):

1. Heating step: heat rate of 1°C/minute from room temperature to target temperature;
2. Dwelling step: dwelling of the selected temperature for 60 minutes;
3. Inertial cooling step: the furnace is switched off, the chamber is kept closed and the temperature decreases slowly.

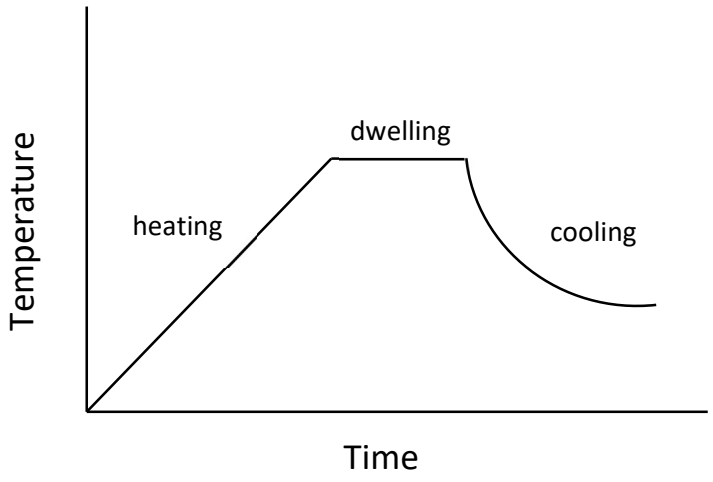

Figure 1.12: Firing treatment heat program.

The duration of each step is adequate for a low water evaporation rate, a higher one can cause the formation of big cracks on samples and their break into pieces. Treatments last differently from a temperature to another, generally for the one at 300°C the overall duration is around 6 hours, for 500°C 9 hours, 700°C 12.5 hours and for 1000°C the total treatment duration is 17.5 hours. This without considering the last step, as it is variable, because it is based on the heating chamber refractory tiles thermal inertia.

1.5 Methods of characterization

This section can be subdivided into two different sections based on the material status: the first one is the inks, the second the samples characterization. The inks characterization includes the rheologic analysis of the freshly made geopolymer, the samples characterization includes mechanical, chemical, optical and thermal analysis performed on 3D-printed lattices after heat treatment.

1.5.1 Inks characterization

1.5.1.1 Rheological characterization

Inks rheology is being analyzed through all the research work period and with different rheometers, to ensure consistency to data collected. 3 different rheometers are used:

- Anton-Paar MCR 302, at the department of Civil Engineering (ICEA), University of Padova, Padova, IT;
- Thermo Scientific Haake Mars III, at the Research and Development laboratories of ITT Motion Technologies S.p.a., Barge (CN), IT;
- Malvern Kinexus Pro+, at the laboratories of Saint-Gobain Research Provence (SGRP), Cavaillon, FR.

The equipment used on the rheometers are the same plate-plate geometry with stainless-steel scratched spindle, designed for high viscous materials, 25 mm diameter. Test parameters are set as 1 mm gap and plate temperature of 20°C, all tests are carried out at room temperature.

All rheology analysis is intended to evaluate the suitability of a paste to the direct ink writing printing process, to do so several experiments are conducted:

- Steady rate sweep: shear rate increasing from 0.01 to 100 1/s;

- Dynamic strain sweep: frequency set to 1 Hz while deformation increases from 0.001 to 100% (200% in the case of filled geopolymer inks);
- Dynamic frequency sweep: deformation set to 1% while frequency increases from 0.1 to 100 Hz;
- Viscosity recovery: two steps:
    1. Constant shear rate of 1.0 1/s for 60 seconds to overcome the initial yield stress and destroy the gel network;
    2. Constant shear stress of 15 Pa for 120 seconds (up to 240 seconds for filled geopolymers) to allow viscosity recovery with a stress lower than the ink yield stress.
- Moduli recovery: two steps as viscosity recovery test:
    1. Constant strain of 10% with 1 Hz frequency (up to 70% strain for filled geopolymers) for 60 seconds;
    2. Constant strain of 0.1% with same frequency for 120 seconds (240 for filled geopolymers.

To evaluate if a paste can be used as ink in DIW, the deflection of a suspended filament can be a good indicator. A printable ink has to have high initial yield stress, as previously said, but also the possibility to withstand its own weight when suspended and to not undergo gravity induced deformation. The stiffness of an unsupported filament can be evaluated by the Smay et al. [40] equation (1):

$$G' \geq 0.35\, \gamma\, s^4 D$$

where γ is the specific weight of the ink, which is given by its density multiply by the gravitational constant, s is the reduced span distance (2):

$$s = \frac{L}{D}$$

where L is the length of the unsupported filament, from two support points, and D the filament diameter, which is set at 800 µm, less than the nozzle tip diameter (840 µm) because some elastic shrinkage is considered, for an easy comparison between different inks (figure 1.13).

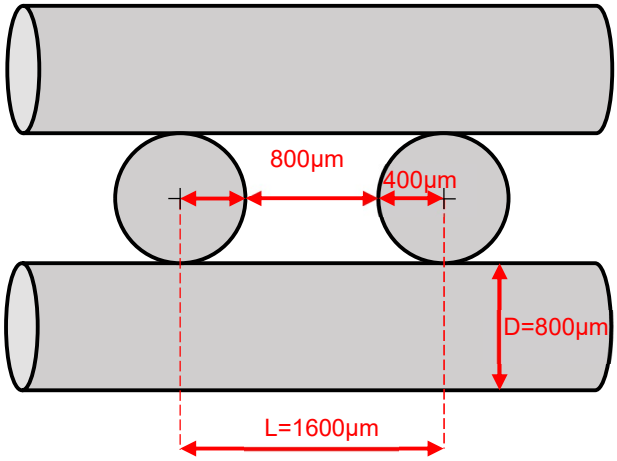

Figure 1.13: Filaments dimensions.

The behavior of a viscous-elastic material is given by the values of the storage modulus G' and the loss modulus G'', the first tells about the elastic characteristic, the second the viscous flow. The equation (1) is a condition on G' on the possibility of having a < 5% gravity deformed suspended filament, if G' << G'_s (i.e. G' calculated with the Smay equation (1)) then the ink is printable, but if G' ≈ G'_s a suspended structure will probably collapse. Moreover, the rheology behavior of a pseudo-plastic Bingham fluid is time-dependent, so it is its viscosity, which is affected also to the geopolymerization degree. Normally, the ink is extruded at high shear rate and low viscosity, but once is deposited to form the layer pattern its viscosity should quickly increase, to minimize the deflection from a support point to the following one. Schlordt et al. [36] were able to connect the deflection $z(t)$ with the paste viscosity $\eta(t)$ (3):

$$z(t) \approx \frac{1}{2}\sqrt{L(t)^2 - L_0^2}$$

where L_0 is the beam initial length and $L(t)$ is the beam time-dependent length (figure 1.14), which can be express as follows (4):

$$L(t) = L_0 \left(1 + \int_0^t \frac{\rho \, g \, L_0}{6 \, \eta(t)} \, dt \right)$$

with ρ ink density, g gravitation constant and $\eta(t)$ ink time-dependent viscosity.

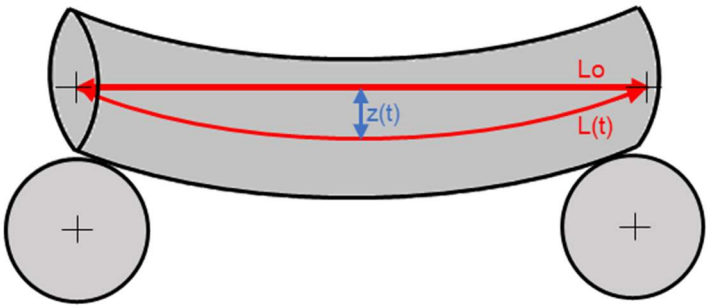

Figure 1.14: Filament deflection.

1.5.2 Samples characterization

1.5.2.1 Uniaxial compression test

Samples tested have geometry plant view of a square with 20.00 x 20.00 mm^2 dimensions. Machine used is an Instron 1121 UTM (Instron, Norwood, MA, USA), with a 10 KN load cell, for the signal digitalization Spider 8 digitalizer (Hottinger Baldwin Messtechnik, Darmstadt, Germany) is used and software Catman (Hottinger Baldwin Messtechnik, Darmstadt, Germany) is used to record data, crosshead speed set at 1 mm/min. The samples compression strength is calculated by (5):

$$\sigma = \frac{F}{S}$$

where F is the maximum compression stress at break and S the value of the surface area in contact with the plates. Hypothetically, S should be 400.00 mm^2, but during production and heat treatments the samples dimensions may vary due to printing issues, like incorrect values of pressure, printing speed or screw rpms, or to thermal shrinkage during drying.

Samples tested are:

- GP 13 PEG, GPS, GPGP after curing and after firing;
- GPMF and GPCF after firing at 300°C;
- GPCF after curing at 80°C for 1 day.

At least, 5 samples for each measurement are tested to have statistical consistency.

1.5.2.2 3-point bending test

According to norm ASTM C 1161 – 18, flexural strength is investigated on samples with 8.00 x 6.00 x 90.00 mm^3 dimensions. Testing machine used is the same Instron 1121 UTS with same digitalization hardware and recording software, equipped with 3-point bending tools, crosshead speed of 1 mm/min.

To evaluate the flexural resistance is used the following mathematic expression (6):

$$\sigma_f = \frac{3}{2}\frac{F\,L}{b\,h^2}$$

where F is the peak load at break, L is the distance between the two support points, b the width and h the height of the sample as shown in figure 1.15.

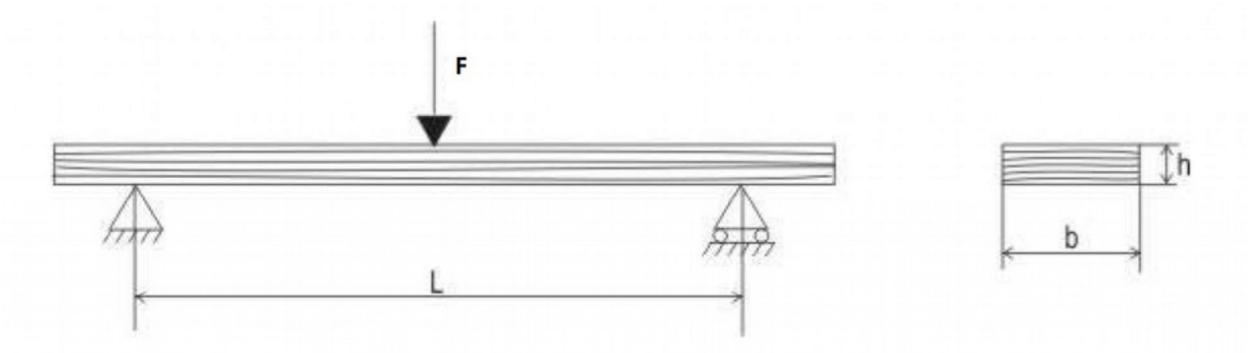

Figure 1.15: Representation of specimen dimensions for bending test.

Samples tested are:

- GP 13 PEG, GPS, GPGP and GPCF after curing at 80°C for 1 day;

At least, 5 samples for each measurement are tested to have statistical consistency.

1.5.2.3 Porosity

The density of a material can be affected by the presence of voids in the structure. These points of discontinuity on the bulk material constitute its porosity, which can be subdivided in two types:

- Open porosity, *OP*: the pores are interconnected;
- Closed porosity, *CP*: the pores are isolated and don't form any connection between them;
- Total porosity, TP: the overall porosity of the sample, open and closed porosities considered.

From this distinction three different classes of density can be determined:

i. Geometric density ρ_g: generally named volume density or bulk density. The sample volume is determined by the measurement of its dimensions using a digital caliper (error 0.05 mm) and its mass with a digital balance (error 0.0001 g);
ii. Apparent density ρ_a: measured with a helium pycnometer (Micrometrics AccuPyc 1330, Norcross, GA, USA) on structures fragments. Compared to the previous measurement, the gas has the possibility to penetrate all the open porosity, therefore it does not include it in the volume measurement. Inserted on the pycnometer cell, a pump creates void to introduce helium inside the sample open porosity, because of the helium less bulky molecular structure than air;
iii. True density ρ_t: like apparent density, is measured with the same helium pycnometer, but instead of using fragments, it uses finely grinded powder to allow the elimination of closed porosity.

Using the densities data, it is possible to calculate the percentage of open (7), closed (8) and total porosity (9) as follows:

$$OP = \frac{\rho_a - \rho_g}{\rho_a} \cdot 100$$

$$TP = \frac{\rho_t - \rho_g}{\rho_t} \cdot 100$$

$$CP = TP - OP$$

1.5.2.4 X-Ray diffraction

The analysis is done thanks to a diffractometer Bruker AXS D8 Advance (Bruker Corp., Karlsrhue, Germany), with a Cu-Kα filament radiation and θ-2θ configuration, operating at 40 kV and 40 mA with 0.05° step width, scanning range from 10° to 70° speed of 3 seconds for each step. Samples investigated are GP 13 PEG, GPS and GPGP after curing at 80°C for 1 day and after firing crushed and powered, to see the evolution of the microstructure through temperature. The crystalline phases identification is possible using the Match! (Crystal Impact GbR, Germany) software with ICDD PDF-2 (International Center for Diffraction Data, Newton Square, PA, USA) database.

1.5.2.5 Thermal characterization

Thermogravimetry and differential scanning calorimetry (TGA/DSC 3+, Mettler-Toledo, Columbus, OH, USA) are performed to pure geopolymer powder, previously cured at 80°C for 1 day, to see the thermic behavior and typical temperatures. Analysis conditions are 5°C/min to 1500°C in static air. Heat treatments are designed around data collected from this analysis.

1.5.2.6 Optical characterization

3D-printed lattices morphology and microstructure are investigated using an optical stereomicroscope (STEMI 2000-C, Calr Zeiss AG, Oberkochen, DE) and an environmental scanning electron microscope (ESEM, Quanta 200, FEI, Hillsboro, OR, USA) at different magnifications to better understand pores and cracks distribution and toughening mechanism in GPCF.

1.5.2.7 Chemical characterization

Punctual chemical analysis is done by EDX (Energy-Dispersive X-ray spectroscopy) probe equipped on the aforementioned ESEM. With this equipment is possible to recognize impurities and differences in chemical composition and to identify every element present.

Results and discussion

Partially published in: Franchin, G., Scanferla, P., Zeffiro, L., Elsayed, H., Baliello, A., Giacomello, G., Pasetto, M., Colombo, P.: Direct Ink Writing with Geopolymeric Inks; J. Eur. Ceram. Soc. 37 (2017), 2481-2489

In this chapter experimental data collected during the research work are shown and discussed.

2.1 Geopolymer rheology optimization

Two inks based on the same sodium-based geopolymer are analyzed and optimized to see which one suits best for direct ink writing printing process. Geopolymers added with rheology agents are called inks, data collected are compared to non-optimized geopolymers, which are pure geopolymers without the addition of rheology agents. The geopolymers are all based on Davidovits patent number 4,472,199 [74], with difference in water contents only. PAA added geopolymer and the geopolymer itself is used as comparison, as this ink is already in use in the labs of the Ceram Glass Research Group of the University of Padova.

The second sodium-based ink is added with PEG as rheology agent, its water and PEG content have to be optimized prior to its use in 3D-printing. This kind of optimization is based on a try-and-error approach, as the only way to recognize a printable ink is to try to print it right after its production and observe if its rheologic behavior is good enough to withstand its own weight without deforming.

2.1.1 Water and rheology agent optimization

The optimization of the Na-based ink starts from a geopolymer recipe already known by adding PEG as rheological agent and tuning the water ratio.

- PEG 400 – H_2O / Al_2O_3 = 14.0: Firstly, 2 wt% of PEG 400 is used in a geopolymer mixture with a water ratio of 14. The gel that formed isn't so strong, but PEG works very well. Then, the amount of PEG is increased to 5 wt%. The geopolymer formed a good gel, and it was possible to use the system as a printable ink.

Figure 2.1: Samples printed with PEG 400 5% wt. and water ratio = 14.0; sample above is printed before the one below.

The ink is easily printable by the cartesian printer and it lasts about half an hour, but there are some problems during printing and with the stability of the results. As it can be seen in the pictures (figure 2.1), there is volumetric shrinkage that leads to internal cracks and different geometric deformation between the two samples, which were produced on the same day. In fact, the high water content of the geopolymer, during the printing, leads to an extrusion of the water first, and then of the geopolymer. But, when the water is all extruded, the mixture inside the printer reacts very quickly, and the viscosity increases as well.

- PEG 400 5% wt. - H_2O / Al_2O_3 = 13.5:

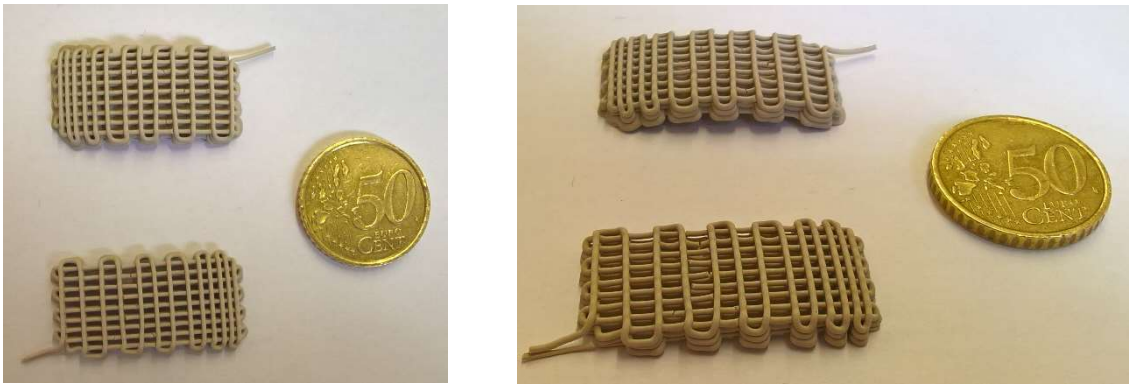

Figure 2.2: Samples printed with PEG 400 5% wt. and water ratio = 13.5; sample above is printed before the one below.

The experiments show that the samples are subjected to less shrinkage, and the results are more reliable. However, there are still problems concerning the deformation after drying and the extrusion of water during printing.

- PEG 1000 5% wt. - H_2O / Al_2O_3 = 13.5: To achieve a stronger gel structure, PEG with higher molecular weight, from 400 to 1000, was added to the mixture. The paste results more viscous with a greater tendency to keep the shape once extruded. However, there are still problems concerning the separation of water from the geopolymer when subjected to pressure.

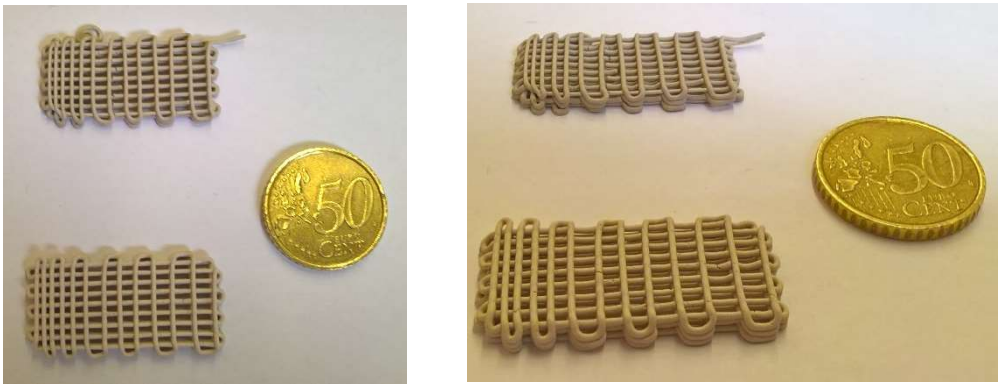

Figure 2.3: Samples printed with PEG 1000 5% wt. and water ratio = 13.5; sample above is printed before the one below.

- PEG 1000 5% wt. - H_2O / Al_2O_3 = 13: Water ratio is lowered to 13 to finally solve extrusion issues. It can observe from the picture (figure 2.4), there is less shrinkage in the printed structures, no evidence of deformation after drying and samples are more uniform through the printing time.

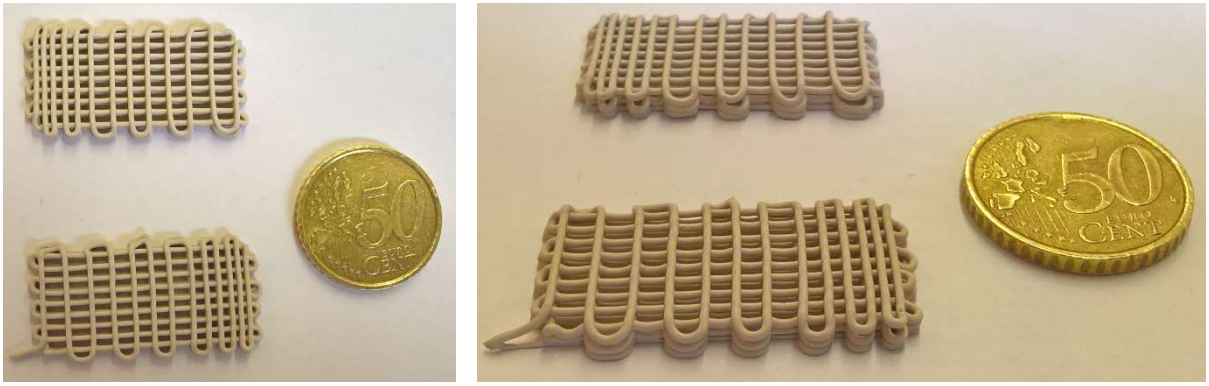

Figure 2.4: Samples printed with PEG 1000 5% wt. and water ratio = 13; sample above is printed before the one below.

However, the viscosity of this last ink is already too high for being extruded by applying only pressure, as the extrusion system of the cartesian printer could do, so, from now on, it will be used the delta printer with the infinite screw extrusion equipment. As a positive side effect, the use of the screw decreases the water separation problem a lot better than just lowering the water amount.

With these initial considerations, the rheology agent type and quantity chosen is PEG 1000 at 5% wt. with a water ratio of 13, on the next paragraph this ink is named GP 13 PEG.

2.1.2 Rheological characterization of pure geopolymers and geopolymer inks

In this paragraph, rheologic behaviors of pure geopolymers GP 13.78 and GP 13 and their inks derived GP 13.78 PAA and GP 13 PEG are compared and analyzed with the methods seen in chapter 2.

Rheology studies the correlations between internal forces with external ones in solids and fluids. Internal forces are driven by particles friction and can generate a counterforce to the viscous flow. In the case of geopolymers, the greater the induced deformation, the greater the tendency of these particles to align themselves to oppose less resistance to the flow. Geopolymeric structure is a three-dimensional network that forms through polycondensation of -OH groups, firstly with the formation of oligomers, then with formation of bridges between neighboring molecules. During the initial reaction of geopolymerization, geopolymeric slurries behave as a weak gel.

Previous studies on metakaolin-based [57] and fly-ash based [75] geopolymers compared the slurries rheology behavior with aqueous suspensions of clay particles, and it has been demonstrated how these materials, when freshly made, have light shear thinning behaviors with low initial yield stresses, and their pseudoplastic behavior can change with solid content. Increasing the quantity of solid particles inside the slurry, both initial yield stress and fluid viscosity can be enhanced. However, the same article cited [57], demonstrated the possibility to even change geopolymer mixtures behavior from shear-thinning to shear-thickening. The addition of organic compounds to the mixture can be used as rheology modifiers to enhance their Bingham behavior, make these materials finely optimizable for the use in direct ink writing.

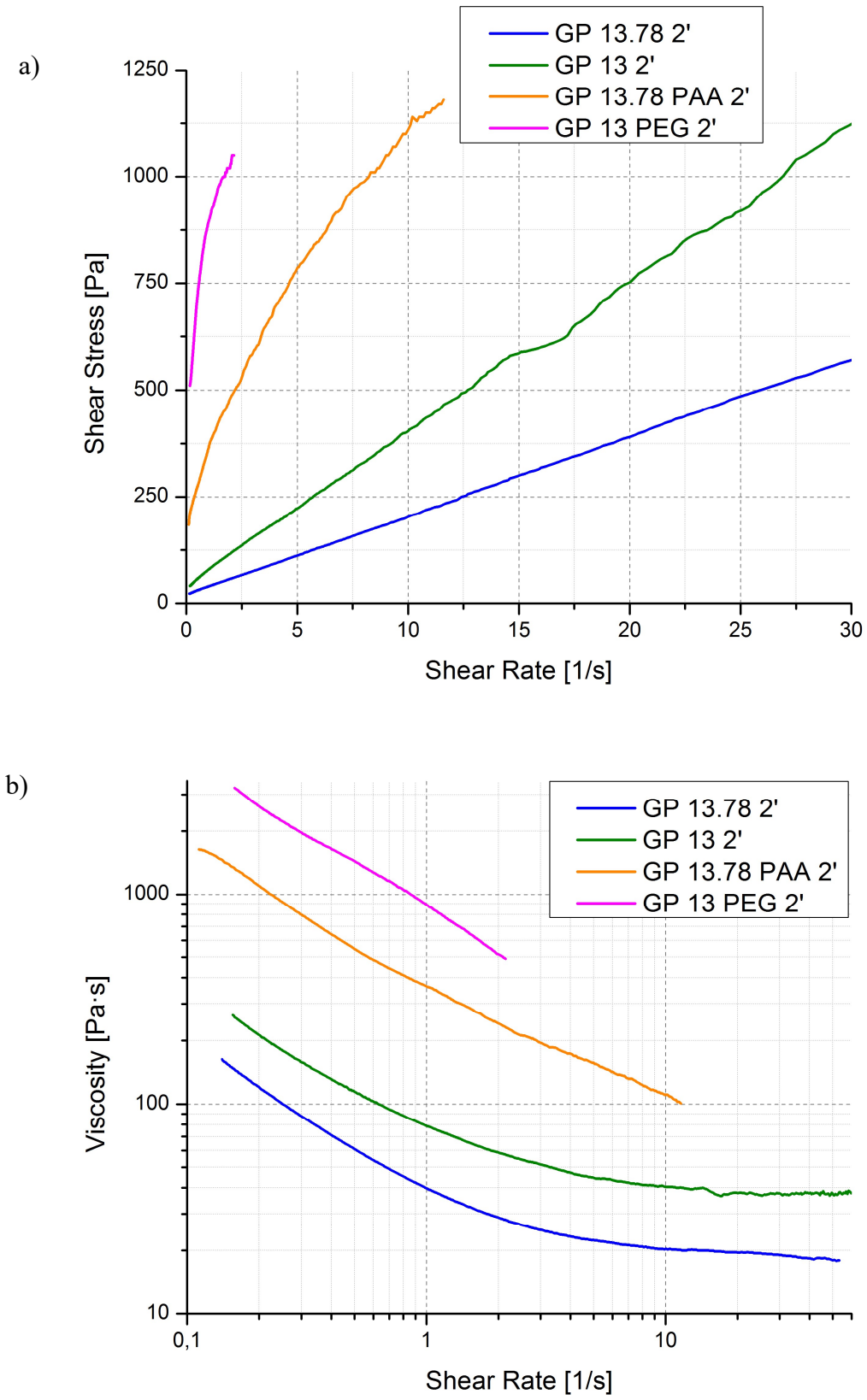

Figure 2.5: Steady rate sweep test: a) Flow curves; b) Viscosity curves.

Figure 2.5 shows the flow (a) and viscosity (b) curves obtained with the steady rate sweep for the four geopolymers after 2 minutes from their production. It can be noted that the inks curves are

interrupted earlier than pure geopolymers ones, especially for GP 13 PEG, because of the lack of adhesion between pastes and rheometer plates, as from mid to high shear rate values the inks tends to leak and be expelled; therefore, only short segments have been plotted, but they can explain the overall rheological behavior of the inks.

Bingham shear-thinning behavior is confirmed for all geopolymers as their viscosity decreases with the increasing of shear rate, pure geopolymers reach a viscosity plateau at 10 1/s with viscosity values of 20 Pa s for GP 13.78 PAA and 40 Pa s for GP 13. The difference in water content, higher on the GP 13.78 side, translates into differences in viscosity and initial yield stress, higher on the GP 13 side. During the test, the breaking at increasing shear stresses of alumino-silicate bonds that continuously form from an oligomer to the next one could be the explanation of this behavior. Inks have higher viscosity through all the shear stress values range and higher values of yield stress than pure geopolymers. In GP 13 PEG shear thinning behavior is enhanced by two sides: low water ratio and presence of PEG, that forms a stronger gel network.

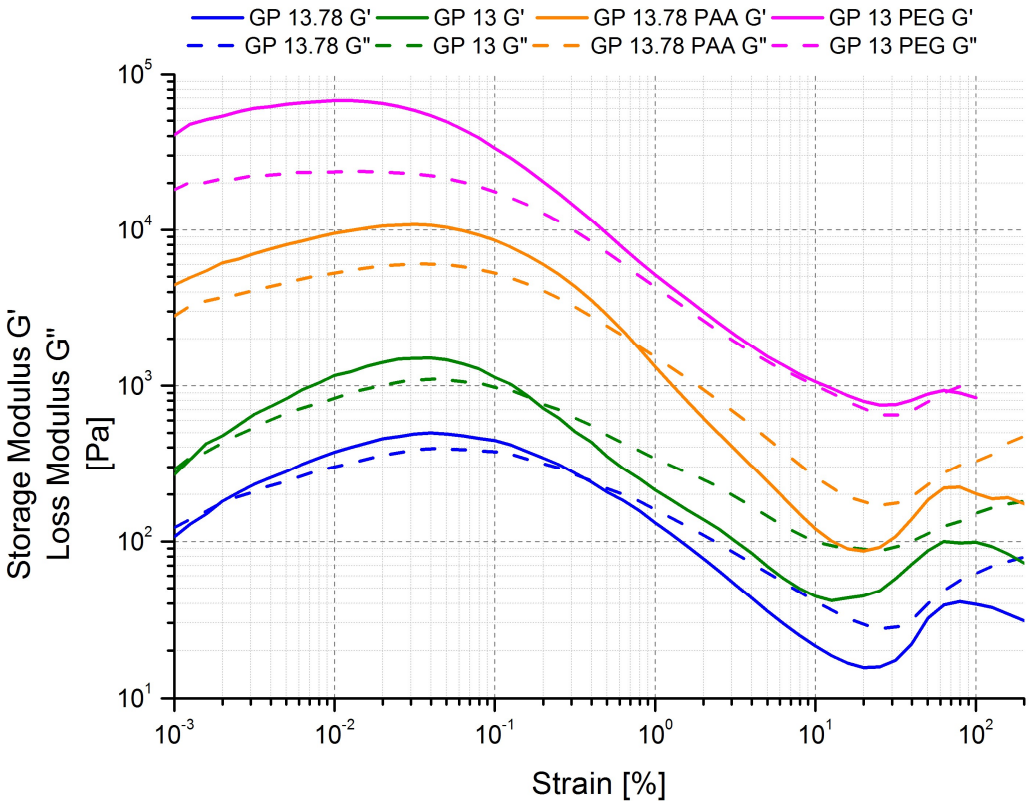

Figure 2.6: Dynamic stress sweep test on the four geopolymers.

The dynamic sweep test results in a diagram (figure 2.6) with G' and G" plotted as a function of strain %. As shown, all the materials, geopolymers and inks, behave similarly and three different zones can be recognized:

1. At low strain (from 10^{-3} to 10^{-1}%) G' and G" slightly increase with the strain, G' > G", materials behave like an elastic solid;
2. At intermediate strain (from 10^{-1} to 10^{1}%) G' and G" decrease rapidly, with different slopes G' quicker than G", and they intersect, transition from elastic to viscous;
3. At high strain (from 10^{1}%) modules stabilize, G" > G' allowing the flow.

This kind of material can be described as a reversible gel: the initial elastic behavior is given by the geopolymer network formation, that can be broken and destructured by stresses above yield stress (τ_y), then the viscous behavior emerges allowing the flow. The transition from elastic to viscous in these kinds of materials is gradual, so yield stress values are determined by the intersection of G' with G" curves. This method results in a more conservative way to determine τ_y values compared to ones seen in literature, for which τ_y is the τ value at G' = 0.9 $G'_{(eq)}$ [40].

As seen for the steady sweep test, pure geopolymers show lower values of the yield stress and their gel network seems to be weaker than inks ones. Also, in this case, the difference in water ratio means a translation of G', G" and ty to greater values. However, the two geopolymers don't have large differences on their rheological behavior. On the other hand, GP 13.78 PAA and GP 13 PEG differ more on G', G" and ty values. For the inks, their rheology is modified and their Bingham pseudoplasticity is demonstrably enhanced, that's because they have to be suitable for DIW meaning that these inks should be able to sustain suspended structure without deforming under gravity and retain the shape once the filament is extruded.

Table 2.1: Values of initial yield stress and comparison between G' collected and G' obtained with the Smay equation for the four geopolymers.

	GP 13.78	**GP 13**	**GP 13.78 PAA**	**GP 13 PEG**
τ_y (Pa)	1.5	2.5	20	80
G'_{max} (Pa)	500	1500	108000	67200
G'_S (Pa)	390	397	341	382

Table 2.1 shows in detail the values of initial yield stress (t_y) and G' (G'_{max}) collected with dynamic strain sweep tests, the value of G'_{max} is the maximum value obtained from the diagram in figure 2.6. Comparing G'_{max} with G'_S, the latter calculated from the Smay equation (1), the differences in printability can be understood. As the G'_{max} is greater than G'_S so it is the suitability to DIW, meaning that all four geopolymers can possibly be used as ink, but GP 13.78 and GP 13 are close to

their limits in term of shape retention and filament stiffness. Considering that rheology agents are added to the geopolymeric mixtures in low quantity, 7% wt. and 5% wt. respectively for PAA and PEG, their impact on rheology behavior of the two inks is dramatic.

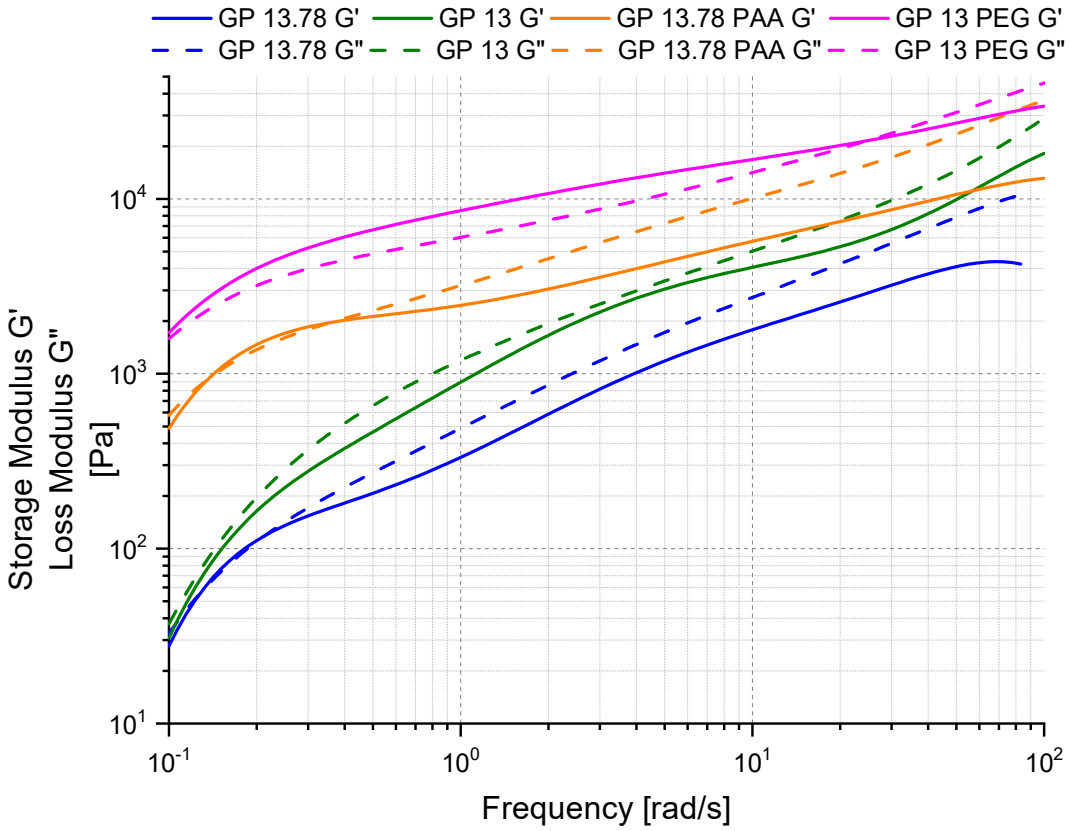

Figure 2.7: Dynamic frequency sweep test performed on the four geopolymers.

Strain sweep tests alone cannot determine the reversible gel nature of a material, therefore, to further analyze the geopolymers, dynamic frequency sweep tests are conducted. Figure 2.7 reports the dynamic frequency sweep curves for the four geopolymers. All geopolymers are beyond their crossover point, as G' and G" increase throughout the frequency range considered. This can be explained considering the pastes as soft gel or weakly bonded dispersion, but also as poorly interconnected geo-oligomers, that have already started to grow and form some entanglements with other molecules. As diagram in figure 2.7 shows, pure geopolymers are over the transition point, with G" > G' for the whole frequency range, in the other hand, inks present the transition, from elastic to viscous region, at some point. For GP 13.78 PAA this transition can be detected at around 0.3 rad/s, for the other ink, GP 13 PEG, the transition point is at around 20 rad/s. This make the PEG added ink more useful for DIW, as it has a wider rubbery region that leads to better workability in an extrusion-

based production process [76]. Anyways, these tests have confirmed the typical reversible gel behavior for all geopolymers and inks.

The typical printing process consists in a continuous filament deposition, this filament has to be extruded from the printing nozzle and to maintain the shape given. So, one of the most important features that a printable ink should have is the shape retention, that is the ability to quickly recover the viscosity, crossing the point of transition from viscous to elastic region, when the stress is no more applied.

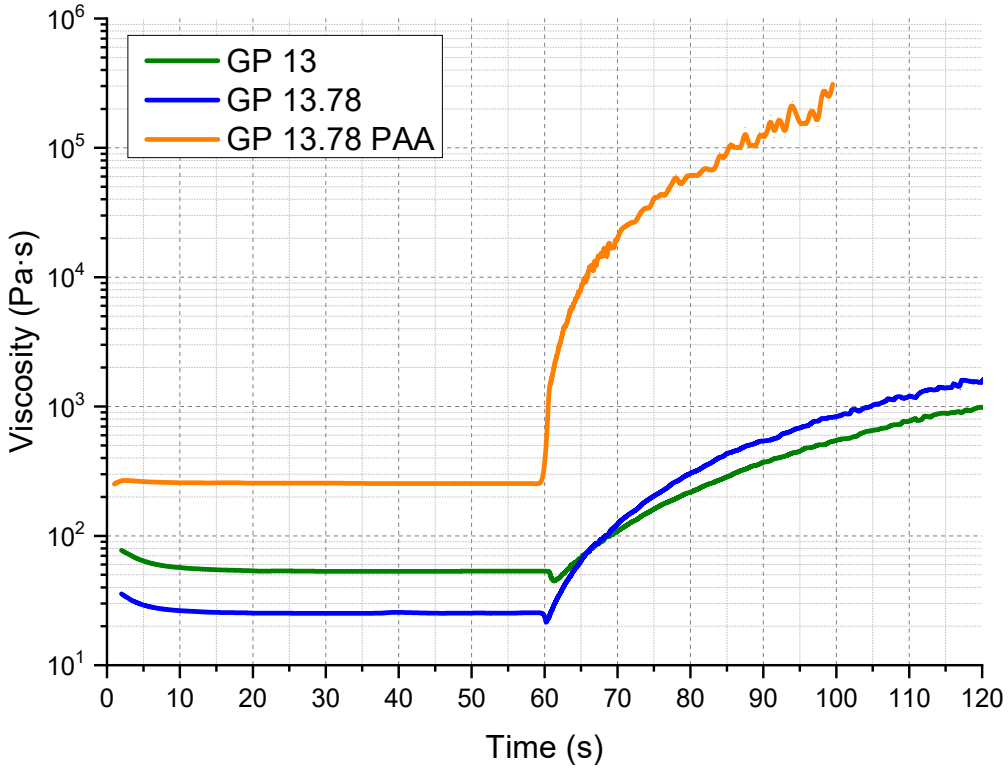

Figure 2.8: Viscosity recovery test performed on GP 13, GP 13.78 and GP 13.78 PAA

In figure 2.8 is reported the diagram of viscosity recovery test performed on GP 13, GP 13.78 and GP 13.78 PAA, the PEG added ink is not listed in the results because of the aforementioned problems of adhesion with rheometer plates, during the first 60 seconds of test, in which a constant deformation is induced to the paste to break the gel structure, the ink tend to leak. As can be seen, all geopolymers tend to recover their viscosity, however, pure geopolymers take more than 20 seconds to recover viscosity but for only one order of magnitude, this is not acceptable for the mechanism of production proposed. On the other hand, GP 13.78 PAA recovers its viscosity more quickly than pure geopolymers, starting from a higher value it recovers by two orders of magnitude on the first 20

seconds of the test second step, quickly reaching a plateau value. This confirms its suitability in the DIW printing process, as the fast viscosity recovery give the possibility to print stiffer suspended structures with more defined geometries.

Schlordt equation (3) permits to evaluate the midspan deflection in the middle of a suspended filament, this calculation is based on the previous one, as the value of η(t), viscosity as a function of time, is considered after 20 seconds on the recovery test, during the low shear step. The spanning distance is set at 2.4 mm, as for the final sample production, the calculated deflection are 9 mm for pure geopolymers, meaning a deflection of over 1000% as the height of the filament is 840 µm, and 0,19 mm for GP 13.78 PAA, deflection of 22,6% confirming its suitability on DIW for printing accurate structures.

To compare these results with GP 13 PEG ink the same test is conducted but in oscillatory mode. The results shown in figure 2.9 are plotted as G' and G" as functions of time.

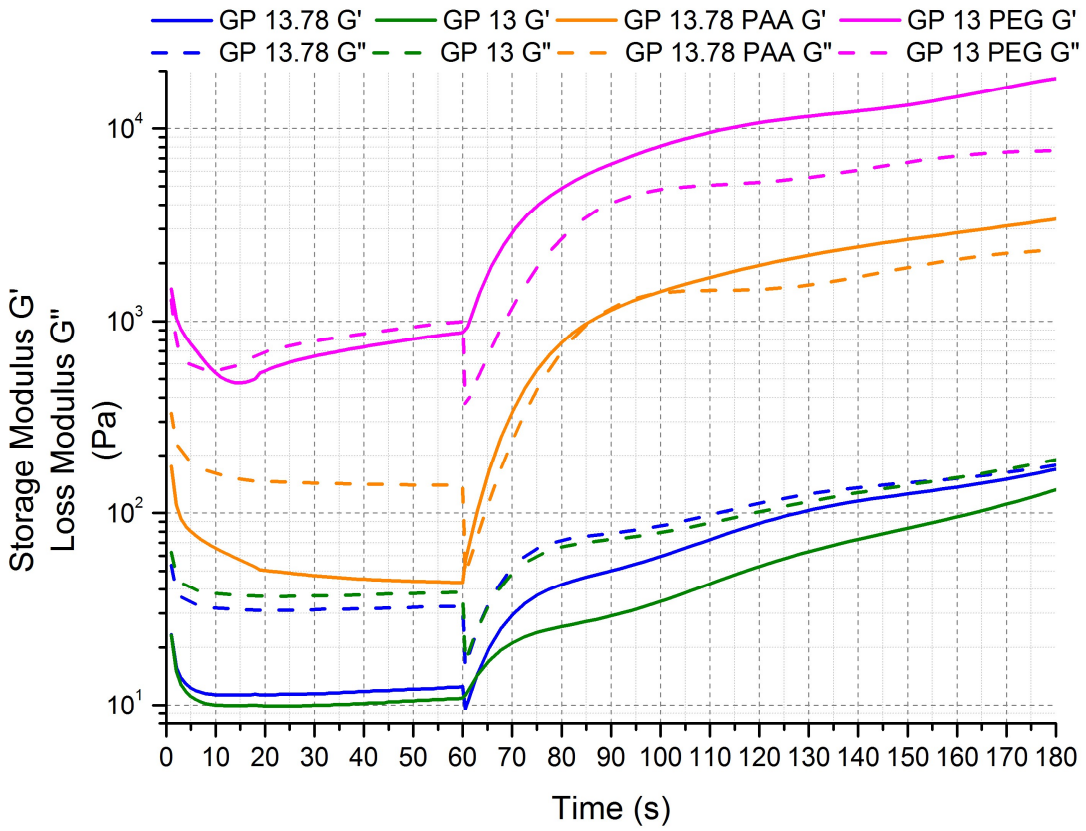

Figure 2.9: G' and G" recovery test performed on the four geopolymers.

The behavior of all four inks are comparable to ones of the previous test. Pure geopolymers start with more or less the same values of loss and storage moduli, the addition of rheology modifiers lead to higher values of G' and G", and thus to higher stresses to overcome the initial yield stress and

allow the flow, as it is already confirmed by previous tests. Especially for PEG added geopolymer, the strain applied during the first step is double compared to that needed to disrupt GP 13.78 PAA ink gel network. The second step of the test shows the difference in the behavior while inks are recovering, on GP 13 PEG G' >> G" meaning a more elastic behavior after extrusion, thus a material keener to retain the shape with lesser deflection. Unfortunately, the Schlordt equation (3) is impossible to apply in the case of GP 13 PEG, but, giving the results of these tests, its deflection can be estimated as lower than the GP 13.78 PAA one. Comparing the slope of the recovery curves during the first 20 seconds of the second step, geopolymers with higher water content seem to recover more quickly and to higher orders of magnitude, a mechanism not yet understood.

Another main feature ceramic printable inks should have is a wide process time, especially for geopolymers, which are subjected to a constant reaction of polycondensation, i. e. geopolymerization. Therefore, working time test (figure 2.10) shows the behavior of the pastes over time and their comparison between them as a G' and G" functions of time diagram.

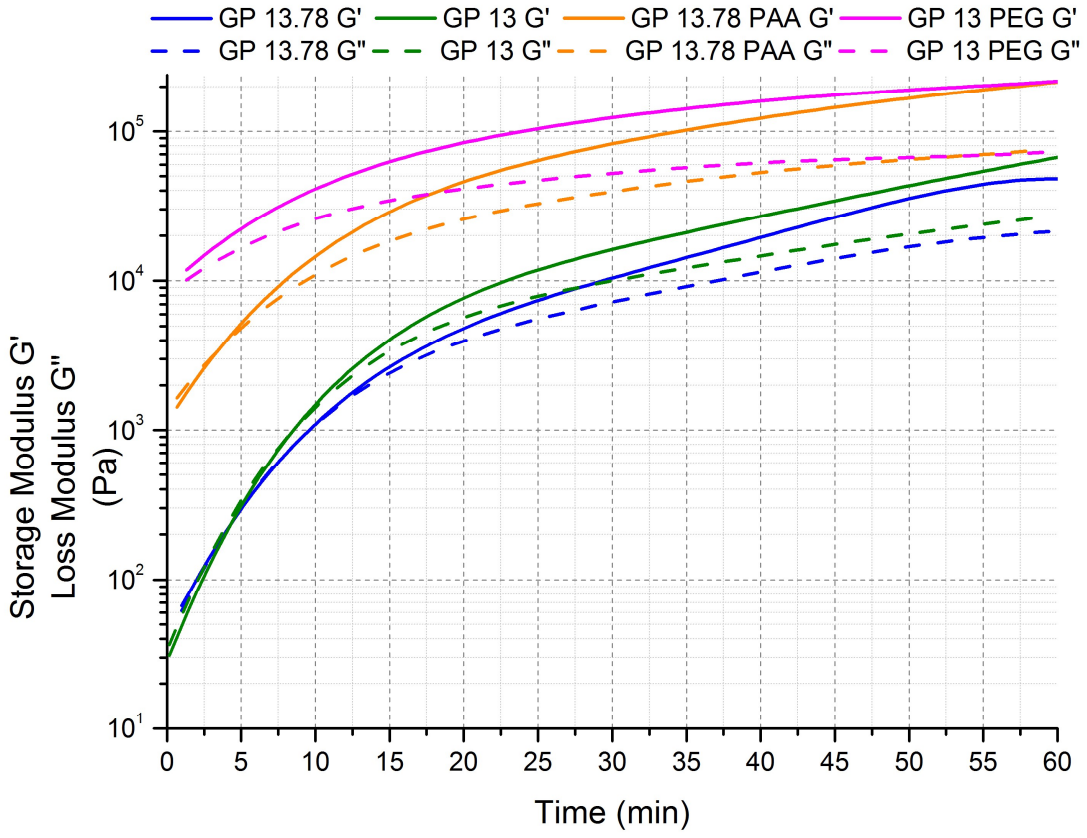

Figure 2.10: Working time test performed on the four geopolymers.

All geopolymers have a similar behavior, with increasing G' > G" over the whole test duration. This is due to the reaction of geopolymerization, geo-oligomers bond with near molecules to form

the tridimensional network increasing the gel strength and its elastic behavior. The slight difference between the two pure geopolymers are to attribute to their water content, GP 13 behave more elastically than GP 13.78, which has more water and thus lower values of G' and G". The curves slope in the initial 10 minutes can be associated to the magnitude of the reaction rate, in fact, pure geopolymers reach a higher degree of geopolymerization than inks. Additives act also as retardants to the reaction, as their curves are significantly less steep. This can be seen especially on GP 13 PEG ink, as G' and G" are more constant over time, they start at higher values, but grow much slower than PAA added ink. The mechanism behind this phenomenon could be explained with the steric interference of the additive gel network introduced inside forming geopolymer chains as their hydrophilic behavior, which hides the -OH groups of the metakaolin, prevents water and ion diffusion needed to its reaction with the activation solution.

During the preparation of GP 13.78 PAA is noticeable the formation of bubbles inside the mixture, due to the reaction of acrylic acid, which has a slightly acid behavior, with geopolymer, that is alkaline. This leads to the formation of samples with more porosity than GP 13 PEG, meaning a loss in the mechanical performances of the final product. Moreover, the more constant behavior of the GP 13 PEG over time, with its wide plateau, made this ink the best choice for the production process of DIW, giving the possibility to produce samples without changing parameters during the production time. It was observed that with this kind of ink is possible to print up to 1 hour after mixing, after that, filaments extruded are less cohesive tending to break into pieces and don't stick with other filaments on the previous layer, because of the advance state of geopolymerization. However, further optimizations of the production process, such as ice bath mixing and refrigerator storing, gave the possibility to print for more time, at least 50% more.

2.1.2.1 Case study: geopolymer ink

The best rheological behavior is reached by GP 13 PEG ink, it is used for the production of samples and examples of what can be printed with this ink. One of the challenges of printing ceramics is the possibility to produce thin walls and complex geometries. Figure 2.11 shows the process of printing (a), while figure 2.11 (b) shows an example of structure. The production process of DIW is a good method for producing samples with unsupported structures, however it is not indicated for the realization of sharp angles, figure 2.12 give the idea of a possible box with straight perpendicular faces that form 90° corners. The ink sagging is clearly visible, as filaments cannot be stiff enough to withstand their own weight without any support point.

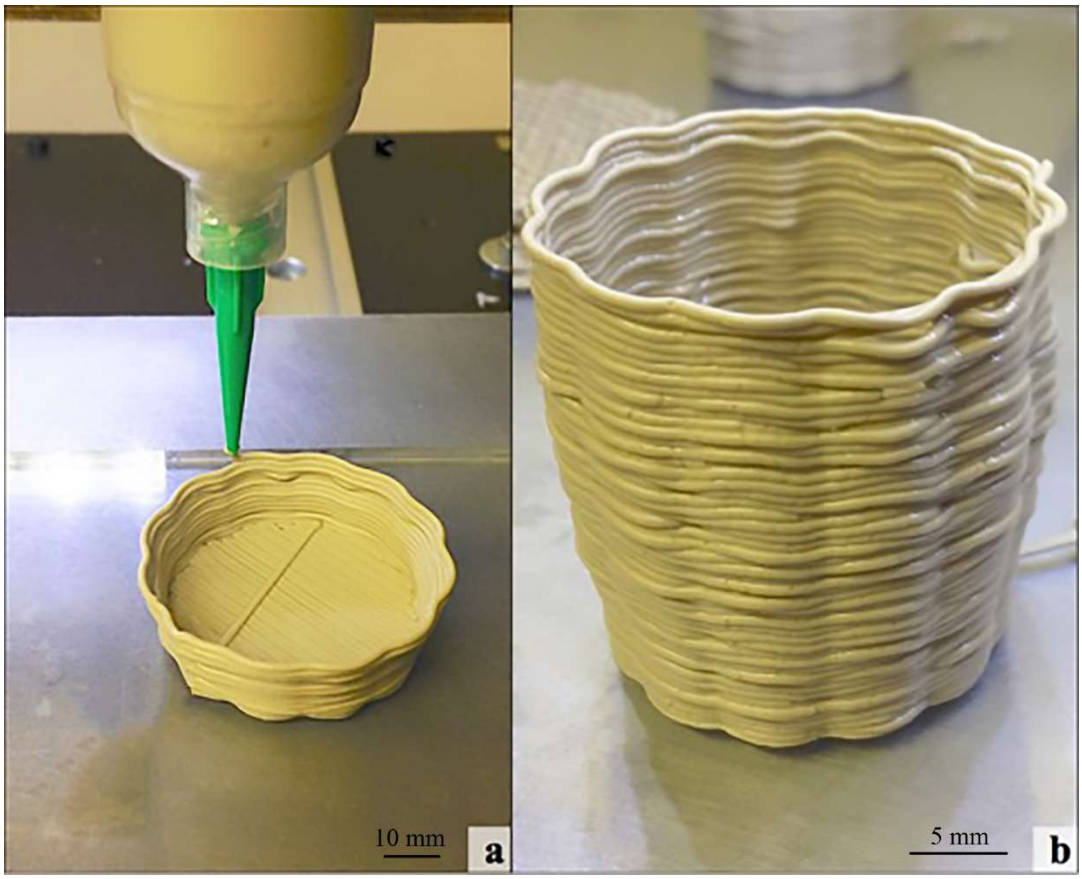

Figure 2.11: (a) printing process; (b) example of printed structure.

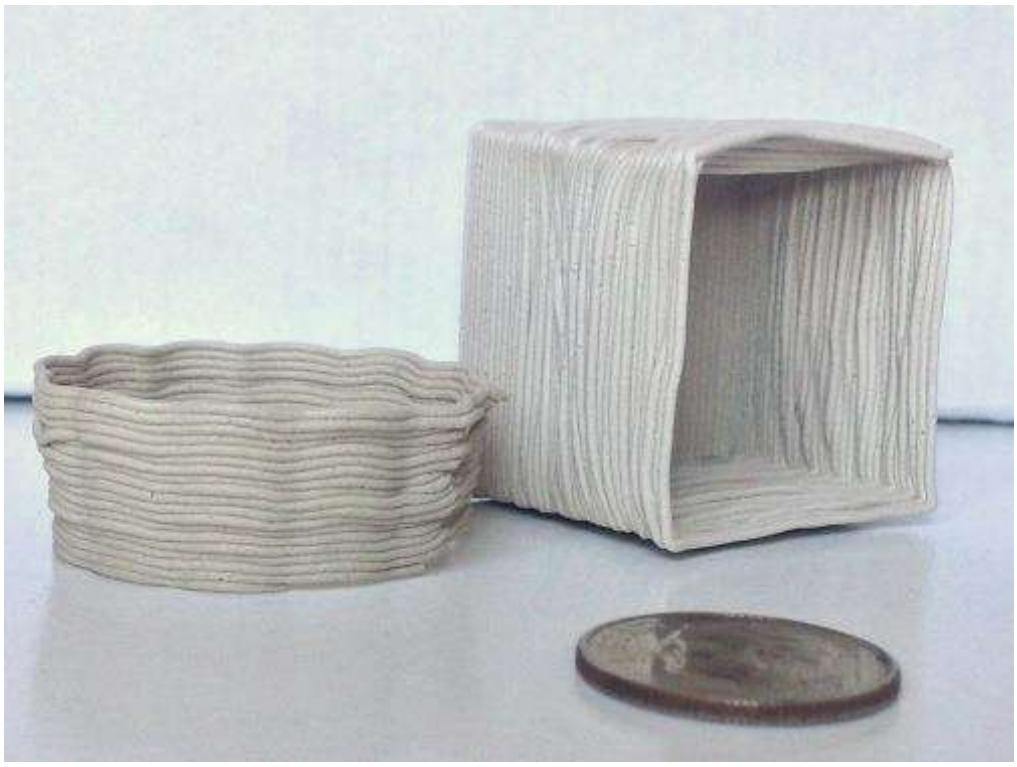

Figure 2.12: Example of structures with thin walls and sharp corners.

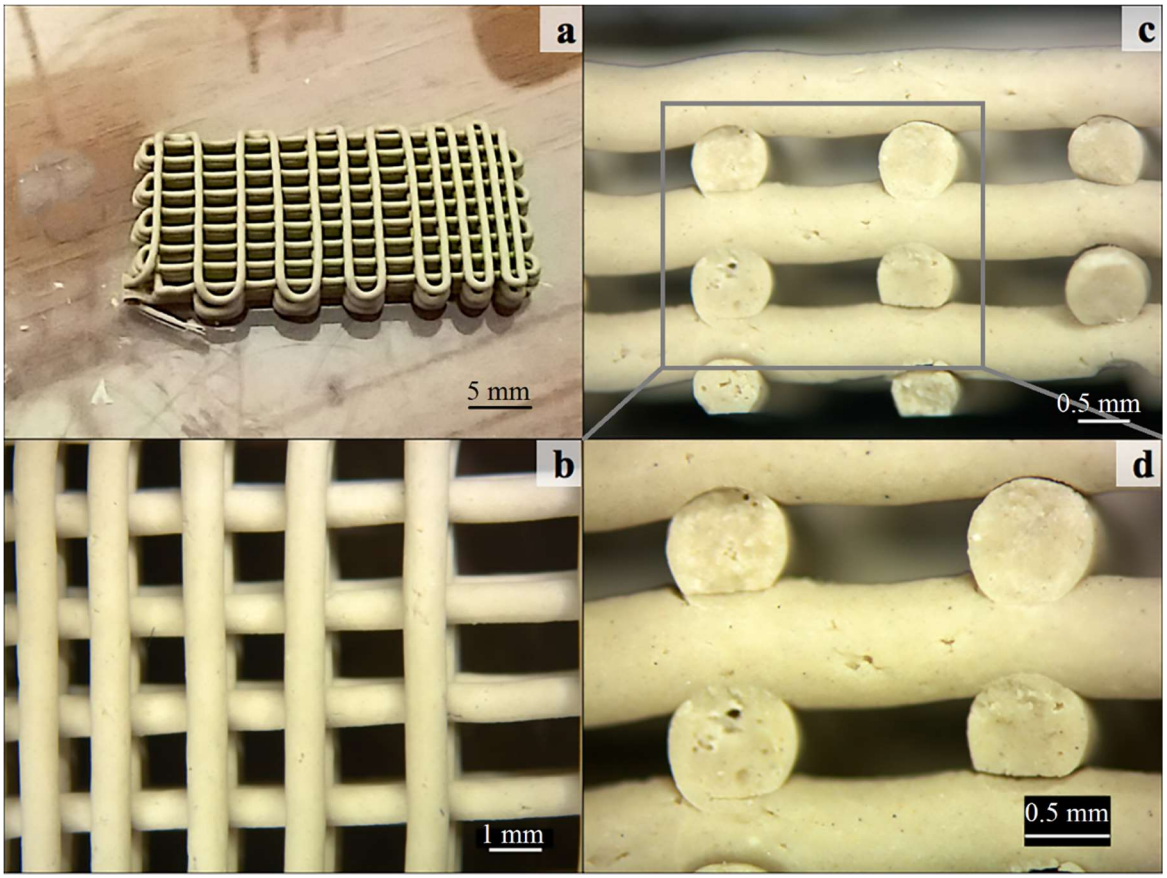

Figure 2.13: Reticular structure with increasing spacing: (a) overview, (b) top view, (c) and (d) side views.

Figure 2.13 shows a printed lattice with increasing spacing between subsequent filaments, the unsupported length increases from 1.5 mm to 4 mm with steps of 0.5 mm. The filaments show limited sagging even with the greatest spacing. The filament diameter measures 0.738 ± 0.024 mm, as it corresponds to a linear shrinkage of about 10% from the desired diameter of 0.840 mm, i.e. the nozzle tip diameter. The sagging of suspended struts is observed to be around 7% of their measured diameter, which confirms the good use of this material, thus optimized, as ink in DIW.

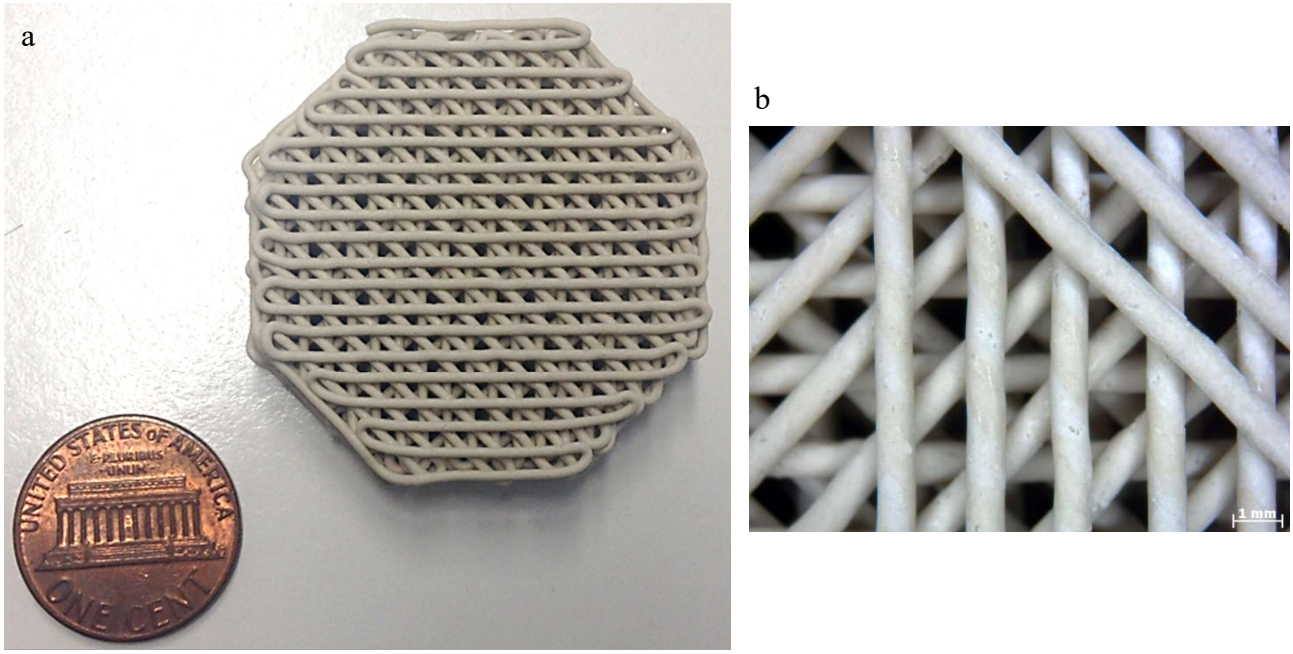

Figure 2.14: Application of a printed structure: (a) overview, (b) in detail.

A possible application, still under development in the laboratories of CeramGlass group in the University of Padova, is the production of filters for fluids treatment made of 3D-printed geopolymer. In figure 2.14 is showed a typical structure, in this case the filaments design is oriented as 0/45/90/-45° for a better filtration.

2.1.3 Rheological characterization of powder added geopolymer ink

In the previous paragraph is discussed the large difference that a minimal amount of rheology modifiers added to geopolymer pastes could make in their rheology behavior, making them more suitable for being used as inks in direct ink writing. However, even the ink with best characteristics, the GP 13 PEG, is still struggling with sagging and gravity-induced deformation. To reduce these issues and to gain better printability properties, a small amount of fine aggregates is introduced into the mixture. The powder added must not chemically interfere with the reaction of geopolymerization, otherwise its setting would be affected, as the final material will result different. In other words, the addition of powder must maintain all the chemical and mechanical characteristics of the initial ink but increasing the printability.

The initial ink, GP 13 PEG, is then added with inert inorganic powder with particle size compatible with the nozzle diameter in order to not have clogging during printing, as the extrusion of 2 or more particles at the same time is highly possible. The powder is previously dried of all water, as it interacts with the mixture changing reaction kinetics, and sieved under 300 μm, it is added as a

20% wt. The resulting ink is labeled as GPP, which stands for powder added geopolymer with 13 as water ratio and PEG as rheology modifier.

a)

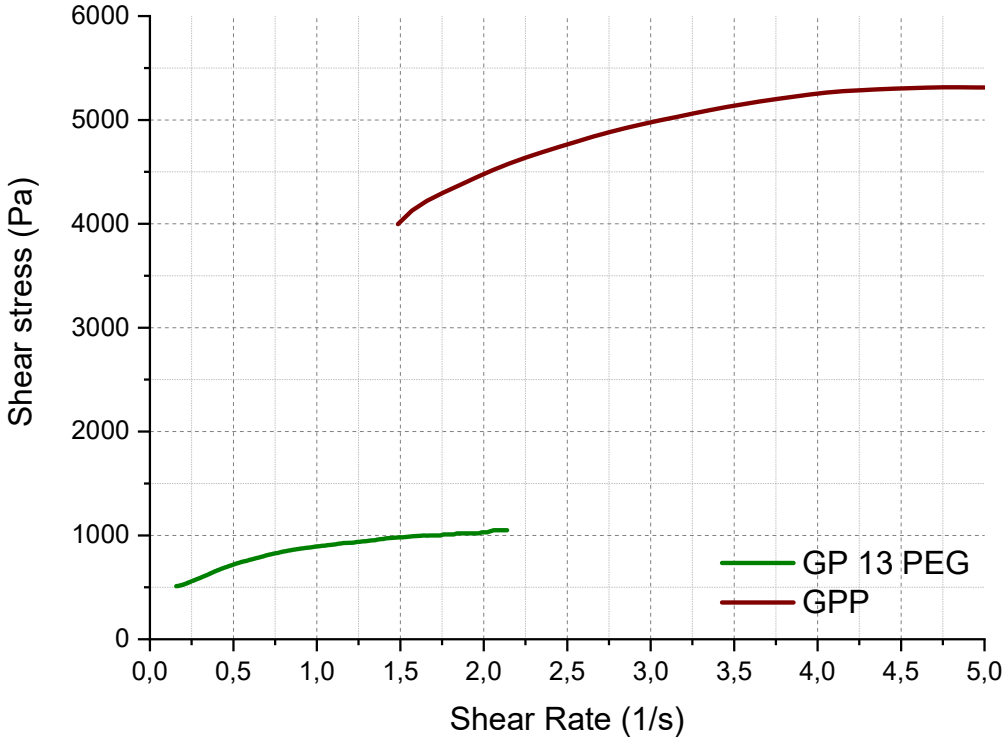

b)

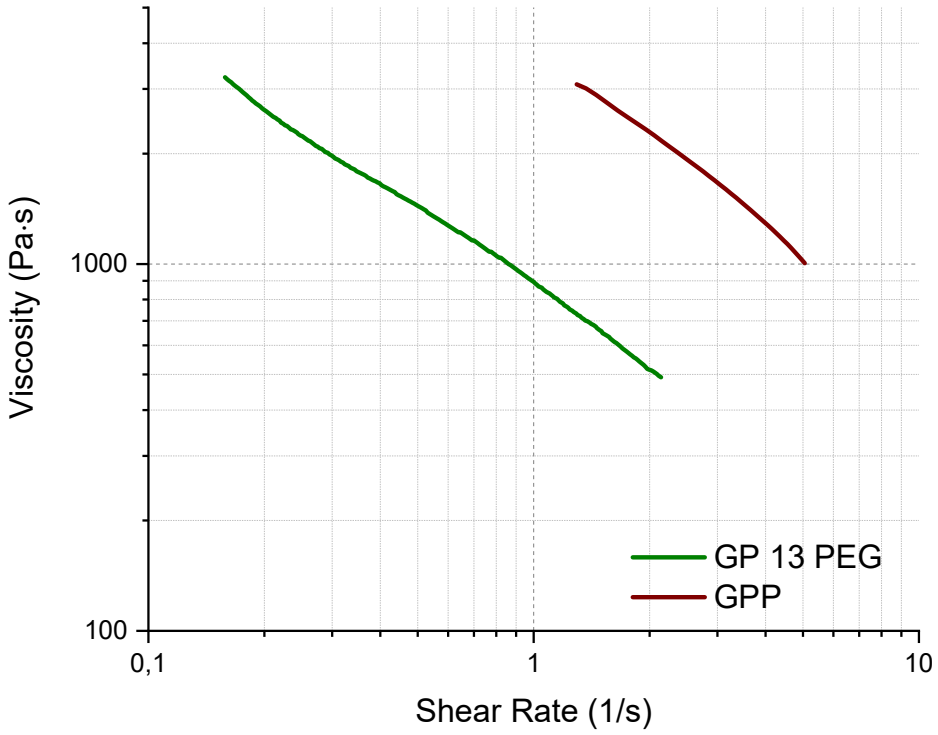

Figure 2.15: Steady rate sweep test performed on the two inks: (a) flow curves, (b) viscosity curves.

Powder added ink behave similarly to GP 13 PEG, as figure 2.15 shows, Bingham pseudo plasticity is confirmed by typical geopolymers trends of increasing shear stress and decreasing viscosity over increasing shear rate, but at greater values. Once again, only small segments of the flow curves are possible to analyze, they don't represent the overall behavior, but are significant in order to understand the tendencies. In comparison with PEG added ink, GPP possess higher initial yield stress and viscosity on similar shear rate values. Unfortunately, it was possible to record flow curves over only a small range of shear rate, from around 1.5 to 5 s^{-1}, because of the aforementioned problem with plates adhesion, but they can be significant to determine their rheological behavior. Anyways, tests in oscillatory mode have overcame this issue.

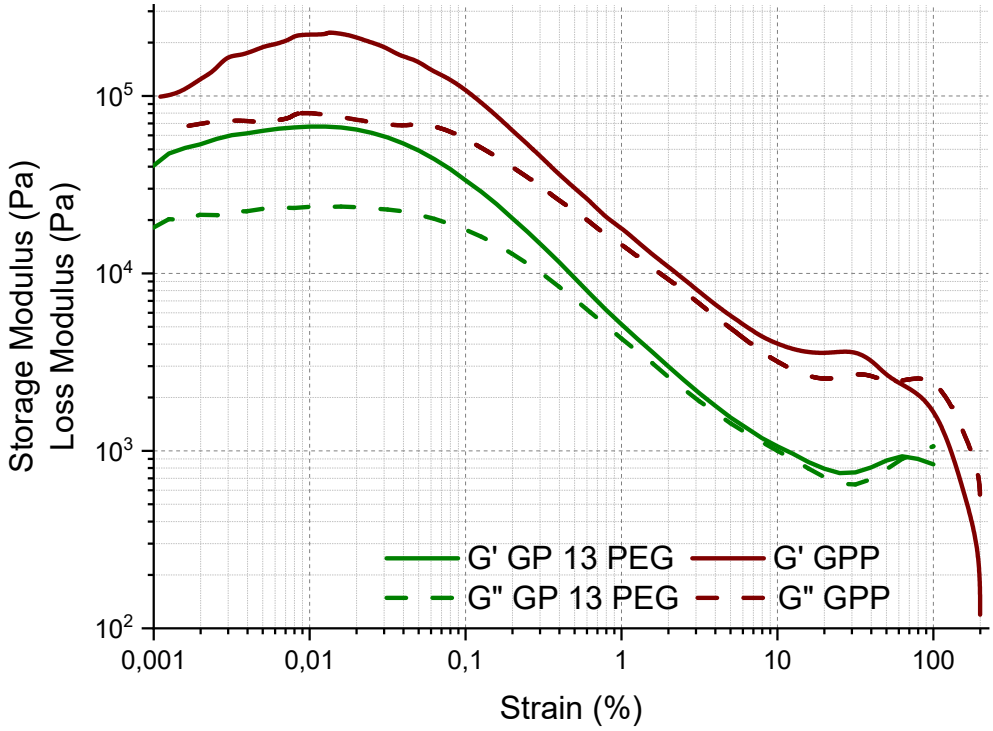

Figure 2.16: Dynamic strain sweep test performed on the two inks: G' and G" moduli over strain.

G' and G" moduli curves obtained through dynamic strain sweep tests (figure 2.16) resemble the same ones for GP 13 PEG ink, but at greater values. As it is possible to observe, at the end of the test, the GPP ink doesn't stabilize to lower values of G' and G", because of the high strain applied that even in oscillatory mode causes the same adhesion problems of continuous strain. The transition point from elastic to viscous behavior is not clear, as G' is very close to G" during the transition, thus yield stress is calculated at the point of intersection between the two curves.

Table 2.2: Values of τ_y, G'_{max} and G'_S for the two inks obtained with the dynamic strain sweep test.

	GP 13 PEG	GPP
τ_y (Pa)	80	2300
G'_{max} (Pa)	67200	234900
G'_S (Pa)	382	412

In table 2.2 are reported the values of initial yield stress (τ_y), G'_{max} given by the greatest value of G' in figure 2.16 and G'_S given by the Smay equation (1) considering D as 800 μm, L as 2.4 mm and γ as 1.73 g/cm^3 and 1.85 g/cm^3, for GP 13 PEG and GPP respectively, multiplied by g = 9.81 m/s^2. For the calculation of specific weight on GPP, the powder added to the ink was considered as quartz sand with a density of 2.76 g/cm^3. Results confirm the better suitability of GPP ink to DIW compared to PEG added geopolymer, allowing better stabilization during extrusion and much bigger suspended structure. Therefore, its high values of yield stress and G' make possible the printing of large samples with a greater number of layers than the ones printable with GP 13 PEG, because the structure won't collapse under its own weight.

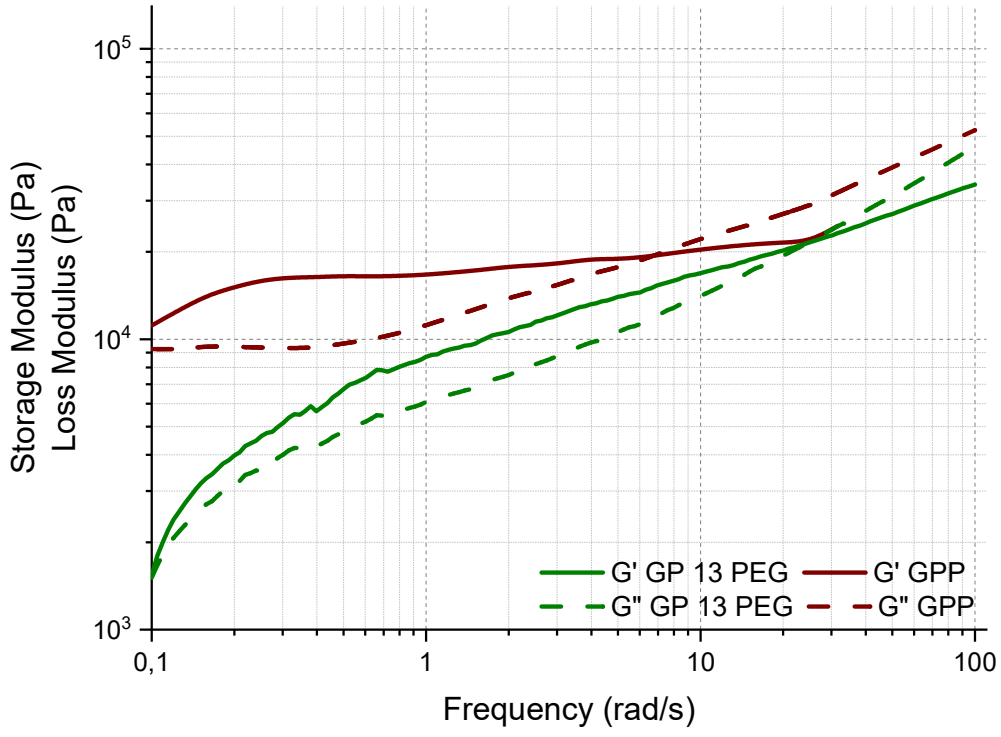

Figure 2.17: Dynamic frequency sweep test performed on the two inks.

Dynamic frequency sweep test, figure 2.17, confirms the behavior of the two inks as reversible gel. The more constant behavior of GPP over the range of frequencies considered could be caused by the presence of aggregates powder, as they are seen as elastic solid particles drowned inside the geopolymeric slurry. In fact, at higher frequency, G" curve shows a similar slope than the GP 13 PEG one, meaning that the elastic component of the ink is driven by the forces given by particles, but the slurry is responsible of the viscous flow. The crosslink point of GPP is clearer than GP 13 PEG, making the ink keener to retain the shape better after extrusion, although more suitable for DIW [76], as it has a clear division between elastic and viscous region.

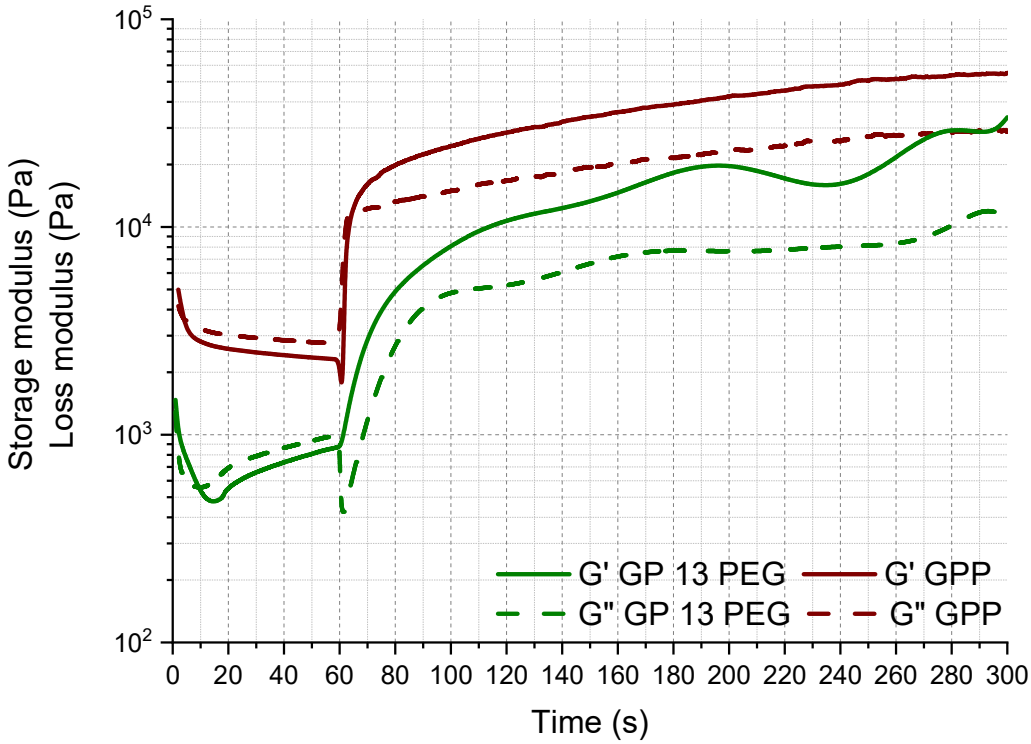

Figure 2.18: G' and G" recovery test performed on the two inks.

Recovery tests are conducted only in oscillation mode (figure 2.18), because of the same adhesion problem as previously said. For the GPP ink, in the first step a strain of 70% was needed to disrupt gel links and allow the flow, G" > G'. In comparison with GP 13 PEG, GPP starts with higher G' and G" moduli of one order of magnitude. The moduli recovery is quicker and in less than 10 seconds it recovers up to 1 order of magnitude, while GP 13 PEG needs about 20-30 seconds. The presence of solid particles inside the geopolymer could explain this phenomenon, when the second step starts and deformation stops, the particles create solid regions in which geopolymer could recover instantly, as close to these particles the material undergoes less deformation.

Due to the well-known adhesion problems, viscosity recovery test is impossible to perform on GP 13 PEG and GPP inks, but the moduli recovery test results suggest a high recovery, with very low deflections. If GP 13 PEG structure images gave a 7% deflection, it is reasonable to expect lower values for GPP.

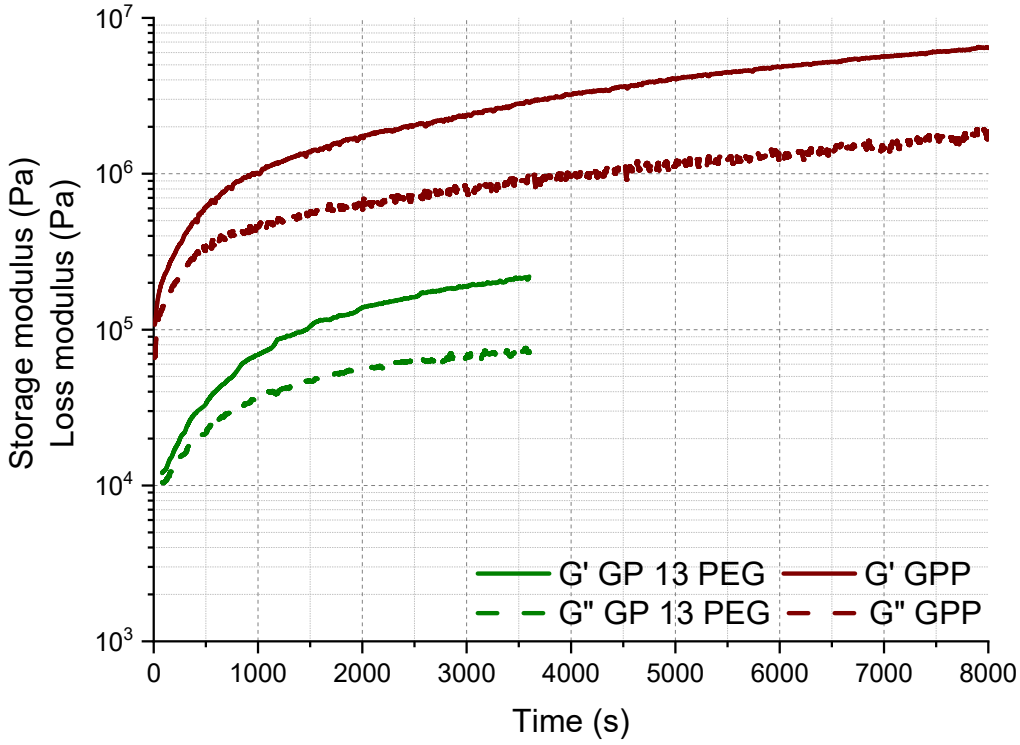

Figure 2.19: G' and G" moduli over time.

Finally, the production time is investigated by testing G' and G" behavior over time (figure 2.19). Both inks have the same trend over time, with a slight increase of G' and G" on the first minutes and then a stabilization to a more or less constant plateau. The geopolymerization occurs during all the period of time considered, but it is prominent only on the first 500 seconds, while the printing parameters has to be adjusted to maintain a constant flow, that doesn't induce inhomogeneity with what printed before. Typically, GPP ink can be printed up to 1.5-2 hours after mixing and storing in a refrigerator, compared to what seen for GP 13 PEG is 1.5-2 times more, allowing to print for longer time to produce bigger objects. Filler acts as a retardant probably because of some sort of interaction with the geopolymer matrix that slows the reaction rate. All in all, the addition of fine aggregates in the geopolymeric mixture previously optimized has made it possible to dramatically improve its printability characteristics.

2.1.3.1 Case study: sand filled geopolymer ink

The first powder used as filler added to GP 13 PEG to enhance its printability is natural quartz sand, as it is inexpensive, easy to find and doesn't require any additional process to be made. The ink is named GPS, same as GPP but with sand as powder filler. Samples printed with this ink are geometrically larger and dimensionally stable, as the addition of filler reduce sagging and shrinkage while drying. It is possible to print more complex structure with more spaced suspended filaments.

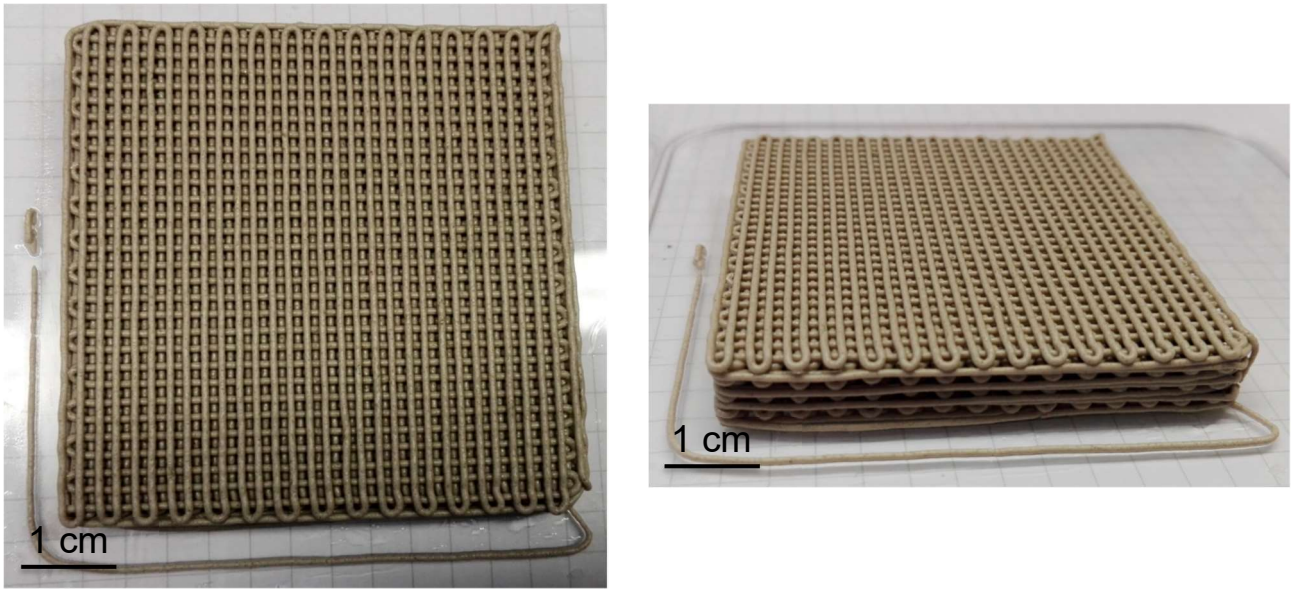

Figure 2.20: Sample printed with GPS ink, left: top overview, right: side overview.

Sample pictured in figure 2.20 is 60 x 60 x 9,60 mm^3, 16 layers, 0-90° shifted cross-section, so, the support points for the subsequent layer are not the same on the previous one. This increases the spacing between consecutive support points, giving less rigidity to the structure. However, the high stiffness of GPS ink permits the production of such geometry. Another problem that GPS ink has overcame is the time of printing, in fact, samples this big require around 50 minutes to be produced, GP 13 PEG ink could potentially be used for the entire time of printing, but the reaction is faster than GPS, forcing changing on the production parameters. The target is to obtain a large sample without major changes on rheological behavior, because this could affect the characteristics of the object. Furthermore, extruding an advance reacted geopolymer results in low cohesion with previous layers and with extruded filament itself.

In figure 2.21 the differences on the same sample geometry between one produced with simple GP 13 PEG (a and b) and the other with GPS ink (c and d) are noticeable. Lower yield stress, lower viscosity and overall weaker gel strength lead to lack of geometry stabilization during printing, as the weight of subsequent layers make the structure collapse merging the first layers together.

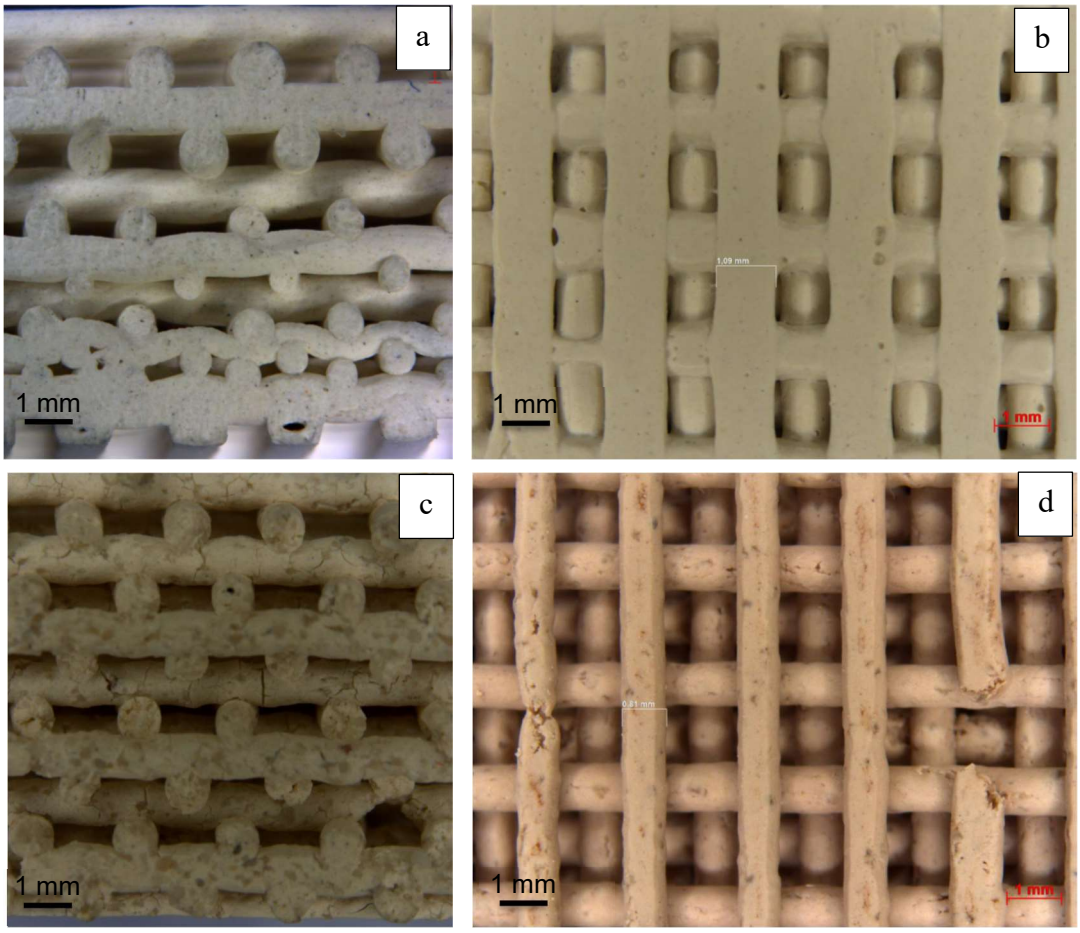

Figure 2.21: Structures printed with the two inks:
(a) GP 13 PEG section view, (b) GP 13 PEG bottom view, (c) GPS section view, (d) GPS bottom view.

Considering the structure in figure 2.21 as an application for aluminum casting filtration, those printed with GP 13 PEG aren't suitable, because their first layers block the flow of what has to be filtered. The geometry of the structure printed with GPS ink is much closer to the desired shape, even on the very first layers some filaments relaxation can be observed, it is yet acceptable considering the overall weight of the structure and its integrity. The first layers aren't blocked anymore, and the sample can fulfill its own application. All in all, the addition of sand has a particularly positive impact on the three-dimensional aspect of the lattice.

Increasing the filler content up to 40% wt. of sand in GP 13 PEG ink, the printability dramatically rises, and printing of more complex structures is possible. On the other hand, the solid content is so high to not allow a full geopolymerization but only a consolidation, because of the lack of water, that is the medium in which the geo-oligomers can diffuse and create links to form geopolymeric chains. In this point of view, the geopolymer isn't the object main material anymore, but becomes an inorganic binder suitable to keep the structure cohesive, which for the most part is formed by sand particles. Moreover, viscosity begins to be a problem for the production method

chosen, in fact, the stepper motor that moves the infinite screw inside the extrusion chamber doesn't have enough power to squeeze the paste through the printing nozzle. Changing the extrusion equipment, from screw to simple air pressure, overcame this problem, but it brought other issues with it like a lesser capability to control the flow or the impossibility to stop the extrusion when the printing is done.

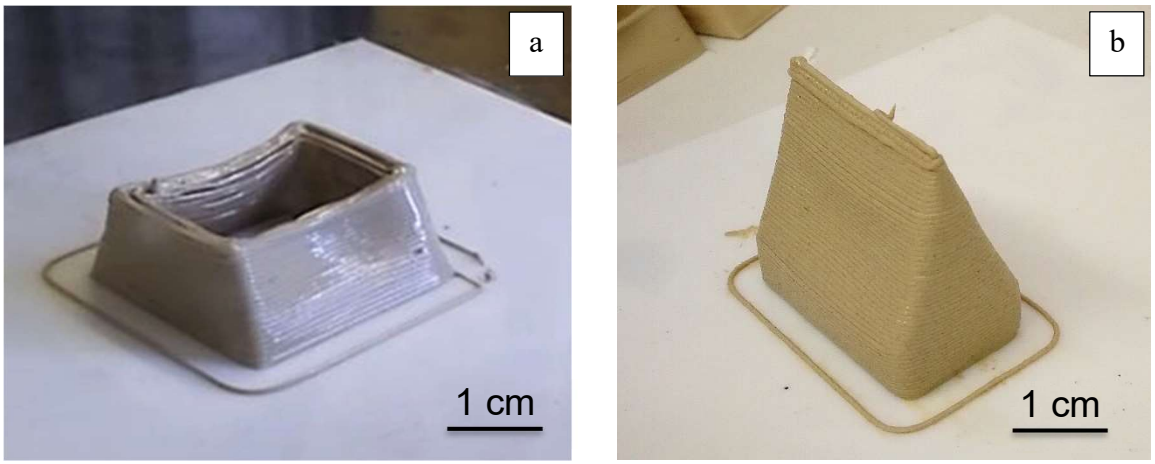

Figure 2.22: Samples printed with GP 13 PEG, different filler content: (a) 0%, (b) 40% wt. of sand.

Figure 2.22 compares structures printed with simple GP 13 PEG ink, on the left (a), with the same one printed with GPS with 40% wt. of sand, on the right (b). The addition of this high percentage of filler allows a great decrease in the sagging, making the printing of such object possible. The roof of the house-shaped sample protrudes with a 60° angle from the horizontal with little geometrical deformation, caused by gravity. The application of these scaled size samples is the study of the quick production of shelters in zones where their use is required, for example during an emergency, such as earthquakes, fires or floods, as their construction could take only few hours and they don't require any specific knowledge. The production of these structures takes more time than anything before, like around 2 hours, and a lot of material is needed, so the need to have more material for more time brings to the conclusion to use the extrusion syringes as cartridges to exchange when the first is finished. Experimentally, during the printing of the first part another batch of ink is being produced and the syringe stored in fridge until the first is finished. Then, the printing is paused, the first syringe is removed and the second is connected to the printer, and the printing can be resumed. For real scale applications, a continuous mixing system at the deposition tip would be preferable.

2.2 Mechanical Optimization of Geopolymer Inks

Geopolymerization can be promoted with either temperature or time. At room temperature (around 25°C) the reaction is complete after about a month, but it is possible to speed up the process by applying heat for the time needed. As a side effect, the completion of the reaction leads to a stronger tridimensional network, that means a stronger material. So, two thermal treatments were designed, one at low temperatures, named curing, and one at high temperatures, named firing, to see which one allow to have the strongest material for applications at low or high temperatures. The higher temperature of firing treatments can affect the microstructure/phase composition, so it is possible to observe the difference in mechanical resistance through the temperature.

2.2.1 Curing

GP 13 PEG and GPS inks are tested mechanically after curing for 1 day and 7 days at room temperature, that is approximately 25°C, 40°C and 80°C to observe if there are differences in mechanical strength. Samples used for these tests are nominally 20.00 x 20.00 x 7.20 mm^3 as shown pictures figure 2.23.

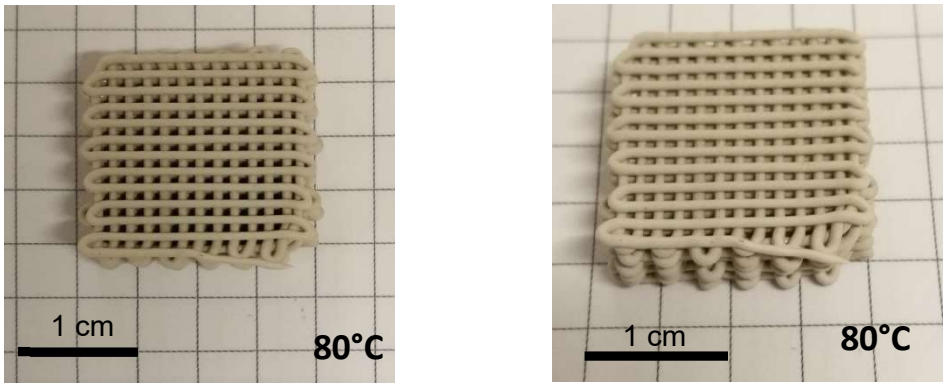

Figure 2.23: Top views of a compression sample, in this case made of GP 13 PEG.

Figure 2.24 shows the compressive strength after curing of samples printed with GP 13 PEG and GPS inks. The trends confirm what can be found in literature [77], geopolymerization can be promoted with temperature with an overall increase on the mechanical properties. However, samples treated for different times, 1 day and 7 days, show strength values are not so different, considering the errors. GP 13 PEG samples cured at room temperature are the weakest with compression values of 6.42 ± 1.85 MPa and 6.93 ± 1.52 MPa, for 1 day and 7 days treatment respectively, and samples cured at 80°C are the strongest with values ~ 13-15% higher. However, the high error values, which

consist on about the 30% of the strength values, don't allow a significative distinction between the results, making them very similar, if not equal. GPS samples show greater differences between samples cured at higher temperatures and those treated at room temperature, but on greater values and with higher step, meaning that probably samples cured at room temperature haven't finished their reaction yet. In fact, it can be assumed that after completion of the geopolymerization reaction all samples would reach a similar compression strength [77]. As an indication, the figure 2.24 also shows the result of a compression test on a sample made of GP 13 PEG of the same geometry but cured at room temperature for two months.

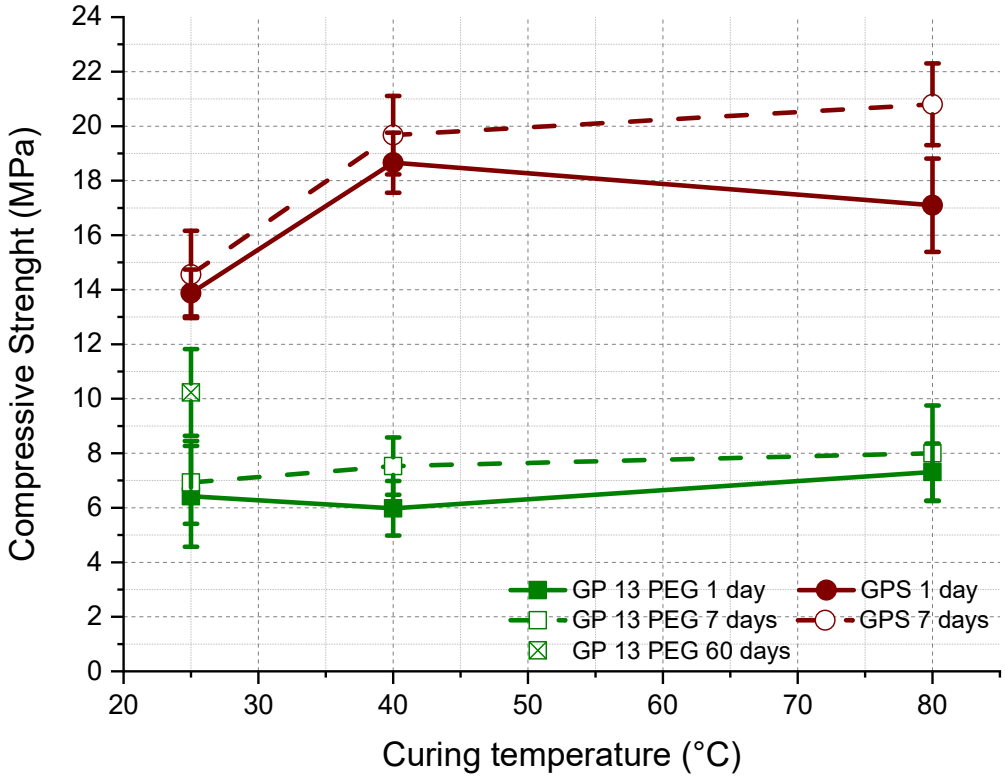

Figure 2.24: Compressive strength for GP 13 PEG and GPS samples after curing.

In comparison, GPS samples show higher mechanical strength than GP 13 PEG ones, with values ~ 2-3 times greater, due to the high content of sand. Quartz has much higher compression strength (ranging from 50 to over 1000 MPa) compared to the geopolymeric matrix, depending on the crystal defects. Similar to cement mortars, the presumed mechanism is that when a crack meets an impenetrable obstacle it becomes pinned. In order to pass, cracks have to bend and thus makes the cracks surface rougher. This would lead to an increase in strength [78]. Sand particles have different geometries with irregular and rough surfaces (figure 2.25), that probably give the chance to the fresh geopolymer to adhere well to the filler particles. A chemical interaction between the siliceous sand and the geopolymer can also be assumed, which would increase the interface strength between the

two materials. The sand is poured inside the activation solution before the metakaolin, so, some of the Si could be attacked helping the full dissolution of aluminosilicate, enriching the geopolymer in silicon, which is responsible to form new geo-oligomers, and creating new branches and more links between near chains. Anyway, sand grains are still visible in SEM micrographs (figure 2.25) as white dots as they have different composition than the geopolymer. In table 2.3 strength values of GP 13 PEG and GPS samples are summarized.

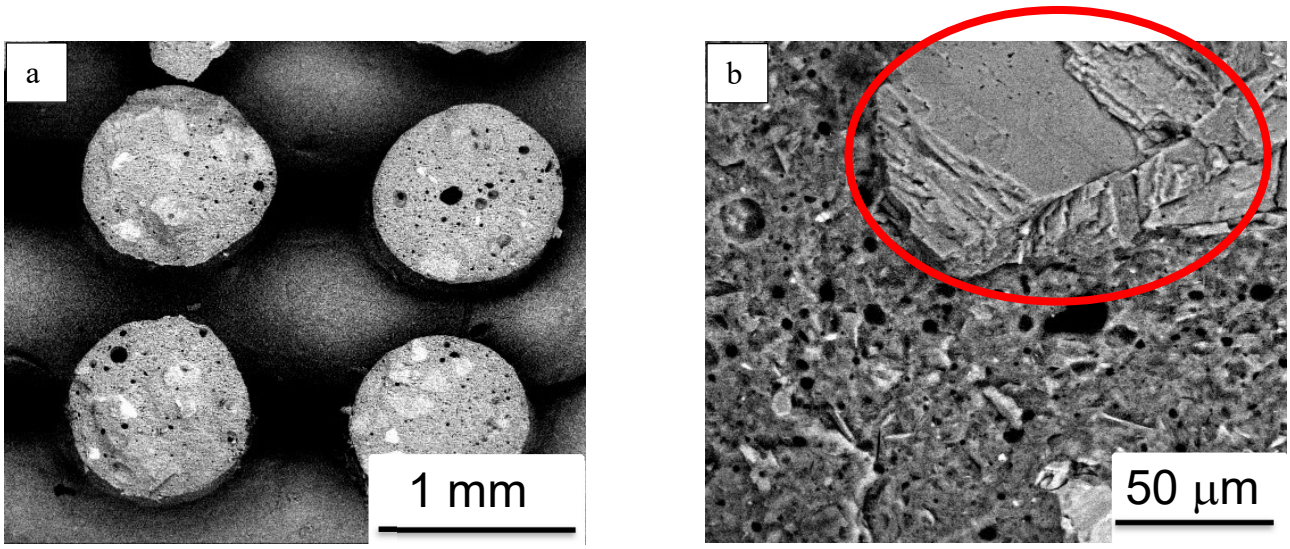

Figure 2.25: SEM micrographs of GPS sample cured at 80°C for 1 day:
(a) side view 50x; (b) detail of sand grain highlighted in red circle 800x.

Table 2.3: Strength values for GP 13 PEG and GPS samples obtained with compression tests.

	GP 13 PEG		**GPS**	
	1 day (MPa)	**7 days (MPa)**	**1 day (MPa)**	**7 days (MPa)**
RT	6.42 ± 1.85	6.93 ± 1.52	13.88 ± 0.86	14.56 ± 1.60
40°C	5.98 ± 1.00	7.53 ± 1.05	18.66 ± 1.10	19.67 ± 1.44
80°C	7.31 ± 1.05	8.00 ± 1.75	17.10 ± 1.71	20.80 ± 1.50

The slight deflection on strength values for samples made of GP 13 PEG cured 1 day at 40°C and for GPS samples cured at 80°C for 1 day is acceptable within a margin of error, anyways, the trend is still positive with the increasing of treatment temperature. However, the increase in compressive strength provided by higher curing time is not so relevant from an industrial perspective. Further tests will be done considering samples cured at 80°C for 1 day.

In order to maximize the compatibility between slurry and filler, previously prepared geopolymer powder, sieved below 300 μm, is added to the mixture as filler. This new geopolymer is labeled GPGP, which means geopolymer powder added to geopolymer.

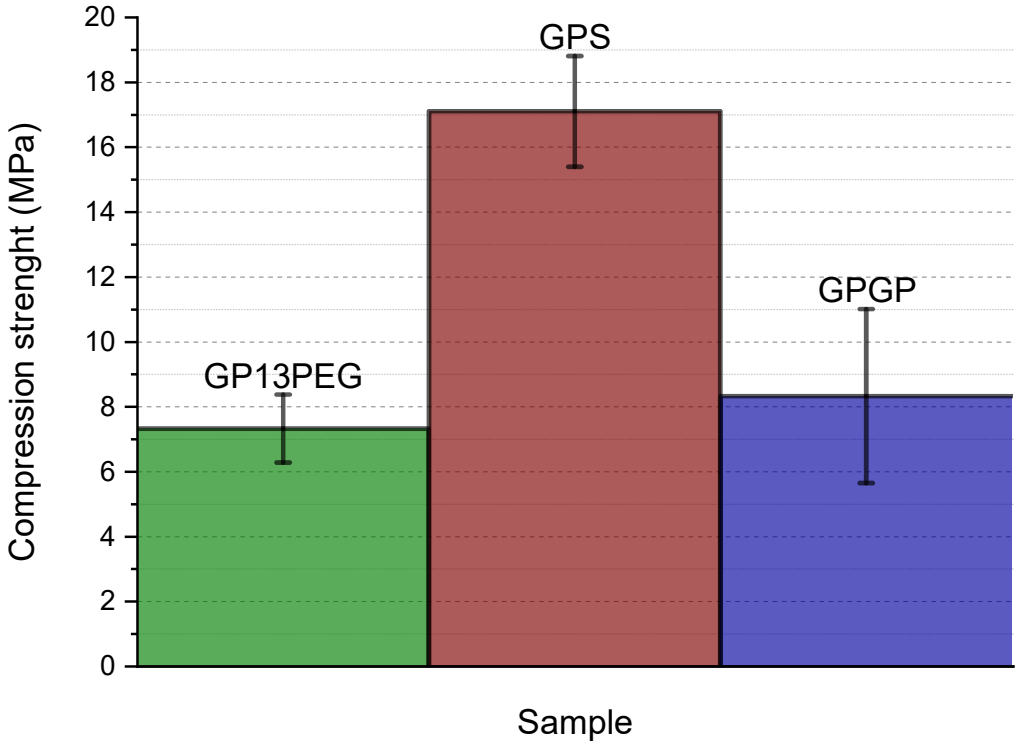

Figure 2.26: Comparison between compression strength of GP 13 PEG, GPS and GPGP samples.

Table 2.4: Compression strength values for GP 13 PEG, GPS and GPGP samples cured at 80°C for 1 day.

	Compression strength (MPa)
GP 13 PEG	7.31 ± 1.05
GPS	17.10 ± 1.71
GPGP	8.31 ± 2.69

Figure 2.26 shows the differences between the samples compression results made with the three inks after curing at 80°C for 1 day. In comparison with GP 13 PEG and GPS, samples made with GPGP ink show compression strength comparable with those made of GP 13 PEG ink, as the filler does not provide with higher compressive strength in this case. Geopolymer used as powder for the ink is stored in an oven with constant temperature of 80°C, thus is surely dried and fully reacted, then is crushed, grinded and sieved. This process helps making the particles aspect ratio different than

sand granules, which don't undergo crushing and grinding steps, from a geometry with non-uniform surfaces to more round particles with smooth surfaces. Geopolymer sand is completely reacted, that gives high chemical inertia, but when it is poured inside the alkaline solution, its chemical similarity with the mixture probably make it slightly soluble, as happens with sand, and can as well provide chemical interaction but at the same time mantains the same matrix composition as in the GP 13 PEG ink (figure 2.27). In fact, it's impossible to distinguish geopolymer matrix to geopolymer powder filler.

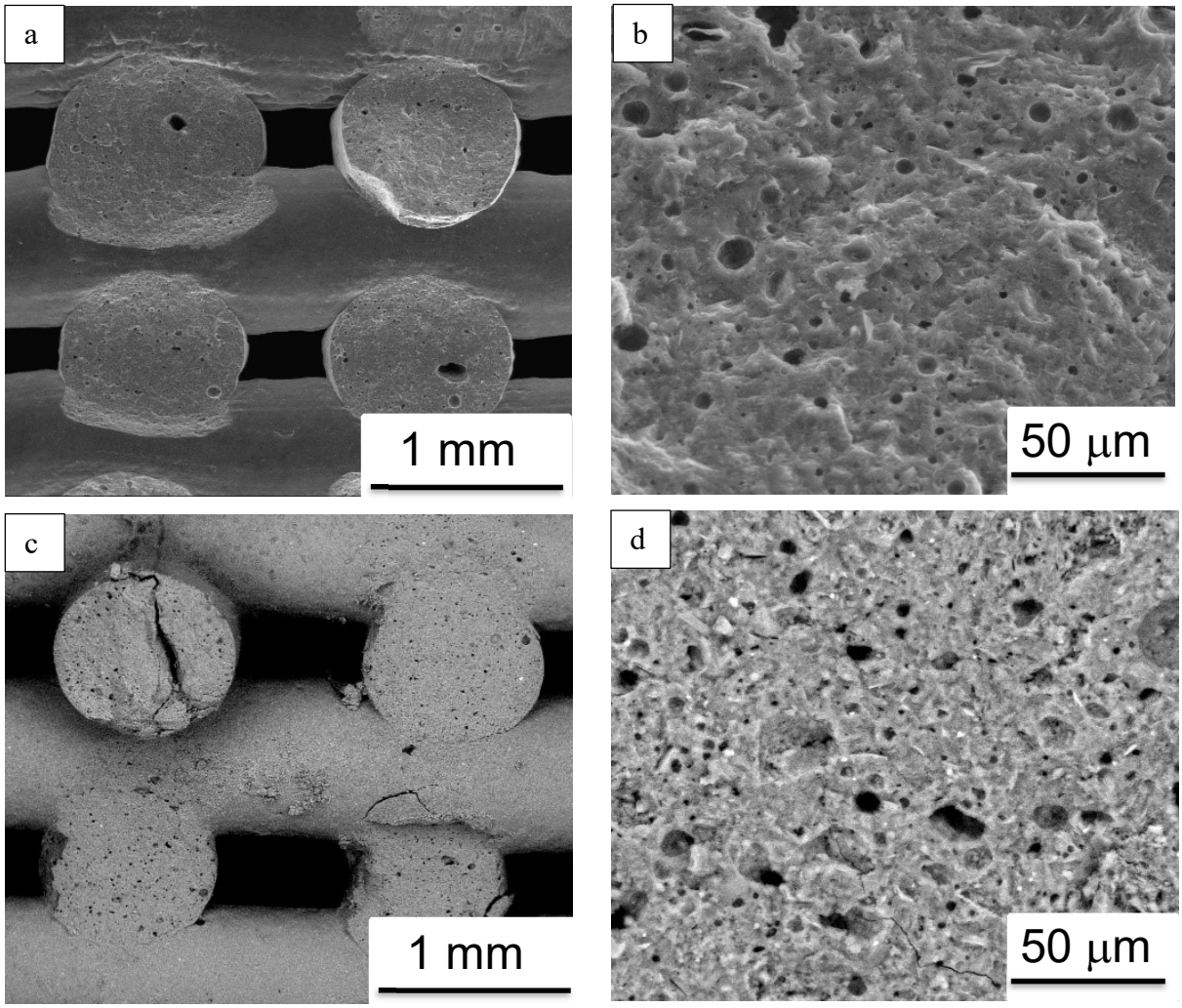

Figure 2.27: SEM micrographs of samples cured at 80°C for 1 day:
(a) GP 13 PEG side view 50x; (b) GP 13 PEG detail 800x; (c) GPGP side view 50x; (d) GPGP detail 800x.

Observing SEM micrographs in figure 2.25 (a) and 2.27 (a) and (c) is understandable the difference in the production of the lattices with the different inks and their rheology behavior. Side view of GP 13 PEG sample show interpenetrating filaments from a layer to the following one, as its overlap results in ~7% of the filament diameter, meaning a low initial yield stress that causes the strut

to be deformed under gravity force as the subsequent layer is printed. This phenomenon is much less pronounced on the structures printed with fillers added inks, filaments are straighter with minor penetration on other layers. Excessive overlap is a consequence of sagging and affects the samples height, if the desired shape is designed to be 7.20 mm tall, GP 13 PEG samples are 6.80 ± 0.15 mm tall while GPS ones are 7.14 ± 0.15 mm and GPGP 7.19 ± 0.15 mm. If the addition of sand gives huge improvement on the properties, geopolymer powder doesn't affect the overall mechanical characteristics after curing, but it increases dramatically the printability of the ink anyway, as previously seen in paragraph 2.1.3.

2.2.2 Firing

Table 2.5 show data obtained with uniaxial compression tests for samples previously cured at 80°C for 1 day and then fired at 300°C, 500°C, 700°C and 1000°C for 1 hour. The methodology and reasons of firing heat treatment have already been explained in paragraph 1.4.2.

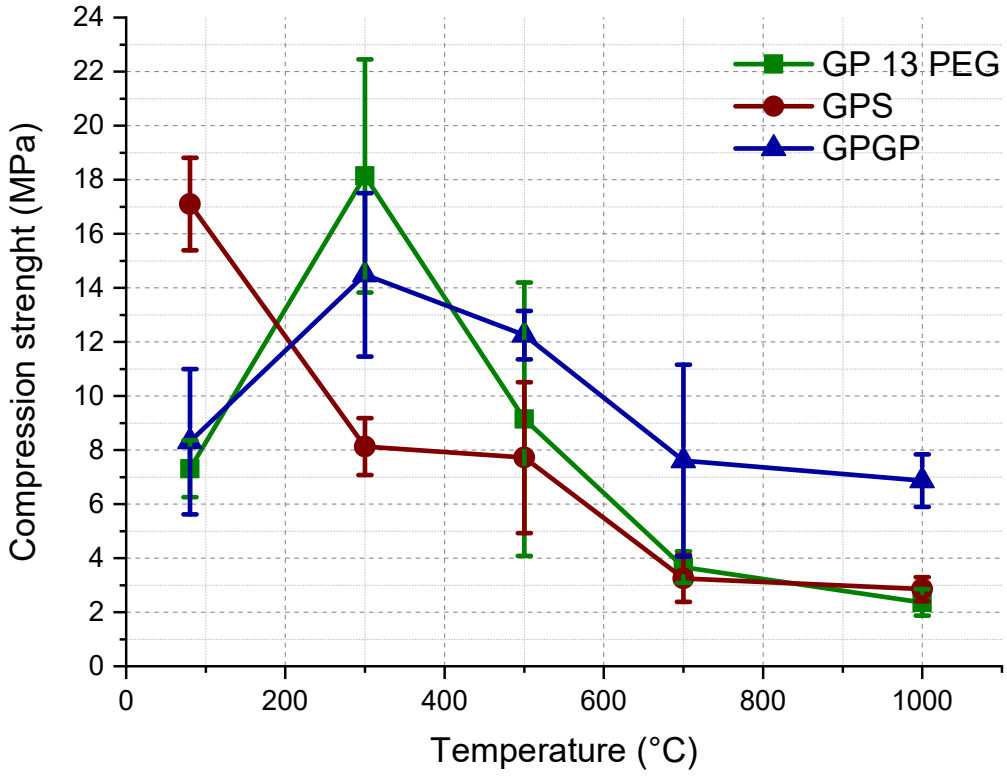

Figure 2.28: Comparison of mechanical strength for samples made with the three inks after thermal treatments.

All inks behave similarly through the increasing of temperature, maximum values reached at 300°C, for GP 13 PEG and GPGP samples, or at 80°C, for GPS samples, then decreasing of mechanical resistance (figure 2.28) if treated at higher temperatures.

Table 2.5: Comparison of compression strength values for samples made with the three inks after thermal treatments.

	Compression strength (MPa)		
	GP 13 PEG	**GPS**	**GPGP**
80°C	7.31 ± 1.05	17.10 ± 1.71	8.31 ± 2.69
300°C	18.14 ± 4.31	8.13 ± 1.05	14.48 ± 3.02
500°C	9.14 ± 5.06	7.72 ± 2.79	12.25 ± 0.90
700°C	3.67 ± 0.58	3.25 ± 0.87	7.61 ± 3.55
1000°C	2.36 ± 0.49	2.85 ± 0.44	6.87 ± 0.97

Figure 2.29 shows load profiles for samples of all inks, cured at 80°C for 1 day and fired at 300°C as indicative to all other treatments. All samples show the typical profile of a foam structure with non-catastrophic failure and residual stress after reaching the maximum strength. Lattices, which are trabecular structures, behave this way because cracks proceed gradually from layer to layer encountering some resistance even when the sample is already broken. The slope of initial load is not always continuous, as the compression proceeds some filaments may collapse, probably because of production defects. Some profiles show residual stresses even greater than first peak load, because the sample surfaces are not always perfectly planar, but can concentrate the load on smaller areas on protruding filaments; after these first break, an increase on the force is needed to keep the pushing speed of 1 mm/min.

Samples treated at 300°C show the best compression strength values for GP 13 PEG and GPGP inks, the physical water absorbed by the three-dimensional geopolymer network is completely evaporated, and the material results completely reacted. SEM micrographs depicted in figure 2.30, doesn't show any presence of cracks in GPGP structures, GP 13 PEG has only superficial cracks, probably made during the preparation of the sample to the analysis, and GPS is severely cracked. The difference in thermal expansion coefficients between geopolymer and sand may explain the appearance of GPS samples: while the first shrinks, the second swells, resulting in cracks growth, when heated, starting from the sand/geopolymer interface, where the load is concentrated. During the compression test the geopolymer acts as a matrix that bonds the sand grains together, and the load is borne especially by the quartz particles, that possess greater mechanical characteristics than geopolymer. However, a damaged matrix cannot perform well enough to result in enhanced mechanical features, because the presence of cracks is extended enough to impair the performance.

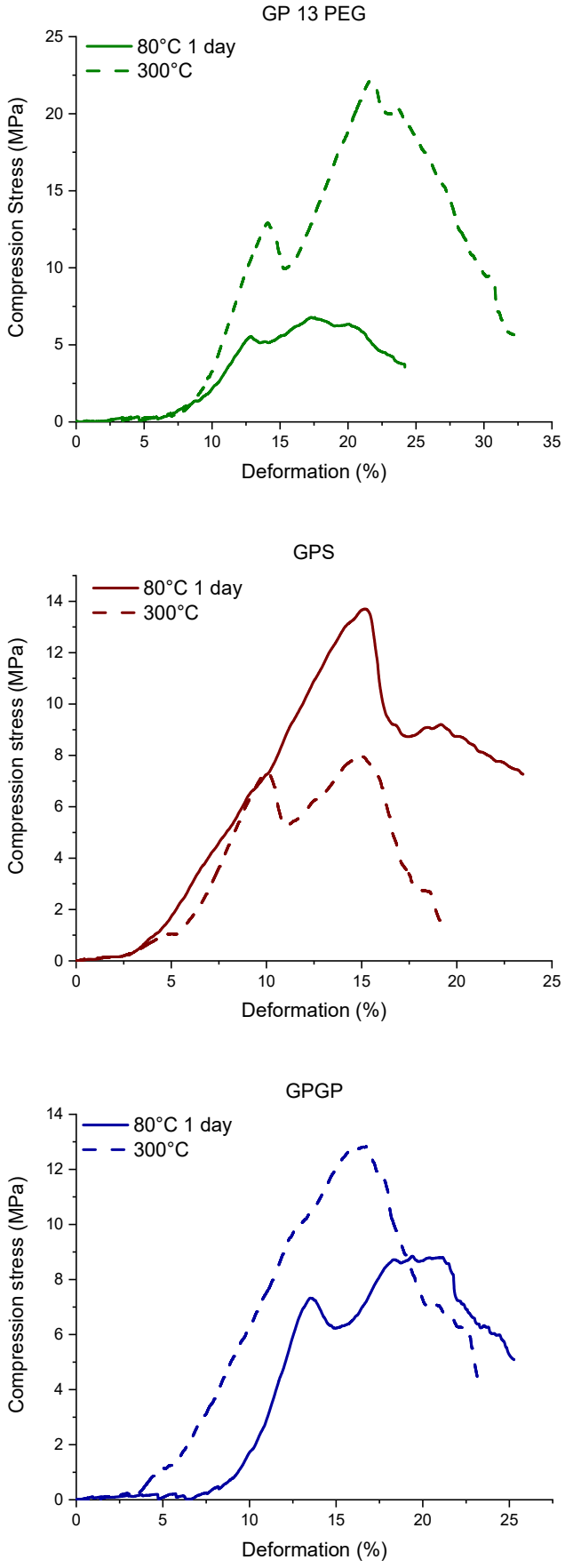

Figure 2.29: Load profiles of GP 13 PEG, GPS and GPGP samples cured and fired.

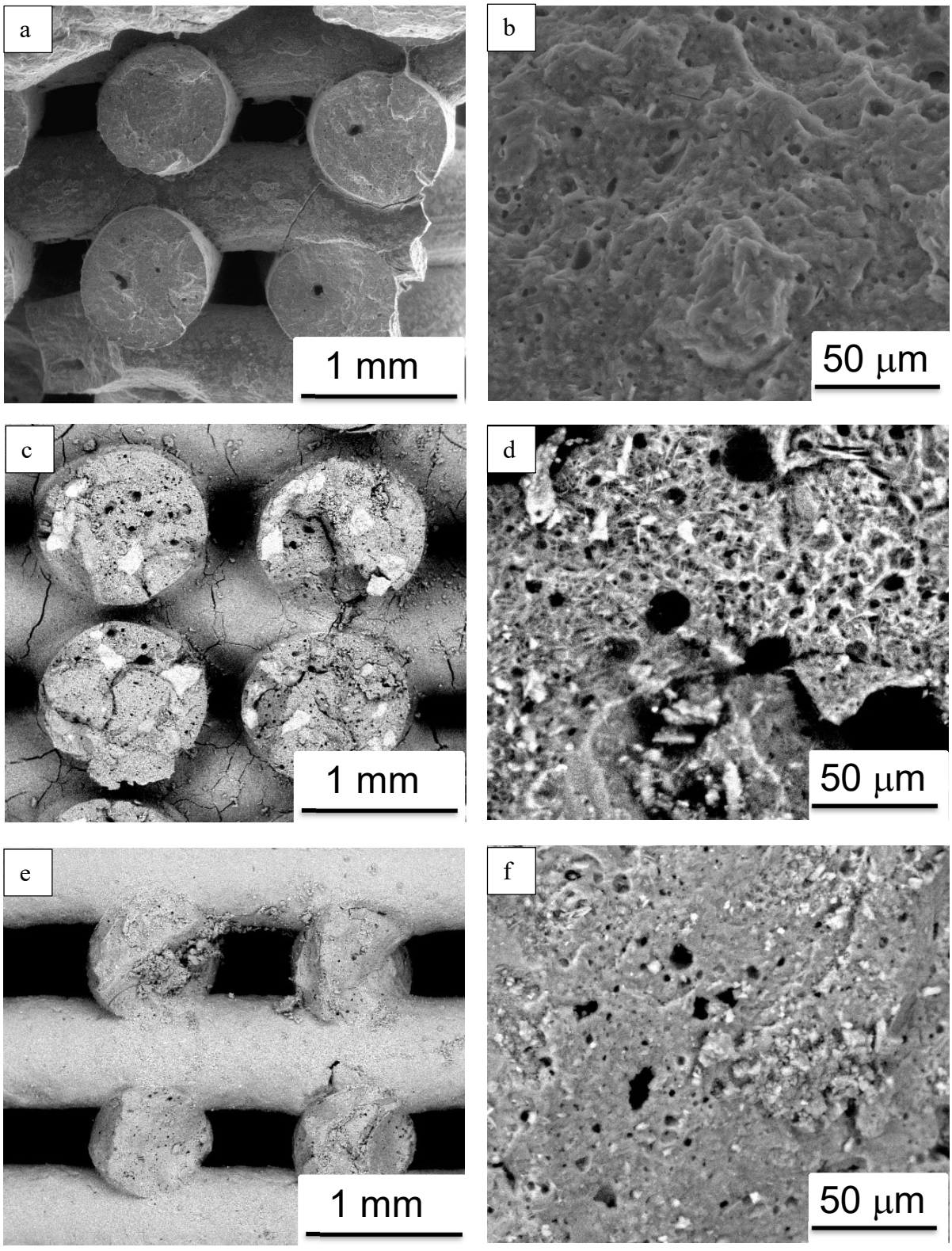

Figure 2.30: SEM micrographs of samples fired at 300°C: (a) GP 13 PEG side view, 50x; (b) GP 13 PEG detail, 800x; (c) GPS side view, 50x; (d) GPS detail, 800x; (e) GPGP side view, 50x; (f) GPGP detail, 800x.

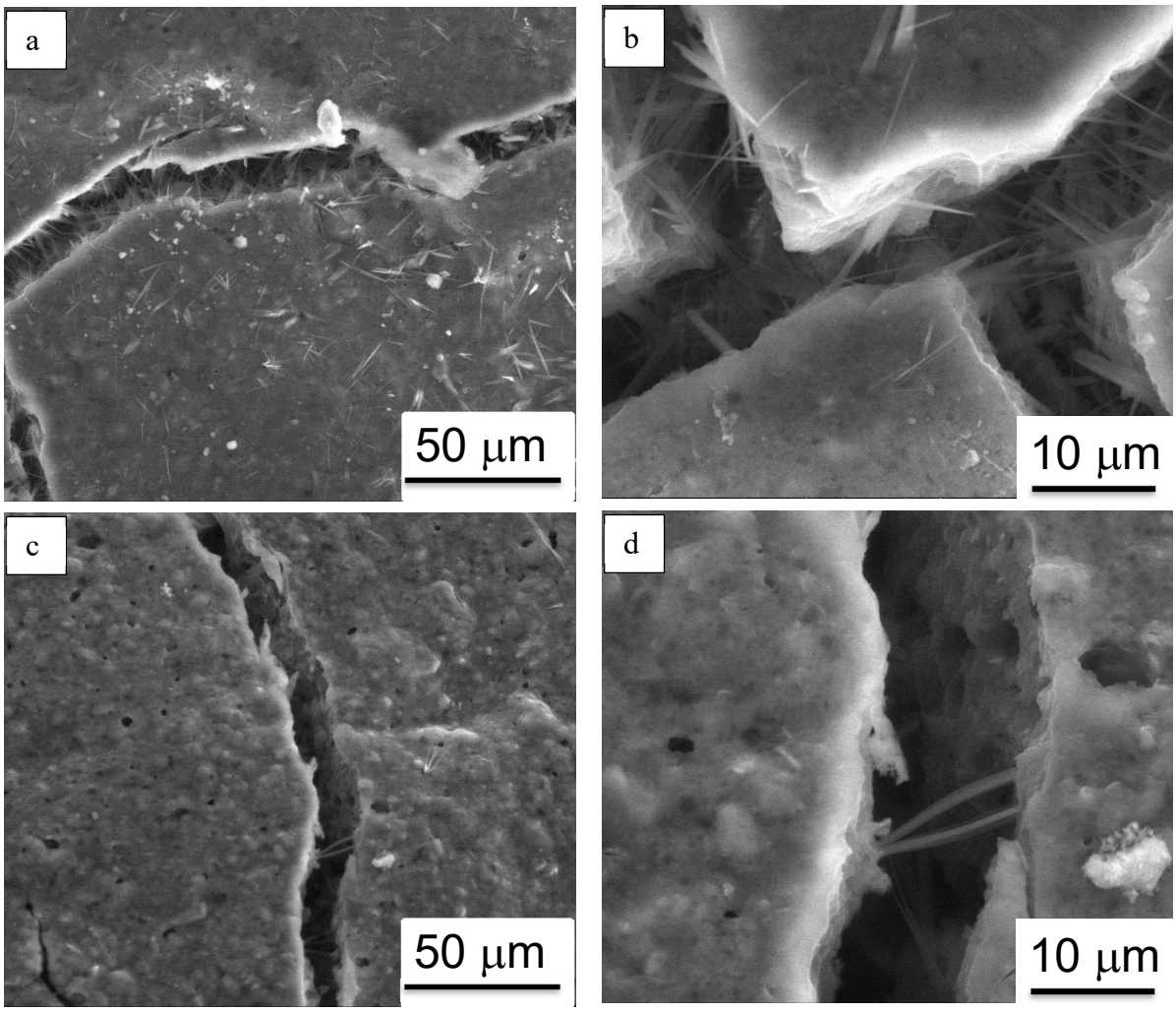

Figure 2.31: Evolution of cracks surface through firing temperature for samples made of GPS ink:
(a) 300°C, top view, 800x; (b) 300°C, detail, 3000x; (c) 500°C, top view, 800x; (d) 500°C, detail, 3000x.

Investigating the morphology of cracks (figure 2.31) in GPS structures fired at 300°C, acicular formations of sodium salts are clearly visible. This phenomenon is often observed in geopolymers with high content of sodium and it is referred as efflorescence [79]. These salts form under humid conditions [81] when an imbalance in the composition makes the alkalis, sodium in this case, more reactive. The addition of sand gives this composition imbalance, probably due to the aforementioned attack of Si by the geopolymer, while the exposition to room conditions, i.e. normal wet weather, allows the growth of such efflorescence. Previous works by Skvara et al. [80] and Zhang et al. [82] explain how such efflorescence can be eliminated by thermal treatment with temperature over 600°C. In fact, their elimination is confirmed in samples fired at 700°C and 1000°C (figure 2.32). This is due to better chemical stabilization possible by geopolymer network consolidation, as all sodium is used in the structure growth. Observing SEM micrographs of GPS samples through temperatures, there is a strong correlation between cracks growth and the increasing of temperature, which implies structures with lower compression strength. In fact, filler and matrix are made of two different

materials, which have different thermal expansion coefficient, positive for the sand, that swells when heated, and negative for the geopolymer, that shrinks at high temperatures.

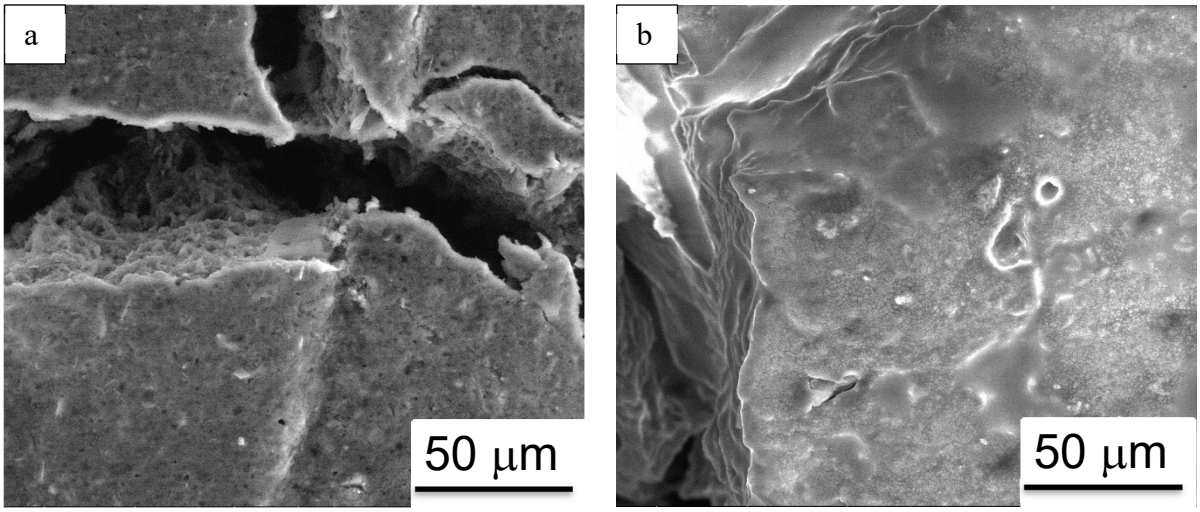

Figure 2.32: SEM micrographs of fracture surfaces in GPS samples after firing: (a) 700°C, 800x; (b) 1000°C, 800x.

At higher temperatures (figures 2.33, 2.34 and 2.35), from 500°C to 1000°C, GP 13 PEG and GPS show similar mechanical proprieties, chemical water elimination and volumetric shrinkage lead to the formation of several cracks, that seems to be more severe in GPS lattices, because of the different thermal expansion coefficient of sand compared to the geopolymer one. GPGP, however, maintains some cohesion resulting in samples with better mechanical characteristics at high temperature, in fact, the filler is the same material as the matrix with the same thermal expansion coefficient, and when heated the structure is free to shrink without constraints. GPGP samples treated at 500°C show a visibly higher porosity, probably due to filler water elimination, which is prevented at lower temperature by high matrix viscosity, but from 500°C a low viscous flow may happened allowing the instant evaporation of water contained in filler grains, resulting in a foamy structure. At higher temperatures, the coordinated shrinkage of matrix and filler leads to samples morphologically similar to the other inks.

On the other hand, GP 13 PEG samples, which don't have any filler added, show lower compression strength values, because of the high thermal coefficient, that makes the structure shrinks up to a 20-30% volumetric, inducing stresses that cause cracks to appear. This ink is, among the others, the one with the highest water content, as volumetric fraction of solid to water ratio, this causes to the structure the need to evaporate more water once heated.

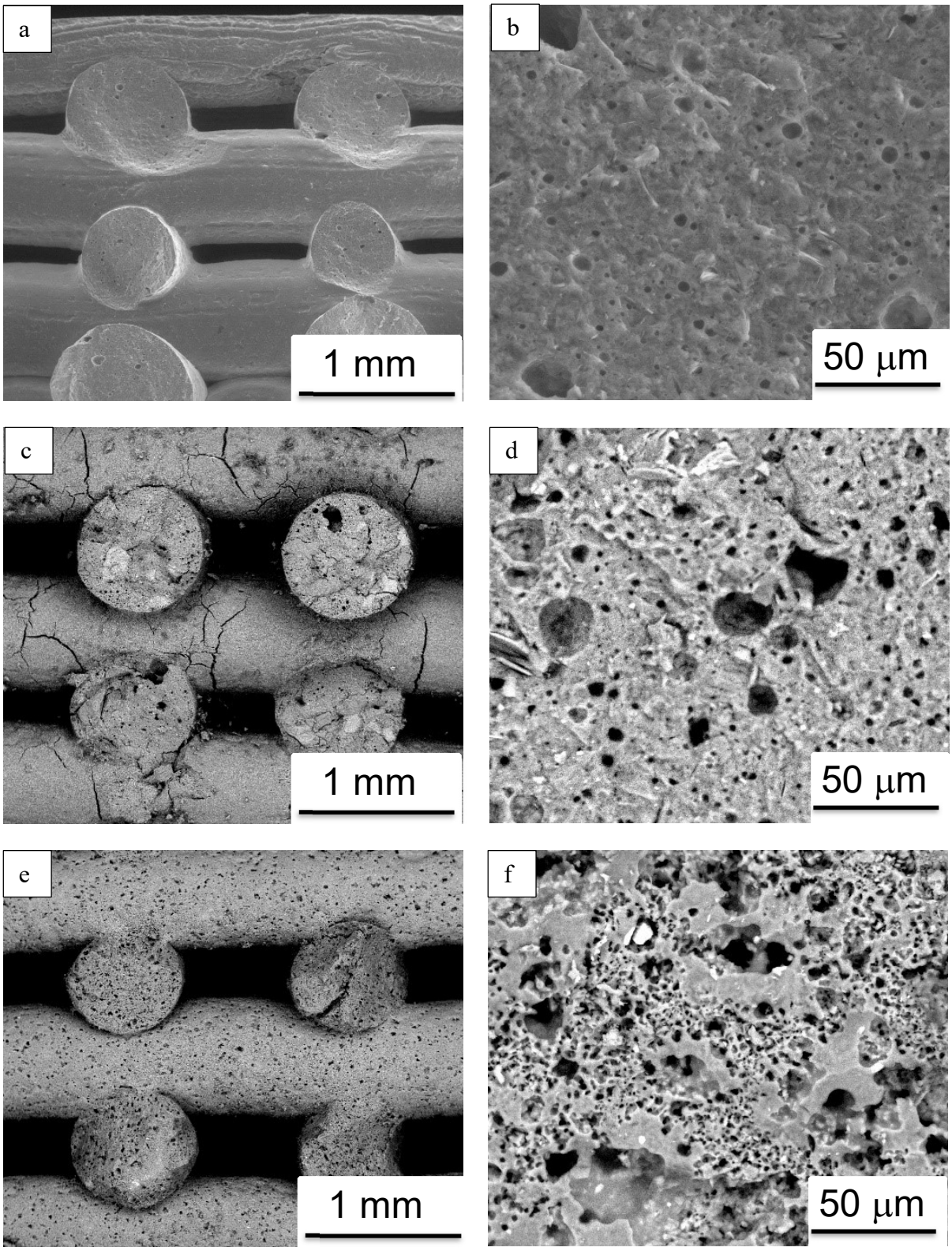

Figure 2.33: SEM micrographs of samples fired at 500°C: (a) GP 13 PEG side view, 50x; (b) GP 13 PEG detail, 800x; (c) GPS side view, 50x; (d) GPS detail, 800x; (e) GPGP side view, 50x; (f) GPGP detail, 800x.

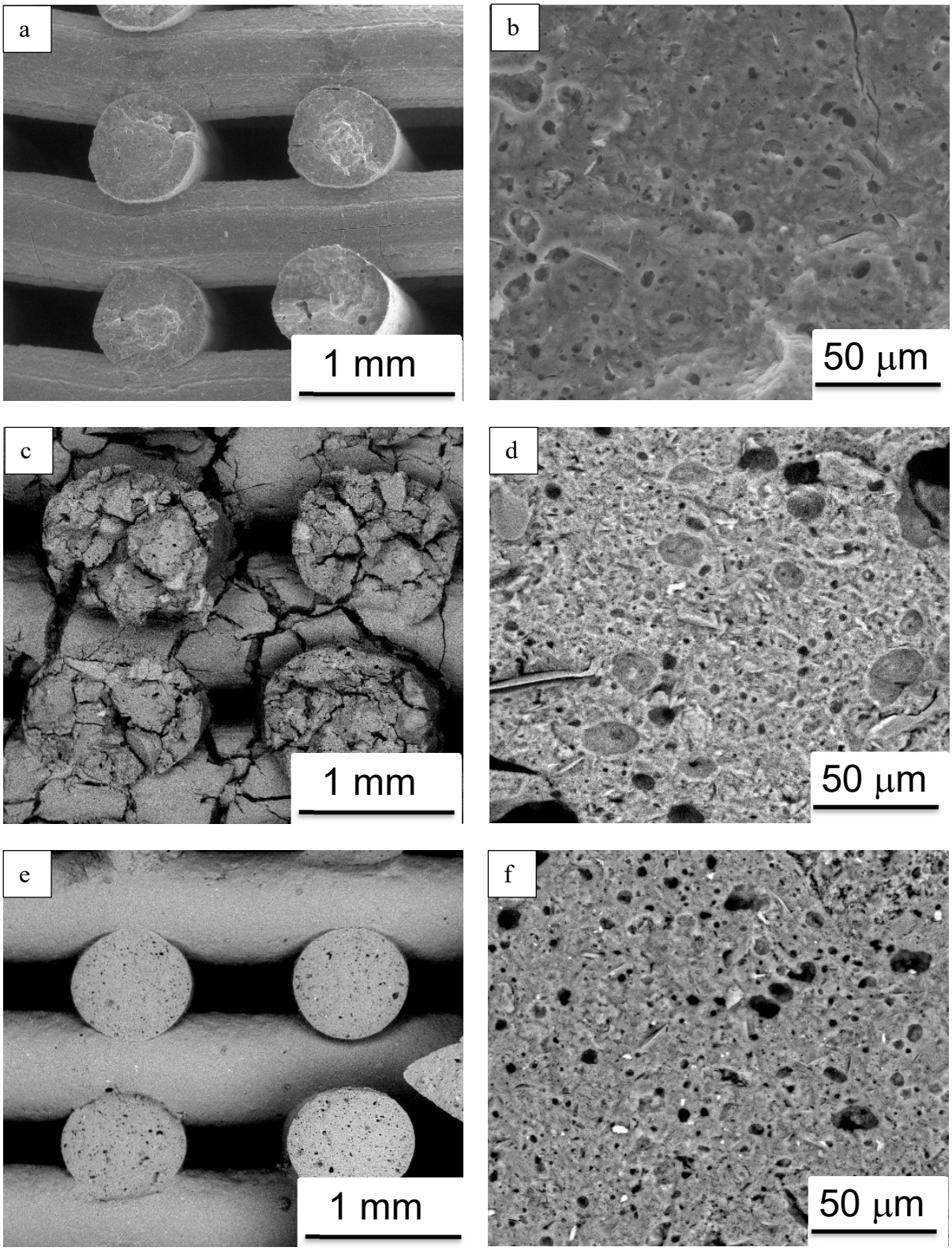

Figure 2.34: SEM micrographs of samples fired at 700°C: (a) GP 13 PEG side view, 50x; (b) GP 13 PEG detail, 800x; (c) GPS side view, 50x; (d) GPS detail, 800x; (e) GPGP side view, 50x; (f) GPGP detail, 800x.

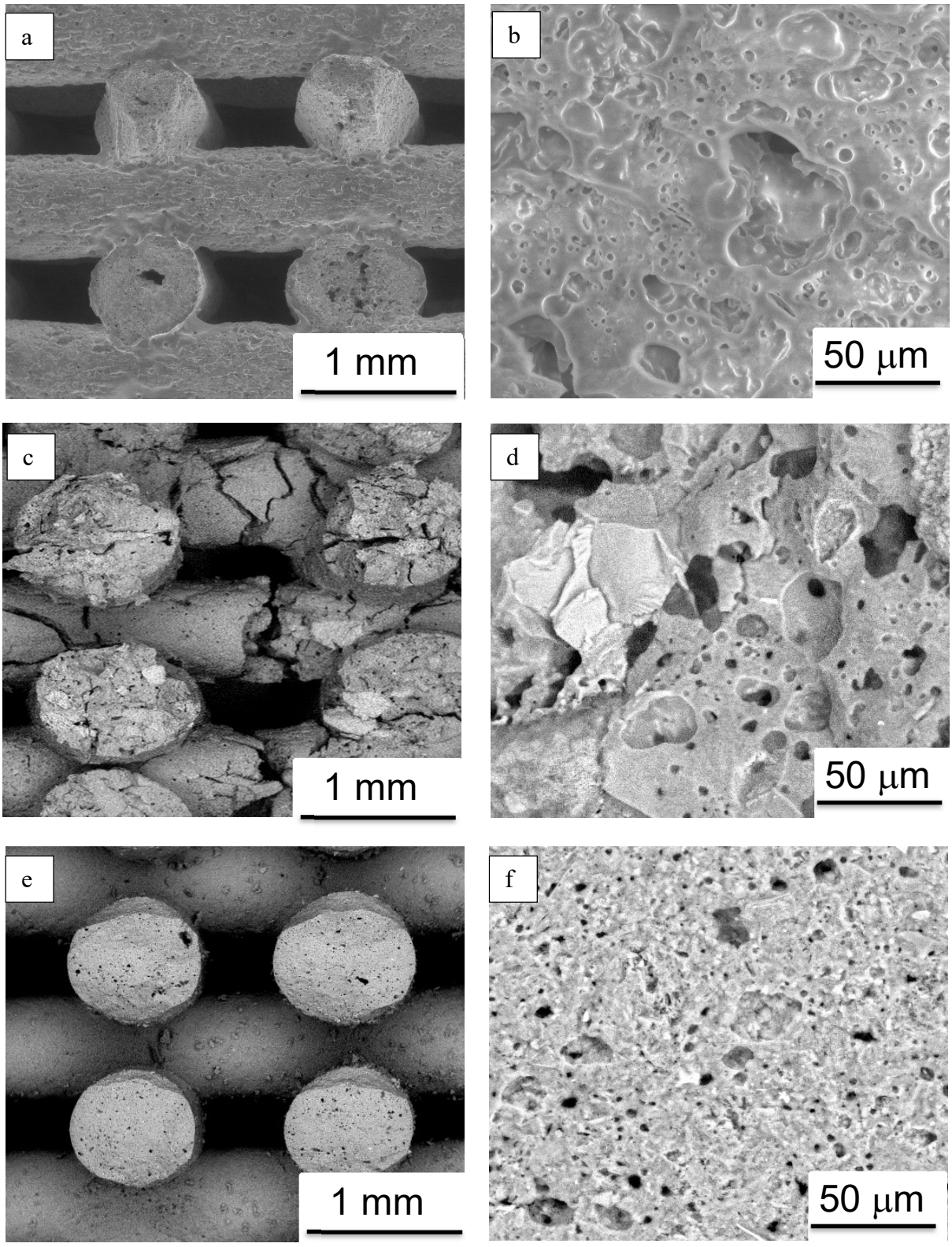

Figure 2.35: SEM micrographs of samples fired at 1000°C: (a) GP 13 PEG side view, 50x; (b) GP 13 PEG detail, 800x; (c) GPS side view, 50x; (d) GPS detail, 800x; (e) GPGP side view, 50x; (f) GPGP detail, 800x.

At 1000°C SEM micrographs of GP 13 PEG (figures 2.35 (a) and (b)) show a structure that seems partially remolten, visible also in the other inks, the material is fully crystalized, as XRD patterns (figures 2.39, 2.40 and 2.41) show the typical peaks of nepheline, and the viscous flow, which causes the matrix to appear this way, may be caused by the TiO_2 and SiO_2 impurities part of raw materials, as chemical composition of metakaolin shows (par. 1.2.1). This phenomenon occurs also on the other inks, in GPS (figures 2.35 (c) and (d)) the contrast between the partially remolten geopolymeric matrix with the sand grains is clearly visible, in GPGP micrographs (figures 2.35 (e) and (f)) distinguishing the matrix from the filler is no longer so easily discernible, as they are made of the same material, but the same remolten structure is noticeable as well in this case.

A quick chemical investigation of inhomogeneities present on samples surfaces is possible by EDX analysis. Observing the micrographs of the various samples made with the three ink through the increasing of temperature, is easy to notice how GPS structures show the widest variety of different species, including geopolymer with its impurities and sand grains. Following is the microprobe EDX analysis of a part of GPS structure (figure 2.36).

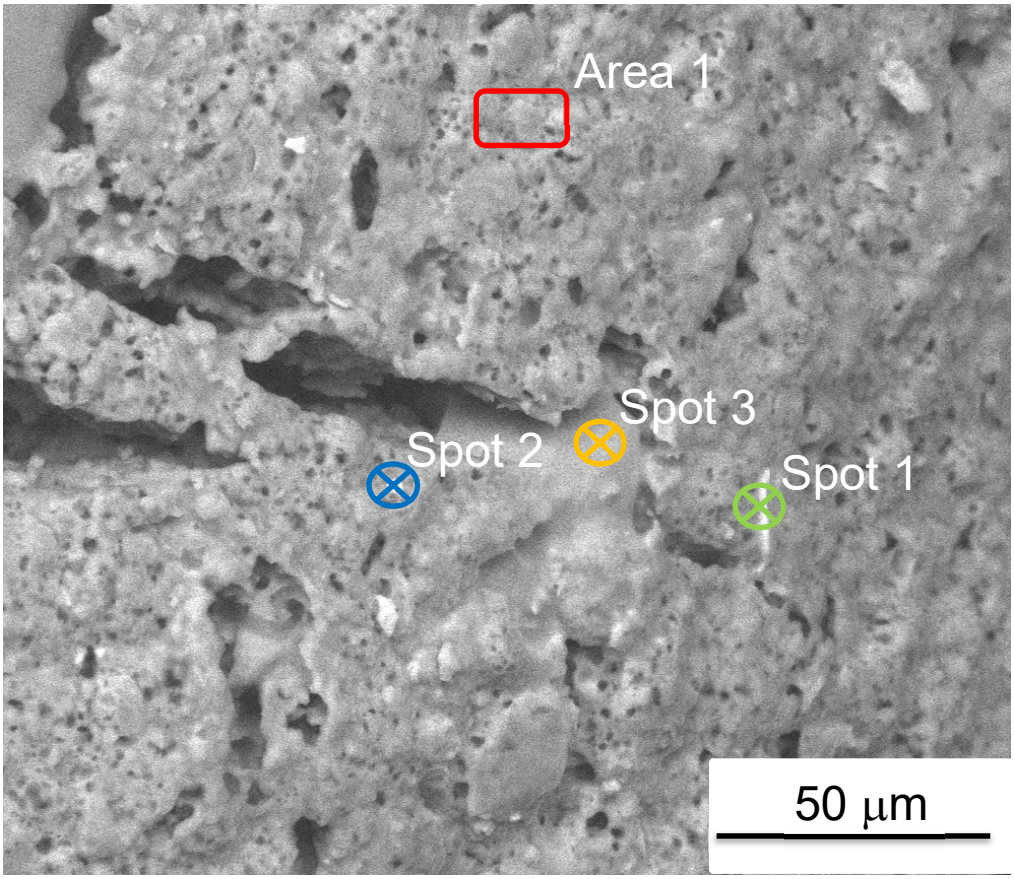

Figure 2.36: SEM micrograph of GPS surface after curing, 800x, EDX spots for microchemical analysis highlighted: (Area 1) geopolymer matrix; (Spot 1) and (Spot 2) impurities; (Spot 3) sand grain.

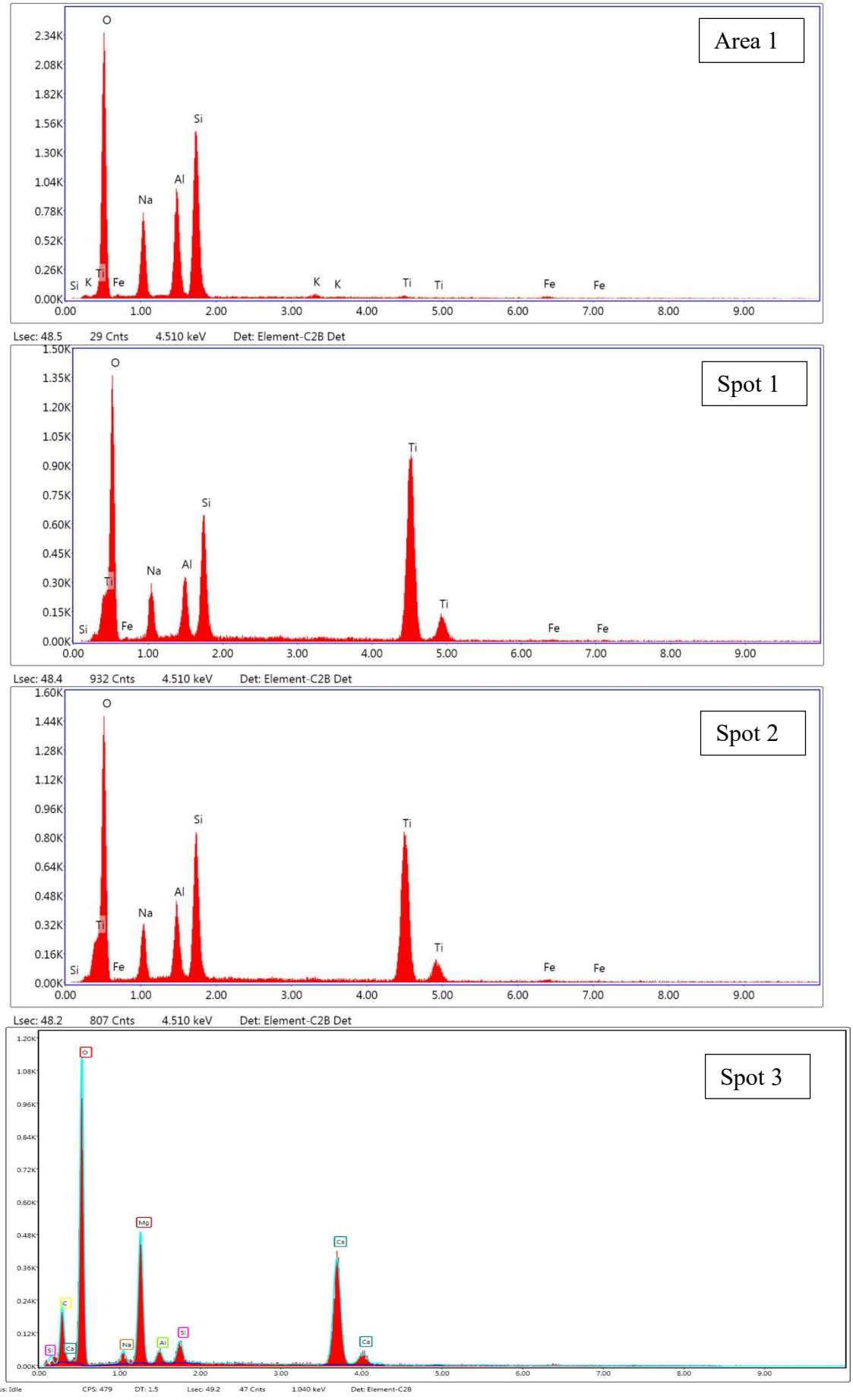

Figure 2.37: EDX spectrograms of the four analysis reported in figure 35.

The EDX spectrogram of geopolymer matrix in figure 2.37 (Area 1) shows the typical chemical elements part of a sodium based geopolymer: Na, Si, O, Al principally and traces of Fe, K and Ti, considered impurities in metakaolin. White spots located in the matrix are recognized as inclusions of titanium, probably TiO_2 in the crystalline form of anatase, as following x-ray diffraction investigation clarifies. Sand grains microanalysis show the presence of chemical elements typical for siliceous natural rocks, like Ca, Mg, O and C, the structure is likely a dolomite formation. All spectrograms show the presence of geopolymer elements because of the diameter of the electronic beam which is large enough to collect data from near areas as well.

2.2.3 Porosity of lattices

The designed porosity is set at 55.5% calculated from the digital file assuming dense cylindrical struts with 840 μm diameter, layer height of 650 μm and a small overlap, which occurs only on the struts intersections. So, it is all open porosity given by the open channels of the structure. Porosities of samples heat treated are reported in table 2.6, values below designed porosity may be caused by sagging, which make the structures denser, higher values, on the other hand, are due to the presence of pores in the material, as confirmed by low closed porosity values. The methodology of production is the first cause of the presence of internal pores on the filaments, as high energy mixing a highly viscous paste leads to air entrapped into the slurry. Then, at high temperatures, i.e. after firing heat treatment, the evaporation of water and the elimination of the organic component, added to the geopolymer to better optimize rheological behavior, create more open pores, resulting in a positive trend of increasing total and open porosity with temperature (figure 2.38). The production of lattices is also one of the reasons of presence of different sizes of air bubbles near the center of the struts, which is clearly visible in SEM micrographs side views (figures 2.25, 2.27, 2.33, 2.34 and 2.35). Larger pores located near the center of struts are due to pressure difference in the printing nozzle, which is greater towards the nozzle walls and smaller towards the center, the use of a screw-driven extrusor has helped to minimize such issue, but it isn't completely eliminated. Smaller pores are geopolymer intrinsic physical characteristic, because of the way it sets, in fact, the reaction of geopolymerization proceeds through condensation of -OH groups creating water molecules that are unable to freely reach the surface for evaporation, which is blocked because of the slurry increasing viscosity. Anyway, results are remarkable, as these structures show compression strength up to 18.14 ± 4.31 MPa, 8.13 ± 1.05 MPa and 14.48 ± 3.02 MPa after firing at 300°C, with total porosity of 53.5%, 59.2% and 60.8%, for GP 13 PEG, GPS and GPGP inks respectively.

	GP 13 PEG			GPS			GPGP		
	Open Porosity (%)	**Closed Porosity (%)**	**Total Porosity (%)**	**Open Porosity (%)**	**Closed Porosity (%)**	**Total Porosity (%)**	**Open Porosity (%)**	**Closed Porosity (%)**	**Total Porosity (%)**
80°C	47.3 ± 2.2	3.5 ± 0.7	50.8 ± 2.0	48.3 ± 1.9	0.7 ± 0.2	49.0 ± 2.1	47.3 ± 2.3	2.4 ± 0.9	49.7 ± 2.6
300°C	53.0 ± 2.2	0.7 ± 0.1	53.7 ± 2.2	57.6 ± 2.0	1.6 ± 0.6	59.2 ± 2.3	57.9 ± 2.2	2.9 ± 1.2	60.8 ± 2.1
500°C	59.0 ± 4.9	0.2 ± 0.1	59.2 ± 4.9	59.2 ± 3.0	0.4 ± 0.1	59.6 ± 3.4	59.6 ± 4.3	3.5 ± 1.0	63.1 ± 3.7
700°C	58.2 ± 4.4	2.0 ± 0.4	60.2 ± 4.2	62.0 ± 3.7	0.3 ± 0.1	62.3 ± 3.3	59.2 ± 4.6	3.2 ± 1.4	62.4 ± 4.8
1000°C	62.8 ± 3.9	2.0 ± 0.3	64.8 ± 3.7	60.9 ± 3.8	2.1 ± 0.5	63.0 ± 4.0	66.3 ± 3.1	0.6 ± 0.2	66.9 ± 3.5

Table 2.6: Porosity values for samples heat treated made with the three inks.

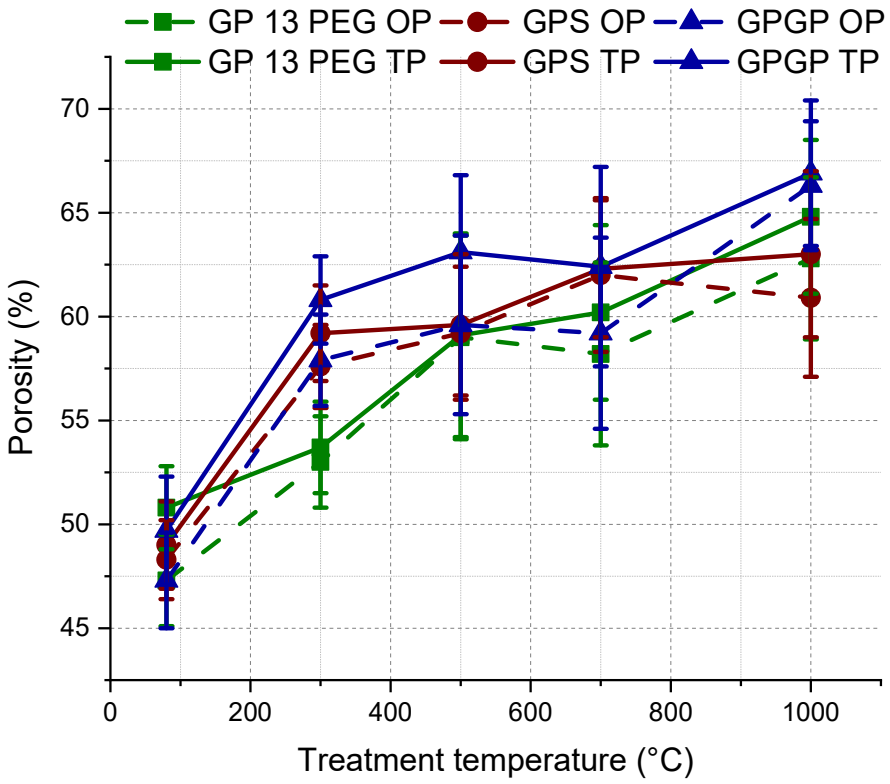

Figure 2.38: Open porosity (OP) and total porosity (TP) trends for samples made with the three inks.

2.2.4 Microstructural evolution

GP 13 PEG, GPS and GPGP after curing at 80°C for 1 day and after firing x-rays diffraction spectra are analyzed.

From XRD patterns shown in figures 2.39, 2.40 and 2.41, is possible to observe how all geopolymers have an amorphous structure until crystallization. In fact, until 700°C spectra don't show typical peaks of any crystal. Most evident peaks located at 27.08° are those belonging to the crystalline titanium dioxide form of anatase (PDF reference: 96 – 900 – 8217) and those present at 20.88° and 26.67° belonging to quartz (PDF reference: 96 – 900 – 5022). These elements are part of metakaolin as impurities and they don't interact with the reaction of geopolymerization, so they remain in the structure once the geopolymer is produced. Figure 2.42 is the diffractogram of the metakaolin used as raw material to make geopolymers. In this spectrum are also clearly noticeable typical peaks of anatase and quartz.

Comparing the various graphs of geopolymers structures through temperatures (figures 2.38, 2.39 and 2.40) is easy to notice that all of them are amorphous until 700°C, then samples fired at 1000°C show the crystallization of the sodium aluminum silicate form of nepheline (PDF reference: 00 – 083 – 2279), as confirmed by differential thermal analysis (par. 1.4.2).

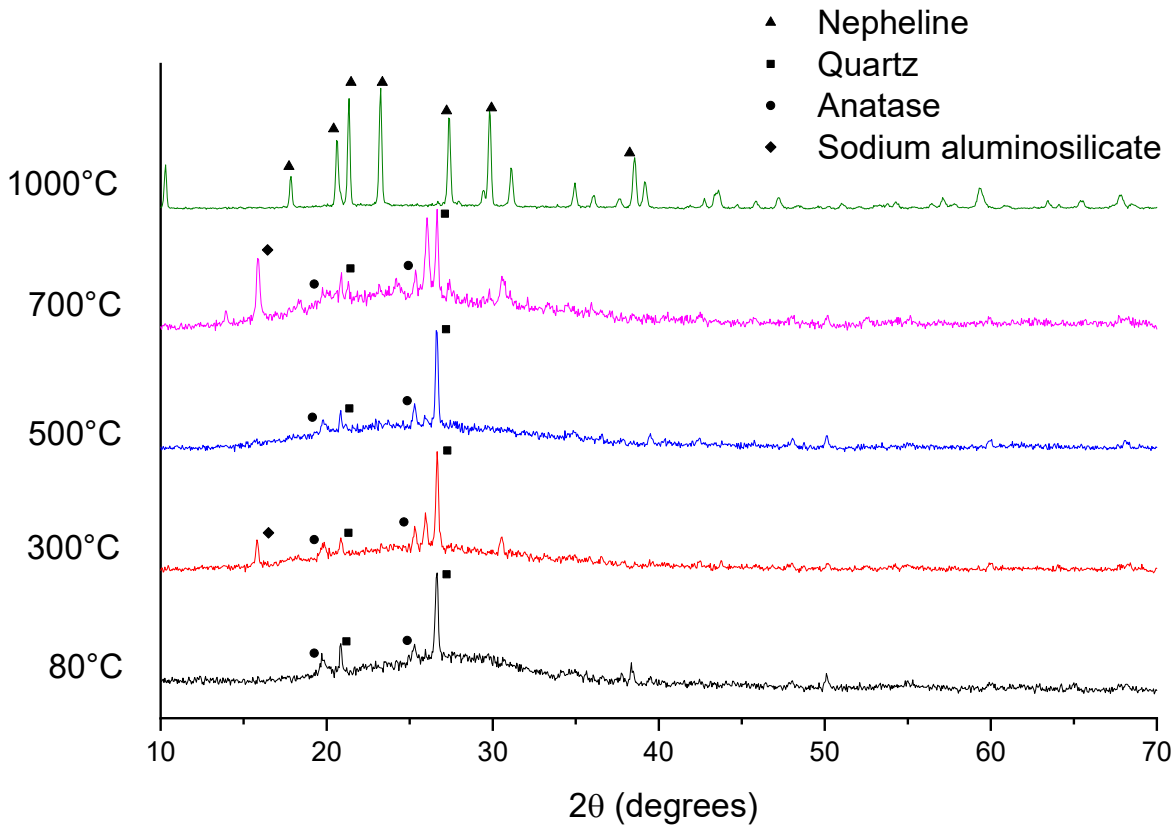

Figure 2.39: Diffractogram for GP 13 PEG after heat treatments.

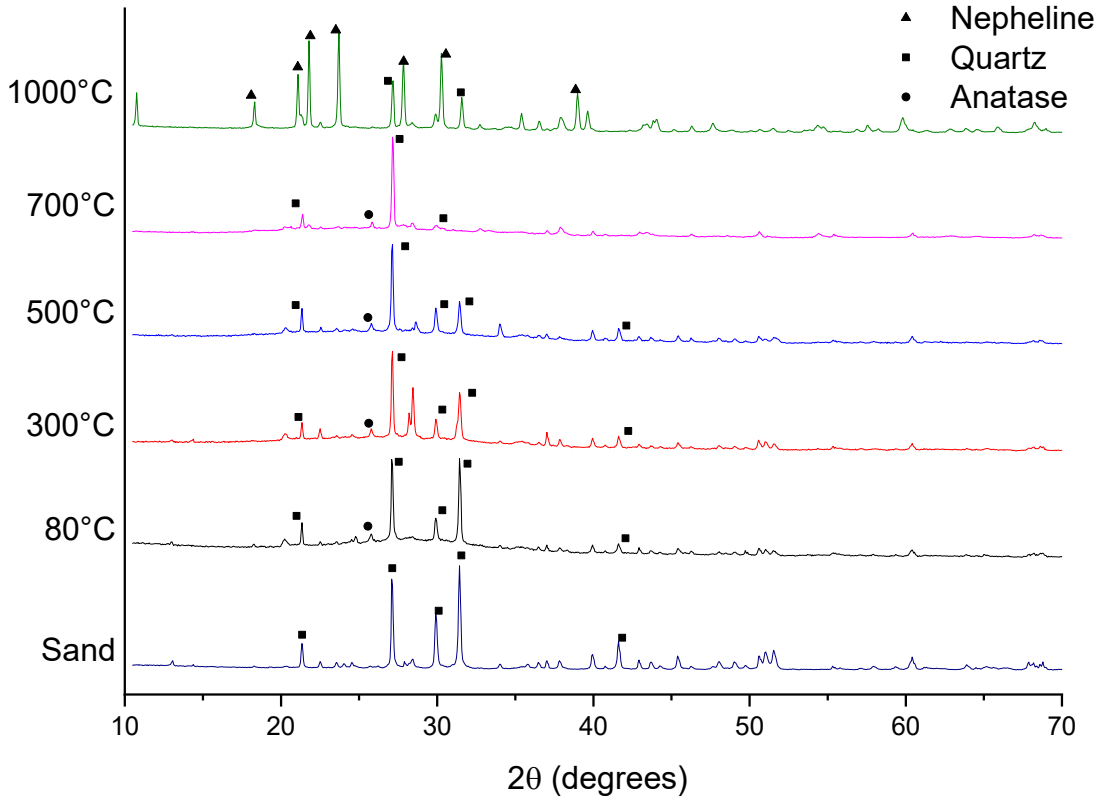

Figure 2.40: Diffractogram for GPS samples after heat treatments and natural siliceous sand.

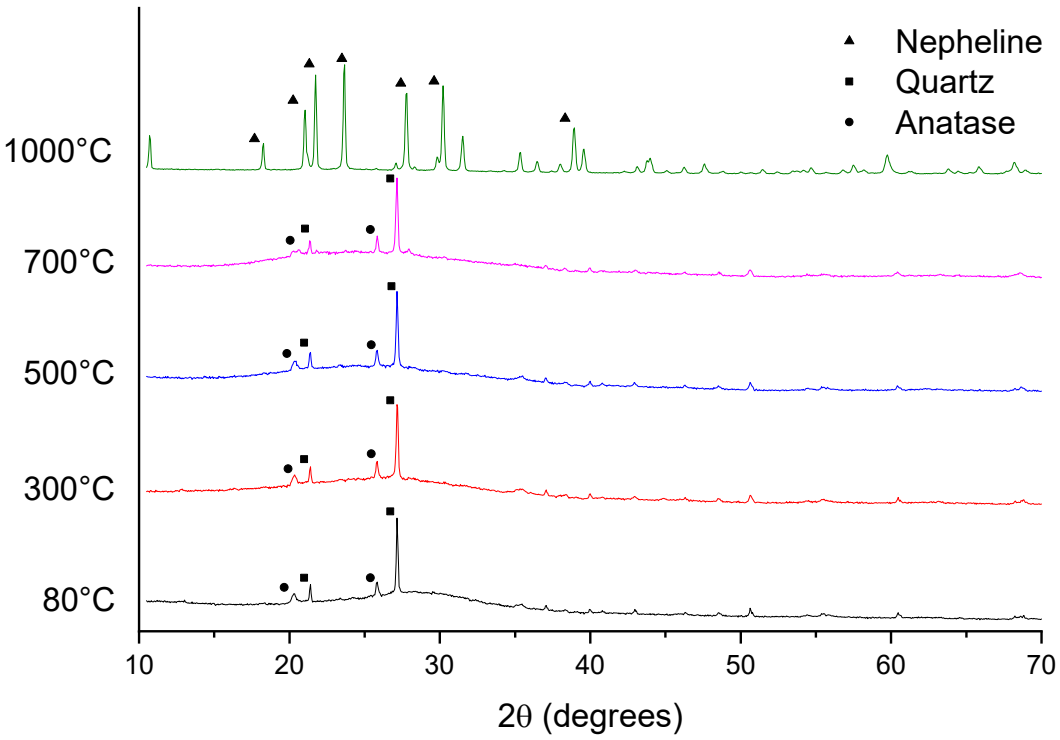

Figure 2.41: Diffractogram for GPGP samples after heat treatments.

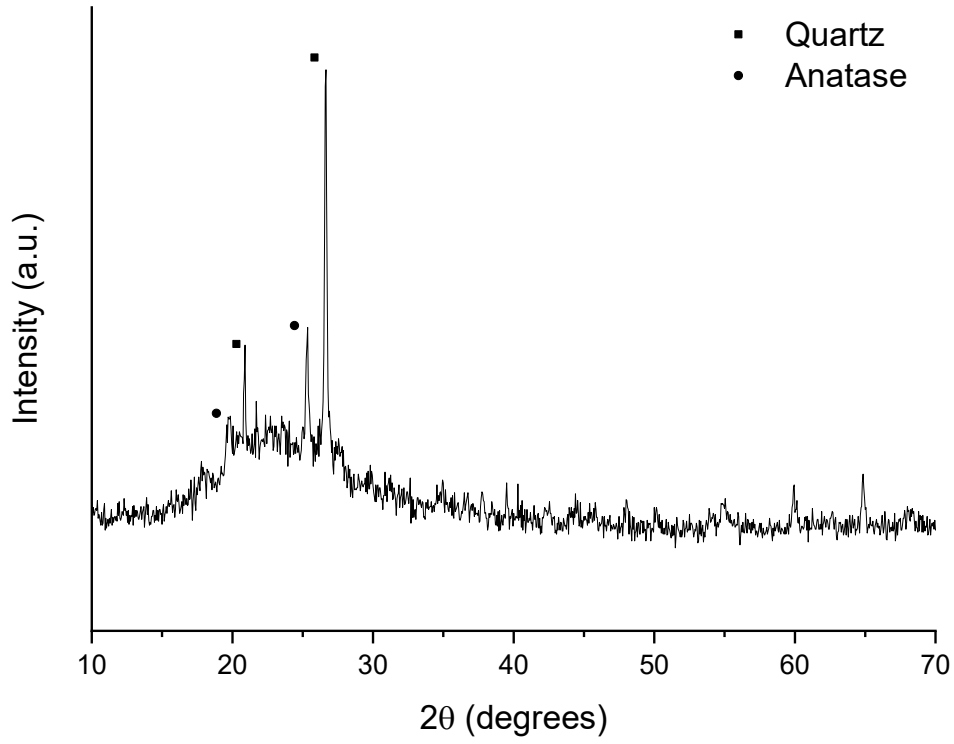

Figure 2.42: XRD pattern for the metakaolin ARGICAL M 1200S.

Diffractograms on figures 2.39 and 2.41, showing XRD patterns of GP 13 PEG and GPGP respectively, are substantially equals. This confirms that geopolymer powder added to GP 13 PEG is the same nature of the geopolymer itself, and, once treated at 1000°C, both filler and matrix crystalize into nepheline. In fact, geopolymeric powder used as filler is previously cured at 80°C, but it isn't crystalized. It should be noted that figures 2.39 and 2.42 as well show a lot more background noise in the data collection, because these analyses were done with the same instrument but with an older radiogenic tube. GPS diffractogram includes the diffraction pattern of natural siliceous sand, used as filler in the ink, that shows all the typical peaks of quartz and they are more evident in the ink patterns. As a side note, the intensity of these quartz peaks is so high that the amorphous structure and anatase peaks of the geopolymeric matrix are almost hidden. However, it is possible to see a small amount of amorphous even in the sand itself.

2.2.5 Case study: DIW of GPGP filters for catalysis [83]

One of the topics under investigation in the laboratories of the Advance Ceramics and Glasses group in the University of Padova is the use of geopolymers for filtration and catalysis. Part of the work presented in this thesis helped to make the first steps in the production of filters made of geopolymer via direct ink writing. Especially, the studies on the rheology of GPP and several trials allowed to optimize the geopolymer composition to better suit the production technology. As an example of structures made, figures 2.43 and 2.44 show samples printed as catalysts to produce biodiesel by transesterification of vegetable oil. In this case, the structures are made of two different kind of geopolymer Na-based and K-based, with different content of geopolymer powder, 25% and 30% wt. respectively.

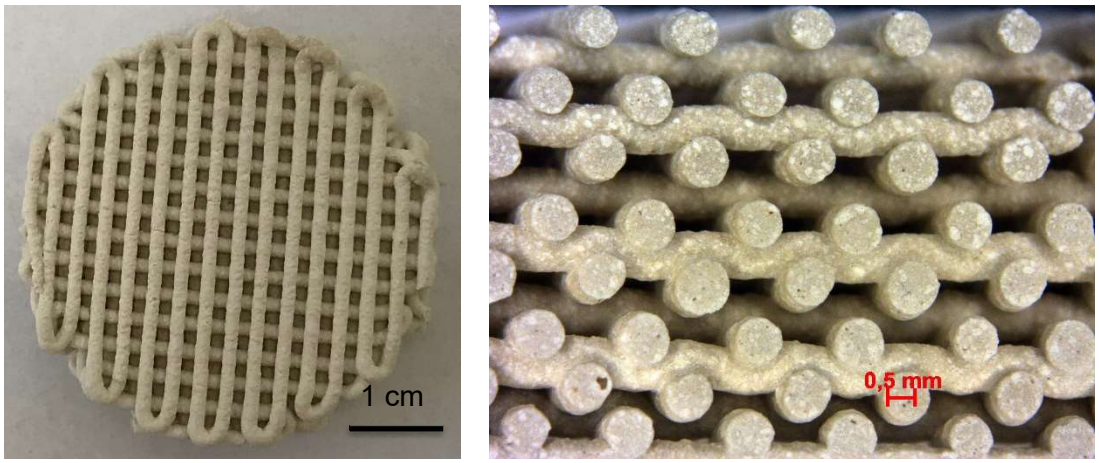

Figure 2.43: Printed filter made of Na-based GPGP.

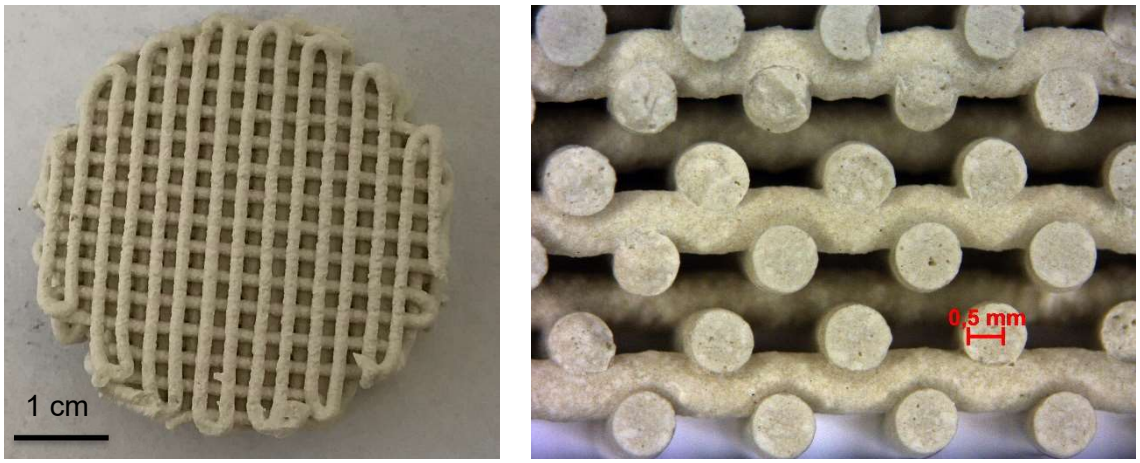

Figure 2.44: Printed filter made of K-based GPGP.

2.3 Direct ink writing of geopolymer fiber composite lattices

After the optimization of the inks by adding powders to the mixture, which led to better printability characteristics first, and then greater mechanical proprieties, especially about compression strength, both at low and high temperatures, the last step to increase and optimize lattices proprieties is the addition of fibers to the geopolymer ink, as they can be a solution to the intrinsic brittleness of ceramics, making inks tougher when subjected to a flexural stress. Therefore, the new ink should have the same optimizations previously seen, such as good printability and high compression resistance, while bringing new positive aspects. The preliminary observations on the rheology behavior of composite inks were satisfying, as these new pastes are printable like powder added geopolymers. They have high viscosity, quick geometry retention and a good production time as well, which make them keen to be used as inks in direct ink writing. The two kind of fibers chosen, already described in par. 1.2.3 , are mineral and carbon fibers, which are added to the GP 13 PEG ink during mixing, the two composite inks are labeled GPMF (figure 2.45), meaning geopolymer added with mineral fibers, and GPCF (figure 2.46), meaning geopolymer added with carbon fibers. Fibers are poured into the alkaline solution before the metakaolin, so the low viscosity and high energy mixing disperse them very well, as pictures 45 and 46 show. In the final samples, fibers alignment through the printing direction is observable (figures 2.45 (d) and 2.46 (d)). This phenomenon is caused by the high shear stresses that develop during ink extrusion through the nozzle tip and it can be exploited to further research on design-based toughening mechanisms.

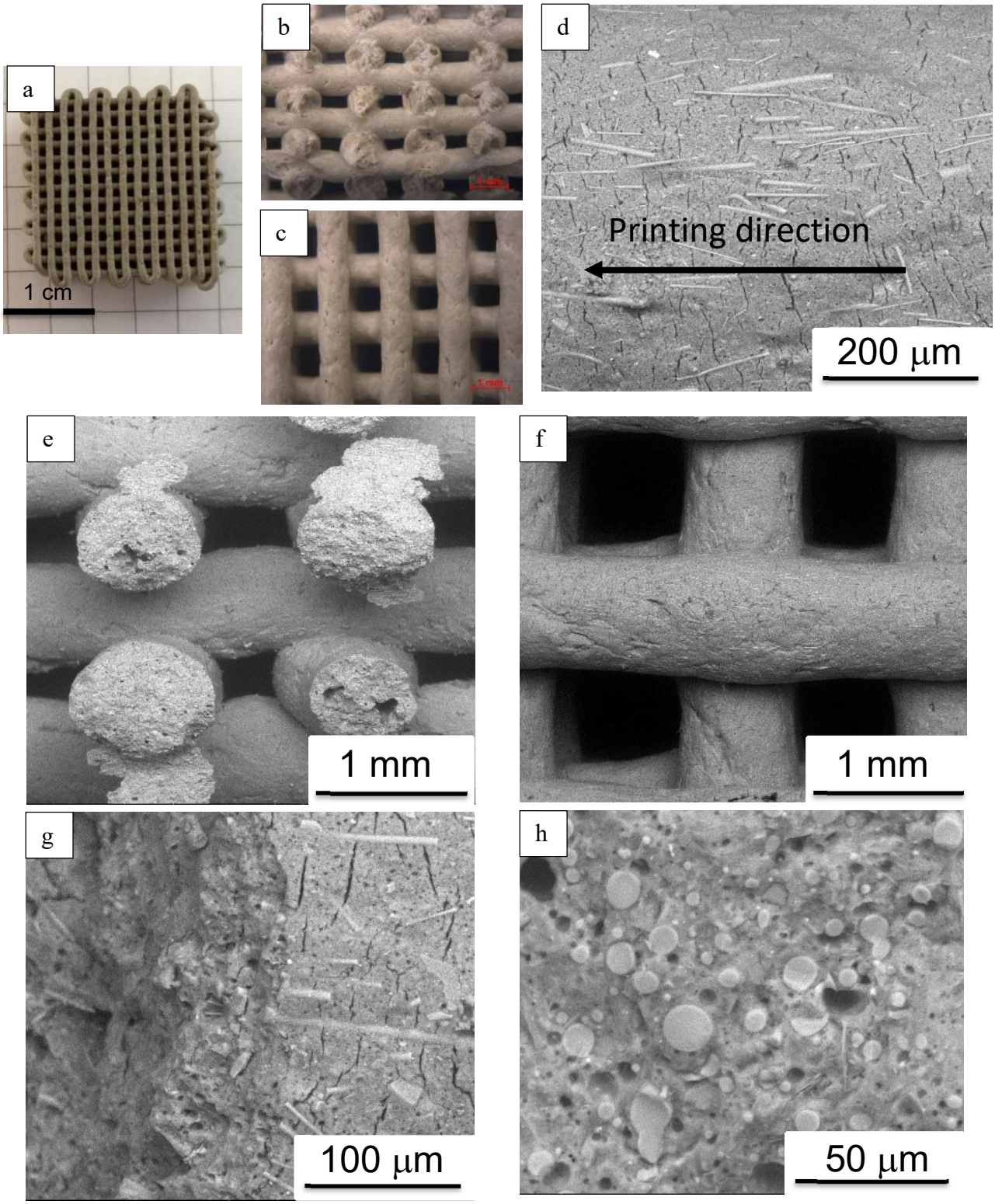

Figure 2.45: GPMF sample fired at 300°C: (a) overview; (b) side view, 10x; (c) top view, 10x; (d) strut surface, detail of printing alignment, 250x; (e) side view, 50x; (d) top view, 50x; (g) surface fracture top view, 500x; (h) surface fracture side view, 1000x.

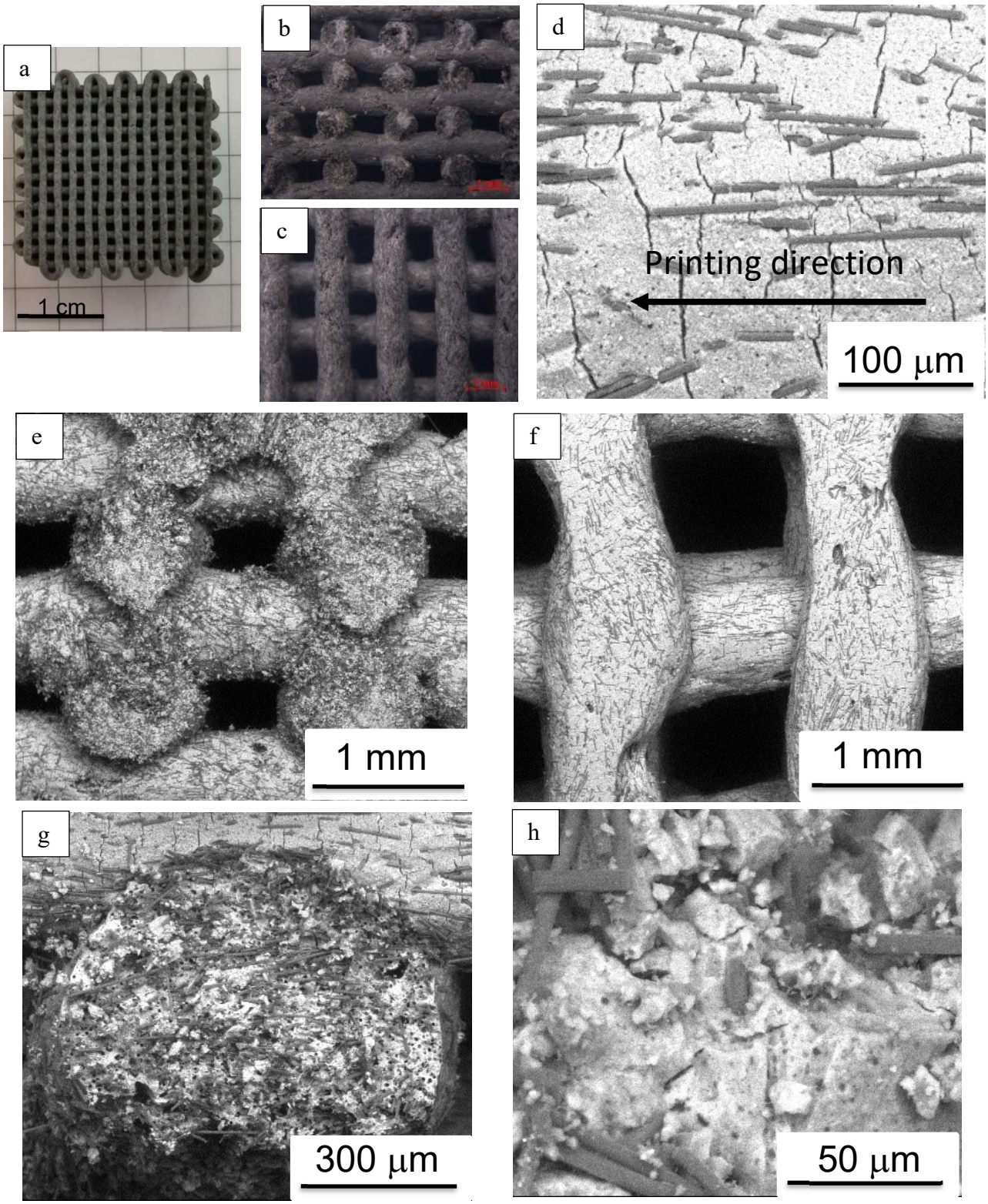

Figure 2.46: GPCF sample fired at 300°C: (a) overview; (b) side view, 10x; (c) top view, 10x; (d) strut surface, detail of printing alignment, 400x; (e) side view, 50x; (d) top view, 50x; (g) surface fracture side view, 150x; (h) surface fracture side view, 1000x.

The purpose to add fibers to a ceramic is to enhance its mechanical behavior, especially to make them less brittle. As previously said, par. 1.1.5, to enhance mechanical behavior in ceramics, ceramic fiber must have low interaction with the matrix, in order to dissipate most of the crack energy

on the interface, and not to be broken by its propagation. The difference in the matrix-fibers interaction between the two composite inks is clearly observable: mineral fibers (figure 2.45 (h)) create a stronger bond with the geopolymer than carbon ones. Thanks to their chemical composition quite similar to geopolymer and the fact that they aren't coated, the alkaline environment chemically attacks the fibers surface using the SiO_2 an Al_2O_3 to make bonds with the metakaolin forming geopolymer. This can influence the mechanical behavior of samples made with this ink possibly resulting in weaker structures, contrary to what previously observed on a similar composite with coated mineral fibers [84]. On the other hand, GPCF micrographs (figure 2.46 (h)) show fibers less bonded with the matrix, resulting in a weaker interaction between them, so higher mechanical performances are expected on this composite ink.

2.3.1 Compression strength

To compete with previously seen powder added inks, GPS and GPGP, these new composite geopolymers are analyzed by uniaxial compression tests after having undergone the same thermal treatments that gave best mechanical performances to previous inks, first cured at 80°C for 1 day right after production, then fired at 300°C, and compared with data already collected. Results are given below in tab 2.7 and figure 2.47.

Table 2.7: Compression strength values for all inks after firing at 300°C.

	Compression strength (MPa)
GP 13 PEG	18.14 ± 4.31
GPS	8.13 ± 1.05
GPGP	14.48 ± 3.02
GPMF	9.53 ± 1.71
GPCF	15.81 ± 1.12

Results confirm what previously said about GPMF composite ink, the addition of uncoated mineral fibers has lowered lattices compression strength. In facts, not only the strong interface does not allow for energy dissipation mechanisms, but the fiber addition also promotes crack growth perpendicular to the fibers direction, due to inhibited shrinkage [85, 86]. Values are around 1.52 to 1.90

times lower than the inks previously tested, and 1.66 times worse than GPCF. On the other hand, the addition of carbon fibers gives to the geopolymer better mechanical response with compression strength values comparable with powder added inks. However, composite inks show a greater homogeneity in mechanical response, which reflects in lower error values, especially for GPCF ink, probably because samples appear already cracked superficially only in direction perpendicular to fibers alignment (figures 2.45 (d) and 2.46 (d)). This gives a more constant and consistent behavior when subjected to stresses, because the cracks orientation is favored by fibers position as they form when heated, rather than growing casually oriented and thus being weak spots favoring the growth of cracks with minimal stresses applied.

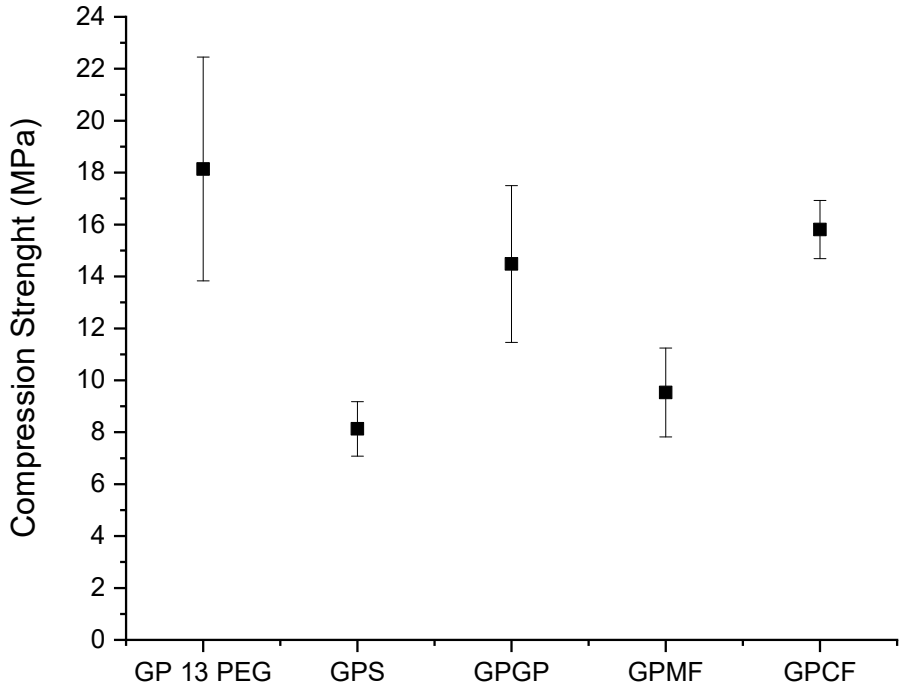

Figure 2.47: Comparison of mechanical strength for samples fired at 300°C made of all geopolymeric inks.

Anyways, the low mechanical performance of GPMF makes it a non-ideal ink to work on, so its optimization won't continue.

GPCF samples are tested mechanically also after curing at 80°C for 1 day, to confirm the fact that cracks formed in the structure after thermal treatment are not the cause of samples failure in compression. In table 2.8 are presented results as values compared to data already collected, GPCF lattices show compression strength comparable to the highest ever achieved with previous samples, meaning that carbon fibers work as a real reinforcement in geopolymer slurry.

Table 2.8: Compression strength values for samples cured at 80°C for 1 day.

	Compression strength (MPa)
GP 13 PEG	7.31 ± 1.05
GPS	17.10 ± 1.71
GPGP	8.31 ± 2.69
GPCF	17.18 ± 3.95

Figure 2.48 shows the scatter plot of mechanical tests compared with previous results with the other inks.

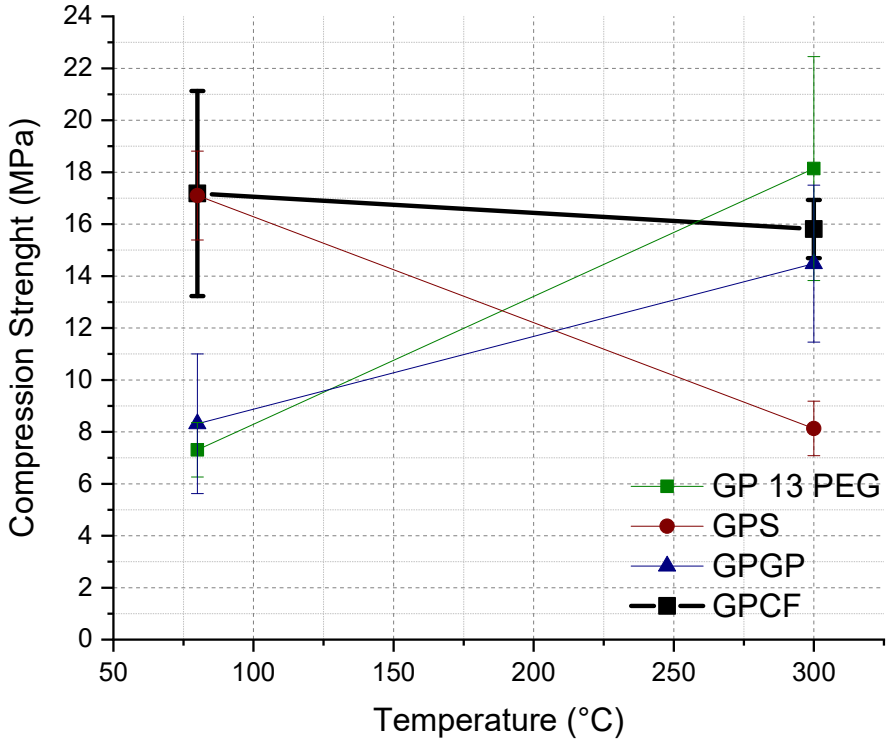

Figure 2.48: Compression strength for GPCF samples (highlighted) compared with previous inks after curing at 80°C for 1 day and firing at 300°C.

The difference on strength values of GPCF samples after curing and after firing are negligible, confirming that the presence of fibers addition induced cracks doesn't affect the overall mechanical performance of the structure, in fact micrographs of GPCF samples after curing don't show the typical cracks perpendicular to the fibers orientation (figure 2.49). Considering the error bars, those samples have mechanical resistance very similar to GPS ones. Thus, carbon fiber added geopolymeric ink is

a valid candidate to further optimizations and to being used for the production of 3-D printed geopolymeric composite structures.

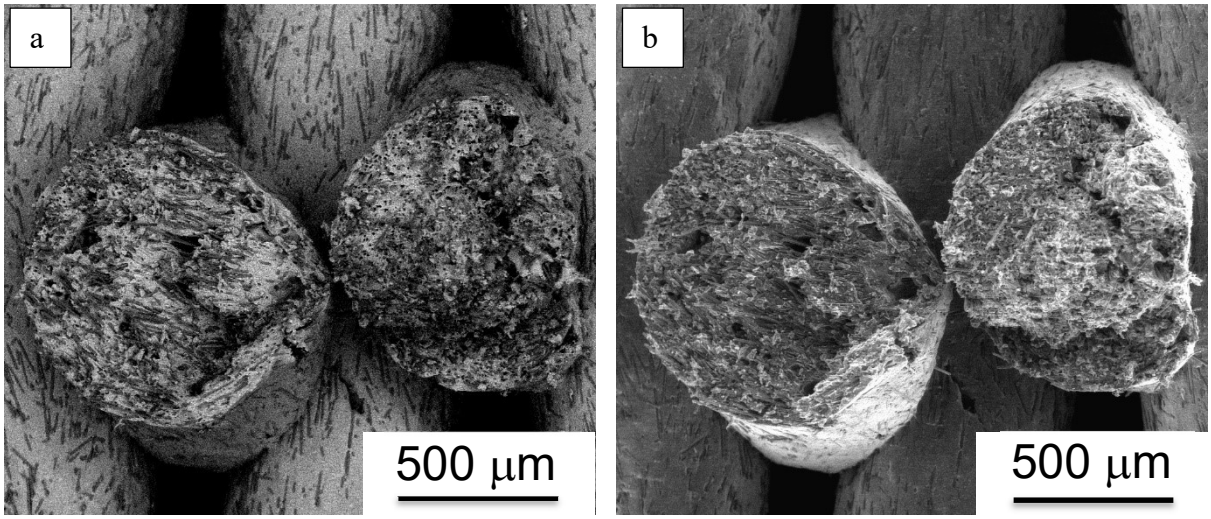

Figure 2.49: SEM micrographs for GPCF sample after curing at 80°C for 1 day, 80x: (a) backscattered; (b) secondary.

Observing the mechanical behavior tendencies of all inks, GP 13 PEG, GPS, GPGP and GPCF, once cured and after firing, 2 hypotheses can be formulated:

1. Geopolymers reach their best mechanical performances after a treatment at 300°C for 1 hour, as their compressive strength values are highly similar, considering the error bars; excluding GPS ink, for which the different thermal expansion coefficients of filler and matrix make the structure weaker than cured one;
2. The starting point, which is samples strength after curing, can be different in two ways, if geopolymer is added with high strength filler (GPS and GPCF) or not (GP 13 PEG and GPGP).

2.3.2 Flexural strength

Following are presented the results obtained by 3-point bending tests done on lattice structures, with geometry modified to suit ASTM C1161 – 18 [87] norm (par. 1.3.2). The target is to acquire a better behavior when subjected to a flexural stress, as geopolymers behave like other ceramics, that are brittle with low flexural resistance, enhancing both mechanical strength and fracture toughness. In table 2.9 are listed the maximum flexural strength values collected for GP 13 PEG, GPS, GPGP and GPCF samples with the 3-point bending tests.

Table 2.9: Flexural strength values for all inks cured at 80°C for 1 day.

	Flexural strength (MPa)
GP 13 PEG	2.50 ± 1.02
GPS	4.15 ± 0.47
GPGP	3.22 ± 1.28
GPCF	6.49 ± 0.11

Flexural resistance values reflect results obtained by compression tests, comparing all the inks used GP 13 PEG and GPGP have the least resistance, but considering the error bars, GPS can be within their range values. GPCF samples show greater bending strength up to around 2.6 times more than unfilled geopolymer, confirming literature similar results [88, 89, 90, 91]. Geopolymer reinforcement with carbon fibers enhance the overall mechanical resistance, but mostly the toughness inducing a post-cracking ductility which leads to graceful failures. This phenomenon is particularly visible on load profiles (figure 2.50) as a "tail" right after the samples have reached the maximum load that can withstand.

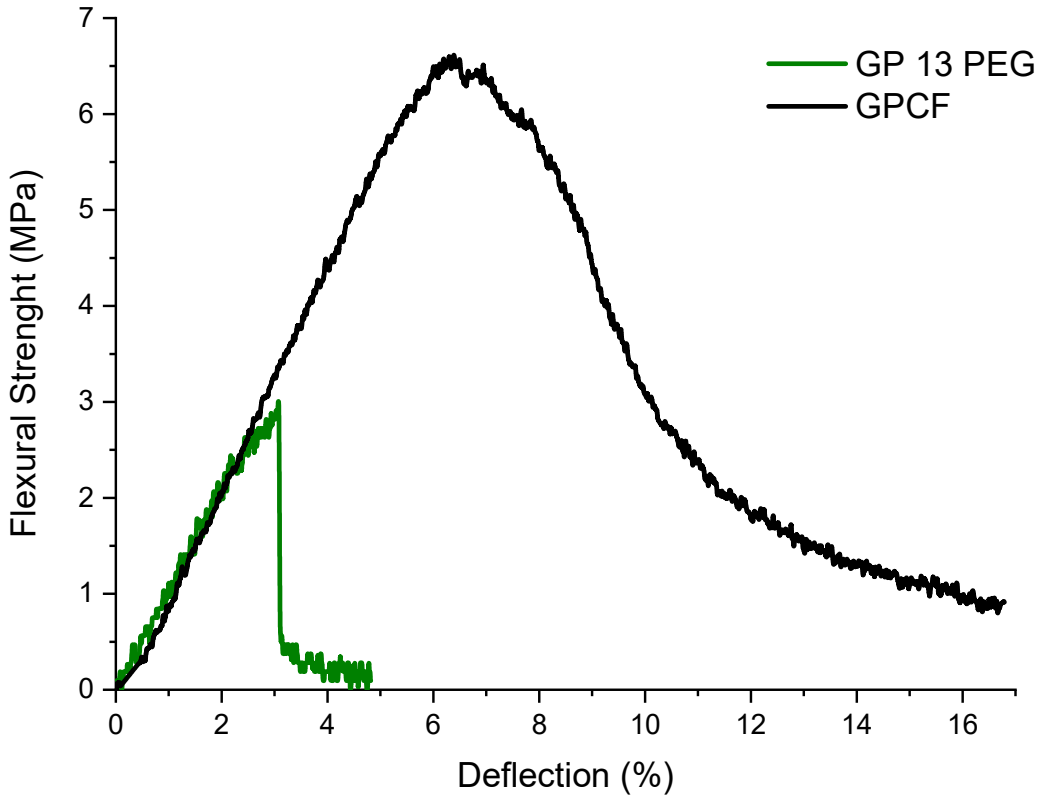

Figure 2.50: Load profile of 3-point bending test done on GP 13 PEG and GPCF samples cured at 80°C for 1 day.

The difference on behavior when stressed by a flexural load between GPCF ink and the others is evident. GP 13 PEG, that is the only present in figure 2.50 as an example of flexural behavior, GPS and GPGP show the typical brittle behavior, for which once reached the maximum load peak, they break catastrophically, because there isn't any obstacle to the crack growth. Composite load profiles, vice versa, show a trend of a ductile or quasi-ductile material. After reaching the maximum load peak, the break isn't catastrophic anymore, but the fibrous reinforcement permits a gradual collapse. In fact, fibers act as real obstacles to the advance of the crack, absorbing the fracture energy thanks to debonding and pull-out phenomena, and they form bridges from a fracture surface to the other.

SEM micrographs (figure 2.51) of lattices struts which underwent flexural failures show these two toughening mechanisms. At low magnifications (figures 2.51 (a) and (b)) it is possible to appreciate the fibers orientation, which is noticeable on the surface and on all the section through the center of the strut. Obviously, it's impossible to have only one orientation, as there will be always some pointing through another direction. Fortunately, in this case the vast majority of fibers is aligned through the printing direction. Hypothetically, to minimize this phenomenon a smaller extrusion tip can be used to better squeeze the paste allowing the extrusion of a smaller number of fibers at a time, but all highly oriented. However, in this case, reducing the tip diameter is impossible, otherwise the nozzle will clog blocking the printing process.

At high magnifications (figure 2.51 (c), (d) and (e)) toughening mechanisms are noticeable. The interaction between matrix and fibers is weak, so the matrix doesn't form strong chemical bonds with fibers. In fact, cracks energy is absorbed firstly by the break of the matrix-fibers interface and then by delamination and extraction of fibers from their seats. As a sign of these toughening mechanisms, in figure 2.51 (e), a broken interface is visible around the fiber, that is the debonding, and the physical footstep of another that has been removed from its seat, that is named pull-out.

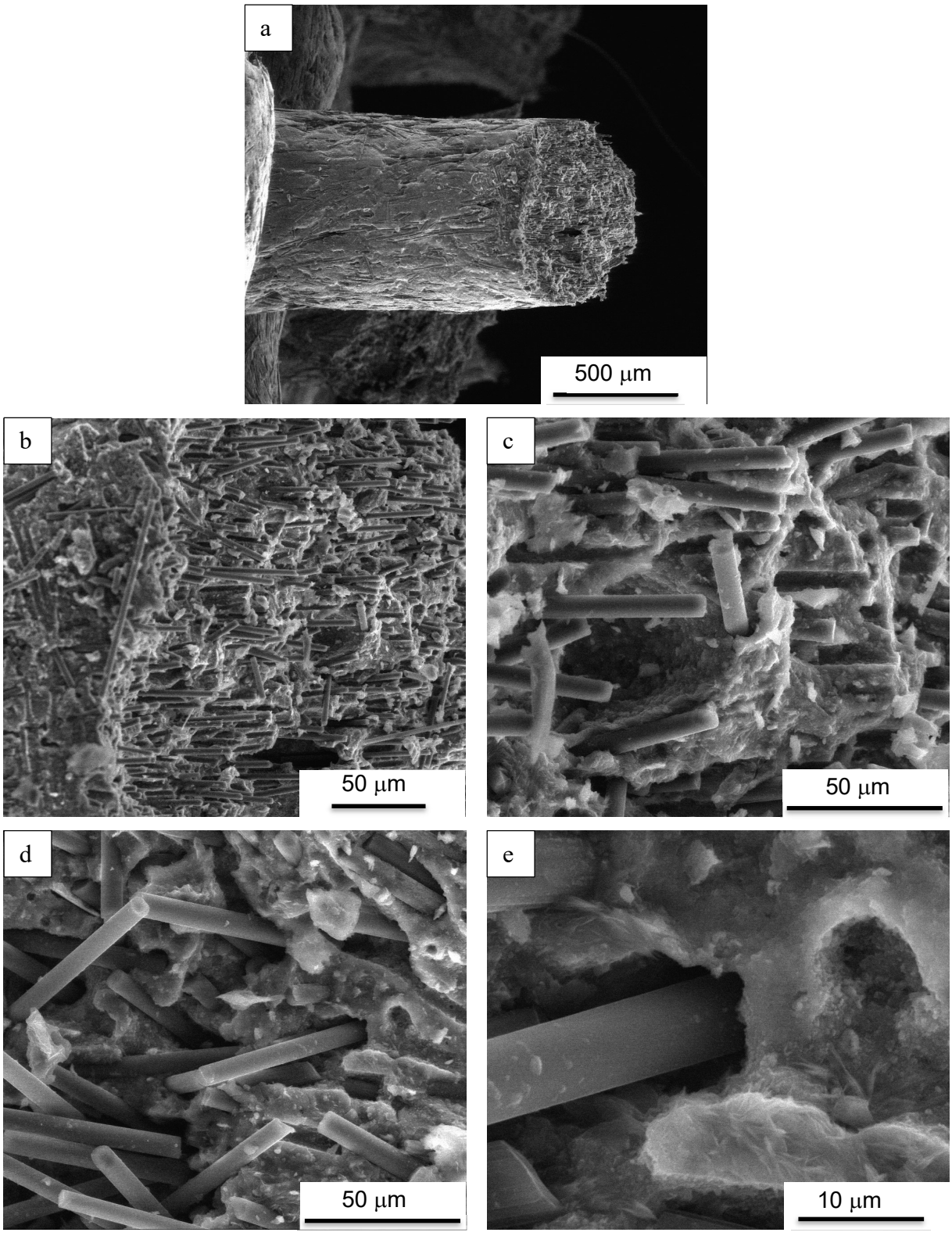

Figure 2.51: SEM micrographs of GPCF sample cured at 80°C after bending test: (a) top view, 80x; (b) fracture surface detail, 300x; (c) and (d) detail of fibers orientation on the fracture surface, 1000x; (e) detail of interface between matrix and fiber, 4000x.

2.3.3 Summary of results

The research presented in this chapter brought the following results:

- Geopolymers can be used as inks in direct ink writing;
- Rheological optimization was possible by using additives;
- Best curing and firing parameters were evaluated to gain best mechanical performance;
- The addition of fine aggregates enhances the printability and the mechanical properties;
- Printing of geopolymeric composites is possible;
- The addition of carbon fibers to the geopolymeric matrix enhances the fracture toughness.

2.3.4 Case study: geopolymer ink added with long Poly (propylene) fibers

Using long fibers to produce 3D-printed lattices gives to 2 major problems:

1. during the preparation of the geopolymer, long fibers tend to tangle together making their dispersion in the mixture very hard to obtain;
2. during the printing process fibers can stick to the extruder screw or on the nozzle tip blocking the production, or if the extrusion is running, long fibers could “escape” from the filament when producing a sharp corner, which is caused by the elastic behavior of fibers material.

Despite these problems, tests were carried out to print geopolymeric composite ink with long polypropylene alkali-resistant fibers at different volumetric percentage to observe how much fibers can be added to the geopolymer without printing issues. Geopolymer used is GP 13 PEG and fibers are MasterFiber 080 (BASF, Ludwigshafen am Rhein, Germany), technical details given by the manufacturer are shown in table below.

Table 2.10: Technical details of PP fibers as given by manufacture [92].

Polymer type	Polypropylene
Diameter (μm)	18
Fiber length (mm)	6
Color	Transparent
Density (g/cm^3)	0.91
Traction resistance (MPa)	600 – 700
Water absorbance	None
Fusion point (°C)	150 – 170
Acids/alkalis resistance	High

Following are presented results obtained:

- High percentages (up to 20% vol.): composite impossible to produce, fibers tangle and stuck together without the possibility to introduce them inside the geopolymeric slurry (figure 2.52).

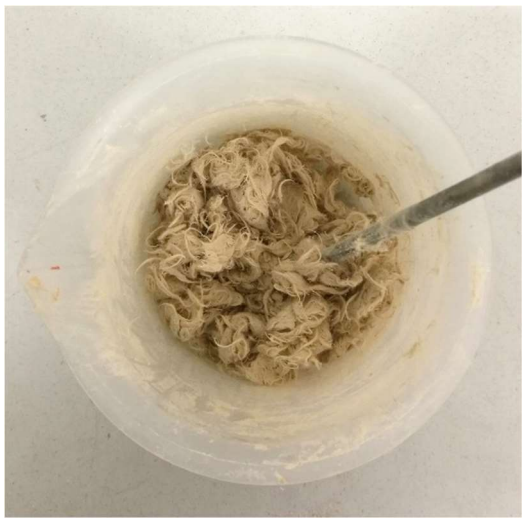

Figure 2.52: Geopolymer added with 10% vol. of PP long fibers.

- Medium percentage (5 – 10% vol.): impossibilities to print the slurry, fibers first stuck to the extruding screw then clog the printing nozzle, which leads to separation of geopolymer from

filler at higher feeder pressures. It is still possible to produce slurries with fibers content up to 10%, but they are only usable as mortars or binders (figure 2.53).

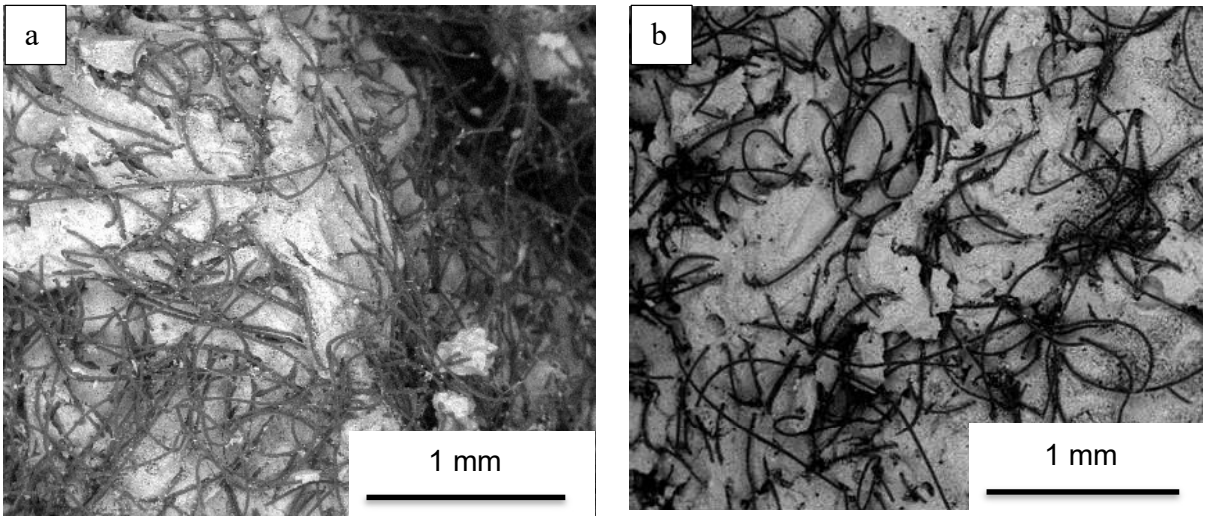

Figure 2.53: SEM micrographs of GP-PP samples, 50x: (a) 10% vol.; (b) 5% vol.

- Low percentage (1 – 1.5%): composites possible to print, but the fibers rapidly segregate causing a difference in their concentration between one strut and the next, as seen in pictures below (figure 2.54). Moreover, with low fibers volumetric content, 1% especially, the ink seems to be less printable with lower viscosity and yield stress, as it's noticeable from subsequent struts merged together in figure 2.54 (b).

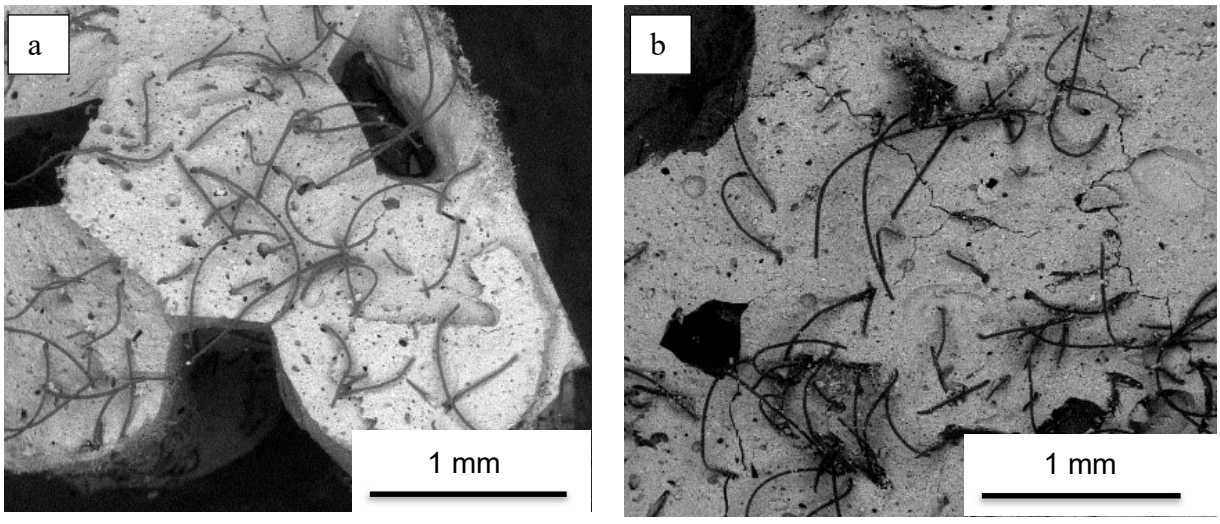

Figure 2.54: SEM micrographs of GP-PP samples, 50x: (a) 1.5% vol.; (b) 1% vol.

Observing the interface between matrix and fibers (figure 2.55), it seems to be weak, polypropylene fibers are elastic and flexible polymeric fibers, so they have to make a strong bond with geopolymer matrix in order to dissipate the cracks energy through fibers deformation and deflection, as previous work on the same composite shows [93]. This problem reflects on the fracture toughness of the composite, making it weaker with a flexural resistance that could be even lower than a sample made of matrix only. Weak interface with a plastic fiber corresponds to an easy extraction of the fibrous reinforcement form the matrix, as in the case of these samples.

To solve this issue, the use of a silane coating on the fibers could be taken in consideration to permit the creation of a fibers-matrix chemical bond.

Considering that the type of polypropylene fibers used in this experiments find their typical applications [92] on concrete addition to make it more tenacious and fire-resistant with volumetric contents of 0.5 to 1%, the results obtained are encouraging, as it was possible to not only produce the slurry with 10% vol. of PP fibers, but also printing it with 1.5 to 1% volumetric content. Anyways, the application suggested is for the production of tenacious and fire-resistant geopolymeric mortars. It is still possible to use such mortars in a DIW production system although nozzle with bigger diameter will be needed [94] (greater than 2mm).

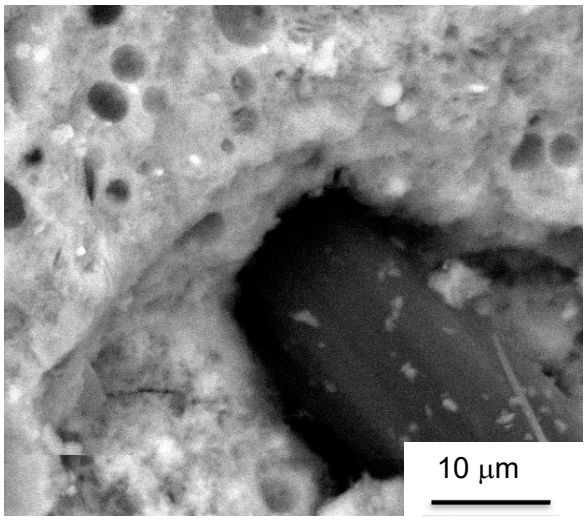

Figure 2.55: SEM micrograph of GP-PP sample, detail of fiber-matrix interface, 3000x.

Conclusions and future works

The aim of the project presented in this work was to produce 3D-printed porous samples using a composite ink with a geopolymeric matrix. The innovation of the research project consists on the implementation of a reacting material as a printable ink. In fact, geopolymers consolidate through polycondensation reaction, which changes their rheology with time in what can be seen as a 4D-printing process (where the fourth dimension is the time of geopolymerization).

The work presented in this thesis can be subdivided into three main steps:

1. The rheological optimization of geopolymer ins;
2. The mechanical optimization of 3D-printed lattices through heat treatment and their microstructural characterization;
3. The fabrication of 3D-printed samples using geopolymer composite inks.

It was used a sodium-based geopolymer based on a Davidovits patent [74] was chosen as a basis and modified with the addition of rheological agents (PEG and PAA) fine powders, natural siliceous sand and already made grinded geopolymer, and fibers, mineral and carbon. The technology used for producing samples was the direct ink writing, which is based on the continuous deposition of an extruded filament in a layer-wise form.

Rheology optimization allowed to choose the best type and amount of rheological agents. Firstly, PEG was observed having a better impact on the rheology behavior than PAA, forming a stronger gel with greater initial yield stress and viscosity. Also, the gel strength was enhanced, as the calculations on G' using the Smay equation (1) shows, as well as the ability to rapidly recover the shape once extruded. Those additives acted also as retardants to the reaction of geopolymerization, giving the slurry more time to be printed. The behavior of PEG added geopolymer and the tendency of foaming of PAA when added to the mixture, made the PEG the best choice to enhance the rheology behavior making the paste more suitable to the printing process. Secondarily, the addition in the geopolymer ink of fine powder as filler, with particle size below 300 μm, was investigated. Results show better printability with enhanced Bingham pseudo-plasticity, meaning higher viscosity, yield stress, gel strength, as well as quicker shape recovery and printing time. The first powder filler used in the geopolymer ink was natural siliceous sand, thus mechanical properties were investigated for both sand added geopolymer, named GPS, and PEG added one, called GP 13 PEG.

3D-printed lattices made of GP 13 PEG and GPS ink were then produced and their mechanical properties optimized. GPS samples showed better performances up to 2.1 times better than GP 13 PEG, because the stress is borne by the sand particles, which have higher strength compared to geopolymers. Best curing conditions were identified in 80°C for 1 day; the slight increase in compressive strength provided by higher time is not so relevant from an industrial point of view. Geopolymer filled geopolymer (GPGP) samples were also tested, resulting in compression strength similar to GP 13 PEG ones; In fact, in this case the filler didn't act as reinforcement. Firing treatment showed a similar trend on mechanical characteristics on GP 13 PEG and GPGP samples, with the maximum strength reached at 300°C, when all the geopolymers can be considered fully reacted and the physisorbed water evaporated. GPS fired samples appeared severely cracked, because of the difference in thermal expansion coefficient between filler and matrix, so their performance is affected resulting in low compression resistance once treated. At higher temperatures, up to 1000°C, lattices showed a decrease in term of compression strength, due to shrinkage and microstructural changes, which occur during crystallization of nepheline, as XRD diffractograms showed. However, GPGP samples showed higher resistance in temperature, probably because of the geopolymeric filler presence that gives better thermal stabilization to the structure during heating inhibiting the appearance of cracks.

Fiber geopolymeric composite inks were also successfully fabricated, thanks to a rheological behavior similar to powder added geopolymer inks. Two different type of fibers were used, mineral (GPMF) and carbon (GPCF), to produce lattices that underwent the same mechanical properties evaluation previously performed. GPMF samples showed the lowest compression strength among all the inks, because uncoated mineral fibers create bonds with the matrix that turns out to be too strong to act as obstacle for cracks growth. On the other hand, GPCF samples showed good compression strength, for which their behavior under flexural stress were observed. In comparison to GP 13 PEG, the addition of carbon fibers worked as a reinforcement against cracks propagation inducing a ductile or quasi-ductile behavior to a material that otherwise would be extremely brittle. The fracture surface analysis has allowed the observation of the two phenomena which lead to increased toughness: delamination and pull-out, which are visible thanks to fibers coming out from the fracture surface and to their physical footsteps once extracted from the matrix.

To conclude, the objectives of the present thesis are mostly reached; in fact, it was possible to implement composite geopolymeric inks in a direct ink writing process to produce porous reticular samples with enhanced fracture toughness.

Further works can be focused on the optimization of geopolymer inks based on other elements, such as potassium or calcium, as well as the solution of clogging problems when using long fibers in the geopolymeric ink and the use of silane coating on PP fibers to make a stronger fiber-matrix interface. Furthermore, an interesting subject could be the development of a design-based toughening mechanism in 3D-printed object with composite geopolymeric inks exploiting the fibers orientation through the printing direction.

Appendix A

Impregnation of 3D-printed geopolymer composite lattices

Ternary/quaternary composites made by 3D-printed lattices with geopolymer composite ink impregnated with a silicone, which can be compatible with the material used for the realization of the printed object, are produced. The idea behind this side-topic to the main research is to give dumping properties to the GPGP lattices, reducing their brittleness.

Ink used, already described, is GP 13 PEG with 20% wt. of geopolymeric powder added as filler, printed in shape of samples used in uniaxial compression tests, ~ 20.00 x 20.00 x 7.20 mm^3, and cured at 80°C for 1 day. The silicone used for impregnation is bi-component Angeloni RTV960 pure and added with 50% wt. of barite, to give some rigidity to the structure and to avoid detachment from the lattice. The method of impregnation consists simply on immersing the 3D-printed object in a square mold in which silicone was previously poured, then the object is kept inside the silicone until its reticulation ends. In figure A.1 are presented some samples made this way, unfilled silicone is yellow, while silicone added with 50% wt. of barite is light brown.

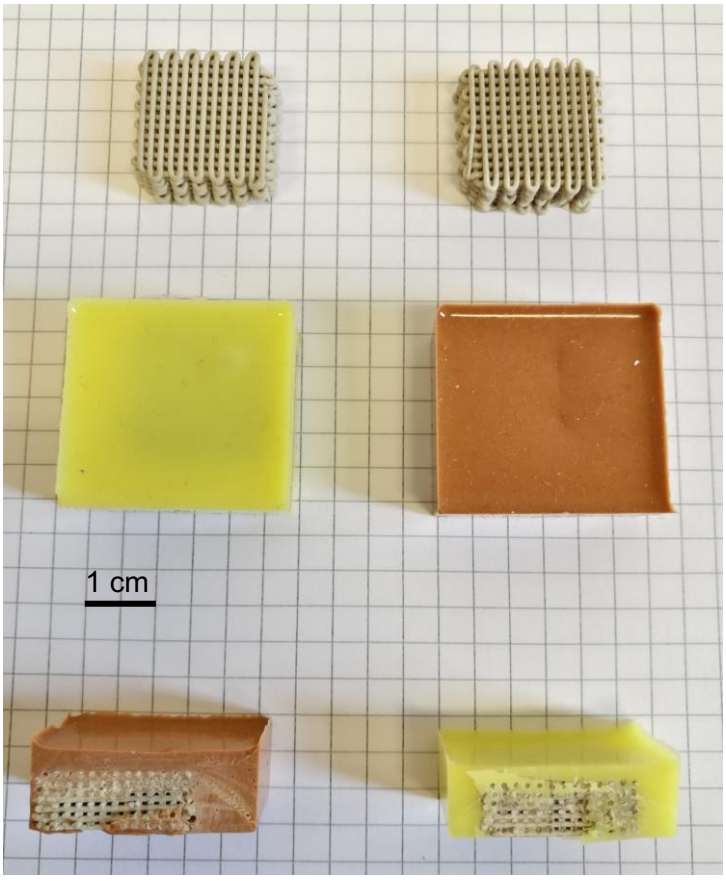

Figure A.1: Ternary/quaternary composite samples produced: (top) starting GPGP lattices, (mid) top view of impregnated composites (in yellow pure silicone, in light brown silicone added with barite), (bottom) cross-section view of composites.

The impregnation is not optimal, as it's possible to see in cross-section views in figure A.1, the viscosity o the silicone is too high, and some air is still entrapped inside the 3D structure. Moreover, the density of silicone added with 50% wt. of barite is greater than the overall density of the lattice, which tends to float, so it has to be kept in position to be fully wetted and infiltrated.

Anyway, the research presented in this appendix can be used for further optimizations on the production process to successfully realize composites this way, by:

- Changing the method of impregnation, by injecting silicone inside the lattice and keeping the mold under vacuum to let the air escape;
- Changing the silicone to another less viscous;
- Using another ink, especially GPCF ink, to enhance mechanical behavior of the structure in both compression and flexural strength, compared to GPGP samples.

Appendix B

AMITIE Secondment in Saint-Gobain Research Provence activities

The research activities were focused on the interaction of printed structures with the substrate in which they have been printed and interactions between subsequent printed layers. Regarding the substrate, it is natural to think about the adhesion of printed materials with the deposition surfaces. A "homemade" tack test was designed to quantify the force of adhesion with different substrates.

An important task that Saint-Gobain research department is trying to solve is the possibility of printing on vertical substrates. Since there isn't any possibility to have a 3D-printer that can actually print on vertical substrates, the problem shifted on another question: how does gravity affect printed structures while kept in vertical? Their behavior was recorded to evaluate deformations as a function of time by using a camera set to take a frame every 30 seconds.

B.1 Tack test

The test was designed around a standardized method ASTM D2979 [95] (Pressure-Sensitive Tack of Adhesives Using an Inverted Probe Machine), using a mechanical machine for uniaxial tensile and compressive strength analysis and changing some parameters to adapt it to non-Newtonian fluids, such as geopolymeric slurries. Probes used are made of steel and tungsten carbide with cylindrical geometry and diameter of 13,97 mm (figure B.1) connected to a 10 N load cell to obtain data with best accuracy possible.

The test procedure consists of 4 steps:

1. approaching the slurry surface at a speed of 10 mm/min;
2. dipping the probes into the slurry until a force of 0,1 N is reached;
3. waiting 10 second to release all the tensions induced in the sample;
4. lifting the probe at the same speed of step 1.

Figure B.1: Steel (left) and WC (right) probes used for tack tests

The result will be a force profile (figure B.2) in which the four steps can be identified.

The fourth step shows a negative peak of the force and can be subdivided into two regions:

a. the probe starts to be lifted, the force increases on the negative field until the cylinder surface encounters the slurry surface;
b. From now the two surfaces begin to lose contact and a cylinder of slurry is being pulled and deformed until the deformation is too high and a detachment occurs (see figure B.3 and B.4).

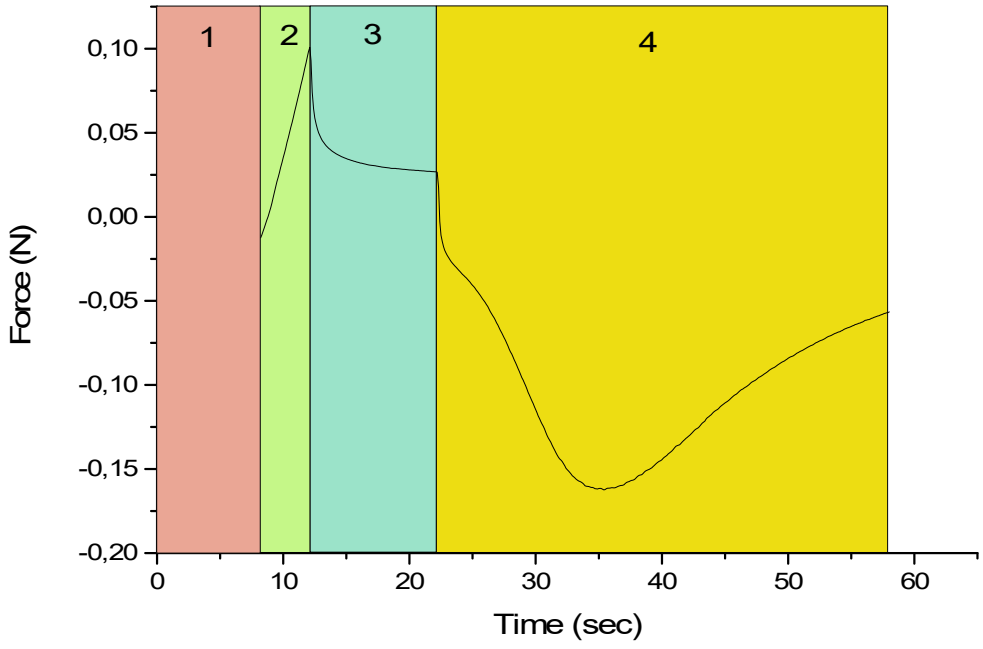

Figure B.2: Diagram of a tack test

Figure B.3: Deformation of the pulled geopolymer cylinder

Figure B.4: Geopolymer cylinder detachment

Tack tests were done on freshly made geopolymer and over time, to observe the evolution of strain while geopolymerization occurs.

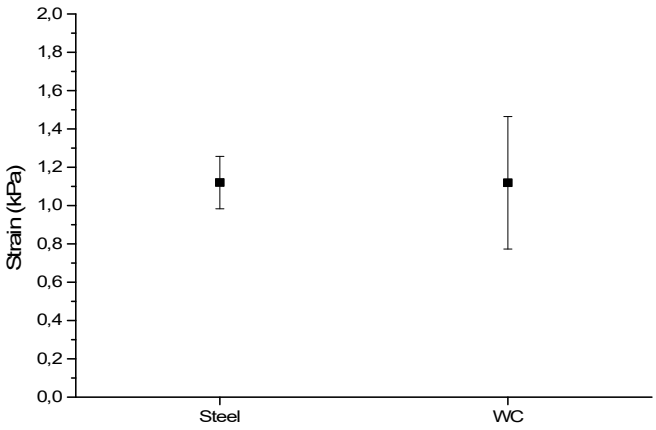

Figure B.5: Freshly made geopolymer strain

Results show no differences between steel and tungsten carbide on the average strain strength. It can be referred to the samples material, the same geopolymer, that has the same behavior in both cases, so, the test can be related to the material intrinsic properties, such as rheology and surface tension. Neither steel nor tungsten carbide show chemical affinity with the slurry for such a short contact time. High error bars are due to the load cell accuracy, that can feel minimum vibrations coming from the machine tabletop.

Tack test over time consists of 16 tack tests done every 5 minutes for 76 minutes of total analysis duration. During the experiment, temperature of material was recorded by a thermocouple in close contact to bulk material.

Geopolymerization is an exothermic reaction of polycondensation that proceeds during time, changing the slurry rheological properties from one test to another. Therefore, the strain increases linearly during subsequent tests, the fitting lines have a slope of 0.014 ± 0.003 with a correlation parameter of $R^2 = 0.626$ for the steel probe, and of 0.023 ± 0.003 with $R^2 = 0.787$ for the carbide probe. The low values of the correlation parameters are due to the fluctuations of the measured strain values.

Thermal curve for steel probe shows a more uniform behavior than carbide one, because of a mistake occurred during the tests, the thermocouple was held too much near to an ice bucket used for transporting samples from where they were produced to the testing machine. At around 25th minute the ice bucket was moved away from the sample and from that moment temperature rose more quickly, reaching, at 76th minute, 24°C, the final temperature of steel (around 25°C), but beginning from two very different temperatures, respectively 16,3°C for steel probe and 10,8°C for the WC one. This can explain the difference on the fitting lines slopes.

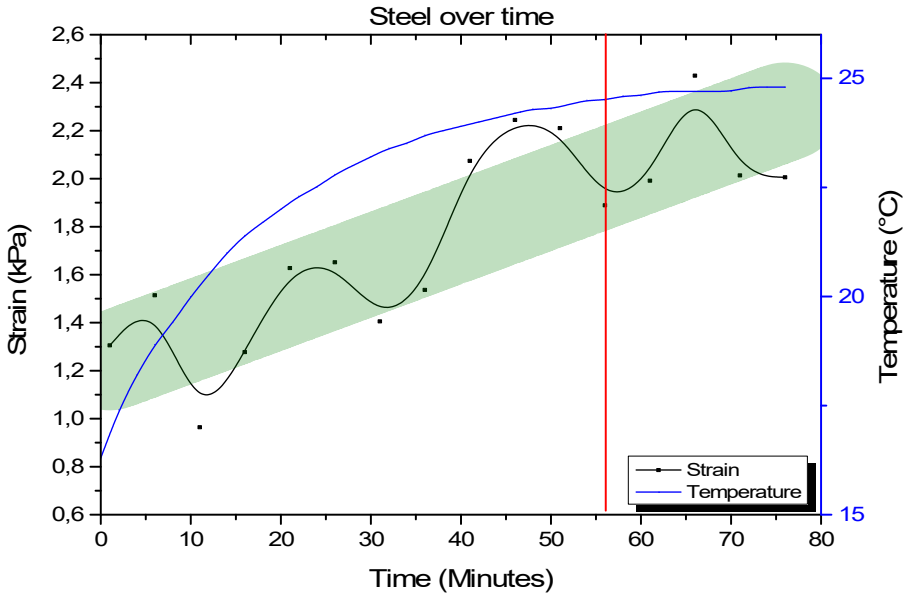

Figure B.6: Evolution of temperature and strain during time for steel probe

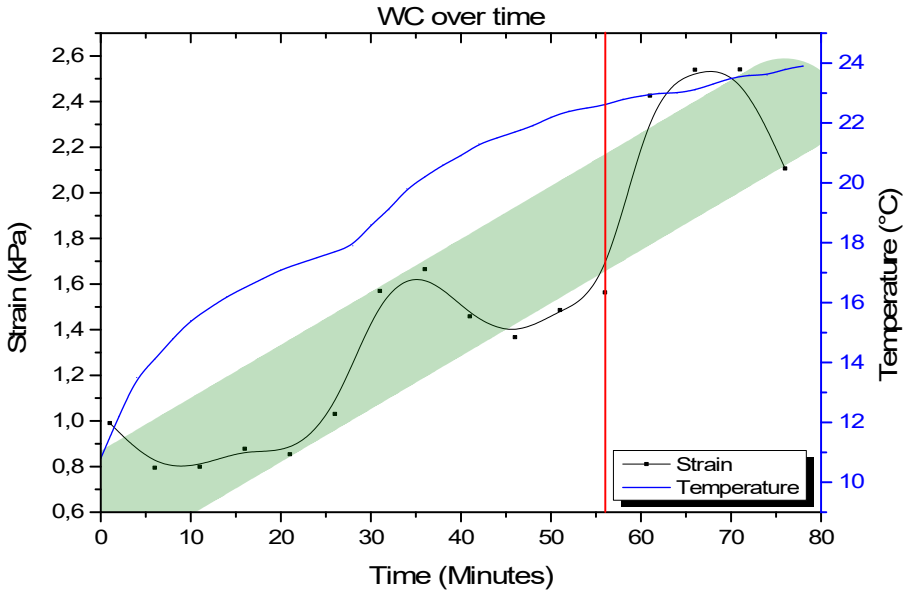

Figure B.7: Evolution of temperature and strain during time for WC probe

After a certain amount of time, the adhesion between the slurry and the probe become worse; this is highlighted by the red lines shown in the diagrams above (figures B.6 and B.7). Probably, bubbles of air entrapped during the first two steps can't escape from the slurry, due to its higher viscosity 1 hour after preparation (figure B.8). However, data over 60 minutes follow the same linear correlation of previous ones.

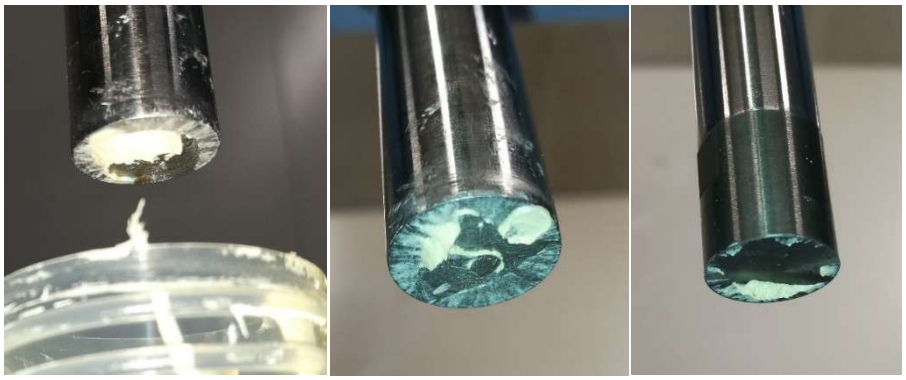

Figure B.8: Adhesion loss with the geopolymeric slurry after 56 minutes

In conclusion, tack tests were done for fresh geopolymeric slurries and over time, to evaluate the adhesiveness behavior during the reaction. All data show a high deviance due to the nature of the test and to the samples characteristics. Analysis through time show a linear trend, which means higher strain on higher times. This may be correlated to the evolution of viscosity during reaction.

B.2 Timelapses

The idea behind this test is to observe the printed structures deformation while their printing substrate is kept in vertical (figure B.9). The test consists of taking frames, by a camera, of the vertical substrate every 30 seconds for several hours. The structures were printed in 3 different number of layers: 5, 10 and 15, same parallel geometry (sections of 15 x 10 mm^2), every layer is 650 μm height with a printing nozzle diameter of 840 μm.

Vertical deformation due to gravity effects can be evaluated via frames analysis by measuring the structures angle of deflection. The main parameters taken in consideration are: the gap between the nozzle and the printing substrate, which determines the adhesion with the metal substrate; the height of subsequent layers, which influences overlap and adhesion between layers; the extrusion pressure and feed rate, which affects the amount of material used and the overall structure mass.

Printing was done on 6 stainless steel substrates, 5 of which scratched with abrasive papers with different particle size (15, 25, 58 and 125 mm) and the latter not scratched (used as it is), to evaluate if there were differences on the adhesion to the surface.

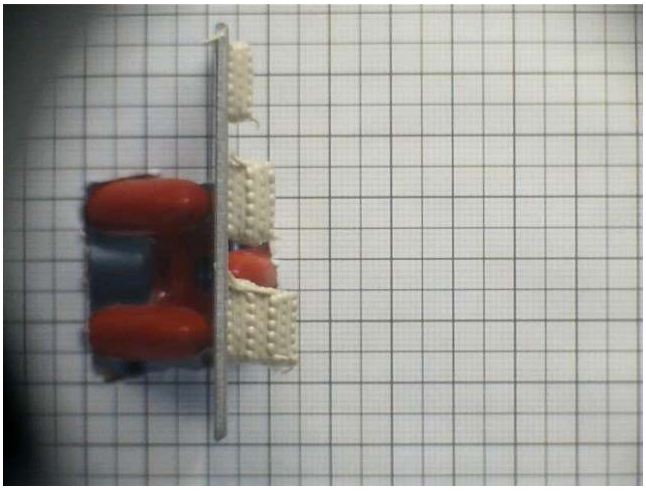

Figure B.9: One of the frames of the vertical timelapses

However, the data collected weren't consistent, as by the end of the experiments the samples seemed attached to the substrate, but they detached with a little external force, for all type of scratches. This means that further works have to be done in order to establishing which kind of interaction occurs between steel and geopolymer, as seen in literature [96].

References

[1] G. M. Paolucci, Lezioni di Metallurgia vol. 1, 90-114, Edizioni Libreria Progetto, 2002

[2] S. Somiya, F.Aldinger, N. Claussen, R. M. Spriggs, K. Uchino, K. Koumoto, M. Kaneno, Ceramics Volume II: Processing and their Applications, 417-443, Elsevier Inc., 2003

[3] J. Davidovits, Geopolymer Chemistry and Applications, Institut Géopolymère, 2011

[4] P. K. Mallick, Fiber-Reinforced Composites Materials, Manufacturing and Design, 2.2.3, Taylor & Francis Group, LLC, 2008

[5] Narottam P. Bansal, Handbook of Ceramic Composites, 10-11, Springer Science + Businnes Media, Inc., 2005

[6] R. A. Stinton, D. P. Caputo, A. J., and Lowden, Synthesis of fiber-reinforced SiC composites by chemica vapour infiltration, 347-350, Am Chem Soc Bull. 65, 1986

[7] J. L. Provis and J. S. J. Van Deventer, Geopolymers Structure, processing, properties and industrial applications, CRC Press, 2009

[8] C. Villa, E.T. Pecina, R. Torres, L. Gómez, Geopolymer synthesis using alkaline activation of natural zeolite, Construction and Building Materials 24 (2010) 2084-2090

[9] P. Hlavácek, V. Smilauer, F. Skvára, L. Kopecky, R. Sulc, Inorganic foams made from alkali-activated fly ash: Mechanical, chemical and physical properties, Journal of the European Ceramic Society 35 (2015) 703-709

[10] A. Zocca, P. Colombo, C. M. Gomes, J. Günster, Additive Manufacturing of Ceramics: Issues, Potentialities, and Opportunities, J. Am. Ceram. Soc., 98 [7] 1983-2001 (2015)

[11] J. Cesarano, P.D. Calvert, Freeforming objects with low-binder slurry, US 6027326, 2000

[12] J. Davidovits, Geopolymers: Inorganic Polymerics New Materials, Journal of Thermal Analysis, vol. 37, 1633-1656, Geopolymer Institute, 1997

[13] J. Davidovits, The need to create a new technical language for the transfer of basic scientific information. Transfer and Exploitation of Scientific and Technical Information, EUR 7716, Luxembourg, Commission of the European Communities, 1982

[14] K. Komnitsas and D. Zaharaki, Geopolymerization: A review and prospects for the minerals industry, Minerals Engineering, 20, 1261-1277, Elsevier Ltd., 2007

[15] P. Duxson, A. Fernández-Jiménez, J. L. Provis, G. C. Lukey, A. Palomo, J. S. J. van Deventer, Geopolymer technology: the current state of the art, J Mater Sci, 42, 2917-2933, Springer Science + Businnes Media, LLC, 2007

[16] T. D. Hung, P. Louda, D. Kroisova, O. Bortnovsky, N. T. Xiem, (2011), New Generation of Geopolymer Composite for Fire-Resistance, Advances in Composite Materials - Analysis of

Natural and Man-Made Materials, Dr. Pavla Tesinova (Ed.), ISBN: 978-953-307-449-8, InTech

[17] C. G. Papakonstantinou and P. N. Balaguru, Use of geopolymer matrix for high temperature resistance hybrid laminates and sandwich panels, Geopolymer 2005 Proceedings, 201-207, 2005

[18] J. Davidovits and M. Davidovics, Composite Materials with Geopolymer Matrix, Geopolymer '88 Proceedings, 325-337, 1988

[19] T. Lin, D. Jia, P. He, M. Wang and D. Liang, Effects of fiber length on mechanical properties and fracture behavior of short carbon fiber reinforced geopolymer matrix composites, Materials Science Engineering, A 497, 181-185, Elsevier B.V., 2008

[20] Q. Zhao, B. Nair, T. Rahimian, P. Balaguru, Novel geopolymer based composites with enhanced ductility, J Master Sci, 42, 3131-3137, Springer Science + Businnes Media, LLC, 2007

[21] Z. Li, Y. Zhang and X. Zhou, Short Fiber Reinforced Geopolymer Composites Manufactured by Extrusion, J. Mater. Civ. Eng., 17, 624-631, ASCE, 2005

[22] A. Natali, S. Manzi, M. C. Bignozzi, Novel Fiber-reinforced composite materials based on sustainable geopolymer matrix, Procedia Engineering, 21,1124-1131, 2011

[23] D. L. Y. Kong, J. G. Sanjayan, Damage Behavior of geopolymer composites exposed to elevated temperatures, Cement & Concrete Composites, 30, 986-991, 2008

[24] ISO/ASTM 52900:2015 [ASTM F2792], Additive manufacturing — General principles — Terminology, 2015 – 12

[25] Loughborough University, The 7 categories of Additive Manufacturing, (n.d.). http://www.lboro.ac.uk/research/amrg/about/the7categoriesofadditivemanufacturing/

[26] D.C. Hofmann, J. Kolodziejska, S. Roberts, R. Otis, R.P. Dillon, J.-O. Suh, Z.-K. Liu, J.-P. Borgonia, Compositionally graded metals: A new frontier of additive manufacturing, J. Mater. Res. 29 (2014) 1899–1910

[27] M. Vaezi, S. Chianrabutra, B. Mellor, S. Yang, Multiple material additive manufacturing – Part 1: a review, Virtual Phys. Prototyp. 8 (2013) 19–50.

[28] W. Kollenberg, Ceramic and Multi-Material 3D-Printing, Keramische Zeitschrift. 66 (2014) 233–236

[29] Z. Chen, Z. Li, J. Li, C. Liu, C. Lao, Y. Fu, C. Liu, Y. Li, P. Wang, Y. He, 3D printing of ceramics: A review, Journal of the European Ceramic Society 39 (2019) 661–687

[30] J. a. Lewis, J.E. Smay, J. Stuecker, J. Cesarano, Direct ink writing of three-dimensional ceramic structures, J. Am. Ceram. Soc. 89 (2006) 3599–3609

[31] S. Eqtesadi, A. Motealleh, P. Miranda, A. Pajares, A. Lemos, J.M.F. Ferreira, Robocasting of 45S5 bioactive glass scaffolds for bone tissue engineering, J. Eur. Ceram. Soc. 34 (2014)

[32] F.C.G. de Sousa, J.R.G. Evans, Sintered Hydroxyapatite Latticework for Bone Substitute, J. Am. Ceram. Soc. 86 (2003) 517–519

[33] Q. Fu, E. Saiz, A.P. Tomsia, Direct Ink Writing of Highly Porous and Strong Glass Scaffolds for Load-bearing Bone Defects Repair and Regeneration, 7 (2011) 3547–3554

[34] S. Yang, K.-F. Leong, Z. Du, C.-K. Chua, The Design of Scaffolds for Use in Tissue Engineering. Part II. Rapid Prototyping Techniques, Tissue Eng. 8 (2002) 1–11

[35] J.A. Lewis, Direct ink writing of 3D functional materials, Adv. Funct. Mater. 16 (2006) 2193–2204

[36] T. Schlordt, F. Keppner, N. Travitzky, P. Greil, Robocasting of Alumina Lattice Truss Structures, J. Ceram. Sci. Technol. 3 (2012) 1–7

[37] P. Miranda, A. Pajares, E. Saiz, A.P. Tomsia, F. Guiberteau, Fracture modes under uniaxial compression in hydroxyapatite scaffolds fabricated by robocasting, J. Biomed. Mater. Res. Part A. 83A (2007) 646–655

[38] P. Miranda, A. Pajares, E. Saiz, A.P. Tomsia, F. Guiberteau, Mechanical properties of calcium phosphate scaffolds fabricated by robocasting, J. Biomed. Mater. Res. Part A. 85A (2008) 218–227

[39] J. Stuecker, J. Cesarano, D.A. Hirschfield, Control of the viscous behavior of highly concentrated mullite suspensions for robocasting, J. Mater. Process. Technol. 142 (2003) 318–325

[40] J.E. Smay, J. Cesarano, J.A. Lewis, Colloidal Inks for Directed Assembly of 3-D Periodic Structures, Langumuir. 18 (2002) 5429–5437

[41] J.E. Smay, J. Cesarano, B.A. Tuttle, J.A. Lewis, Directed Colloidal Assembly of Linear and Annular Lead Zirconate Titanate Arrays, J. Am. Ceram. Soc. 87 (2004) 293–295

[42] J. Choi, O.-C. Kwon, W. Jo, H.J. Lee, M.-W. Moon, 4D printing technology: areview, 3D print, Addit. Manuf. 2 (2015) 159–167

[43] A. Sydney Gladman, E.A. Matsumoto, R.G. Nuzzo, L. Mahadevan, J.A. Lewis, Biomimetic 4D printing, Nat. Mater. 15 (2016) 413–418

[44] Q. Ge, C. K. Dunn, H. J. Qi, M. L. Dunn, Active origami by 4D printing, Smart Mater. Struct., 23 (2014)

[45] Y. Zhou, W. M. Huang, S. F. Kang, X. L. Wu, H. B. Lu, J. Fu, H. Cui, From 3D to 4D printing: approaches and typical applications, Journal of Mechanical Science and Technology 29 (10) (2015) 4281~4288

[46] G. Franchin, P. Colombo, Porous geopolymer components through inversereplica of 3D printed sacrificial templates, J. Ceram. Sci. Technol. 6 (2015) 105–112

[47] J. Zhong, G.-X. Zhou, P.-G. He, Z.-H. Yang, 3D printing strong and conductive geo-polymer nanocomposite structures modified by graphene oxide, Carbon 117 (2017) 421-426

[48] B. Panda, S. C. Paul, M. J. Tan, Anisotropic mechanical performance of 3D printed fiber reinforced sustainable construction material, Materials Letters 209 (2017) 146–149

[49] B. Panda, GVP B. Singh, C. Unluer, M. J. Tan, Synthesis and characterization of one-part geopolymers for extrusion based 3D concrete printing, Journal of Cleaner Production 220 (2019) 610-619

[50] B. Panda, C. Unluer, M. J. Tan, Investigation of the rheology and strength of geopolymer mixtures for extrusion-based 3D printing, Cement and Concrete Composites 94 (2018) 307–314

[51] B. Panda, S. C. Paul, N. A. N. Mohamed, Y. W. D. Tay, M. J. Tan, Measurement of tensile bond strength of 3D printed geopolymer mortar, Measurement 113 (2018) 108–116

[52] S. Al-Qutaifi, A. Nazari, A. Bagheri, Mechanical properties of layered geopolymer structures applicable in concrete 3D-printing, Construction and Building Materials 176 (2018) 690–699

[53] V.D. Glukhovsky, Ancient, modern and future concretes, in: P.V. Krivenko (Ed.), Proceedings of the First International Conference on Alkaline Cements and Concretes, VIPOL Stock Company, Kiev, 1994, pp. 1–9

[54] Apis cor, Boston, Massachusetts, USA, https://www.linkedin.com/company/apis-cor/

[55] P. Duxson, S. W. Mallicoat,G. C. Lukey, W. M. Kriven, J. S. J. van Deventer, The effect of alkali and Si/Al ratio on the development of mechanical properties of metakaolin-based geopolymers, Colloids and Surfaces A: Physicochem. Eng. Aspects, 292, 8-20, 2007

[56] P. Duxson, J.L. Provis, G.C. Lukey, S.W. Mallicoat, W.M. Kriven, J.S.J. van Deventer, Colloids Surf. A 269 (1–3) (2005) 47

[57] M. Romagnoli, C. Leonelli, E. Kamse, M. Lassinantti Gualtieri, Rheology of geopolymer by DOE approach, Construction and Building Materials 36 (2012) 251–258

[58] A. Poulesquen, F. Frizon, D. Lambertin, Rheological behavior of alkali-activated metakaolin during geopolymerization, Journal of Non-Crystalline Solids 357 (2011) 3565–3571

[59] M. Romagnoli, P. Sassatelli, M. Lassinantti Gualtieri, G. Tari, Rheological characterization of fly ash-based suspensions, Construction and Building Materials 65 (2014) 526–534

[60] Vv. Aa., Rheology Theory and Applications, Volumes I-II, 1958, Academic Press Inc., Publishers, New York

[61] P. Scanferla, Sviluppo di Compositi a Matrice Geopolimerica, Master's thesis, A.A.

2014/2015

[62] X. Guo, A. A. Abdala, B. L. May, S. F. Lincoln, S. A. Khan, R. K. Prud'homme, Rheology control by modulating hydrophobic and inclusion associations in modified poly(acrylic acid) solutions, Polymer 47 (2006) 2976–2983

[63] V. A. Hackley, Colloidal Processing of Silicon Nitride with Poly(acrylic acid): II, Rheological Properties, J. Am. Ceram. Soc., 81 [9] 2421–28 (1998)

[64] A. Tsetsekou, C. Agrafiotis, I. Leon, A. Milias, Optimization of the rheological properties of alumina slurries for ceramic processing applications Part II: Spray-drying, Journal of the European Ceramic Society, 21 (2001) 493-506

[65] S. R. Raghavan, H. J. Walls, S. A. Khan, Rheology of Silica Dispersions in Organic Liquids: New Evidence for Solvation Forces Dictated by Hydrogen Bonding, Langmuir 2000, 16, 7920-7930

[66] P. Alphons, R. Bleta, R. Soules, Effect of PEG on rheology and stability of nanocrystalline titania hydrosols, Journal of Colloid and Interface Science 337 (2009) 81–87

[67] R. N. Dasa, C.D. Madhusoodana, K. Okada, Rheological studies on cordierite honeycomb extrusion, Journal of the European Ceramic Society 22 (2002) 2893–2900

[68] A. M. Deliormanli, M. N. Rahaman, Direct-write assembly of silicate and borate bioactive glass scaffolds for bone repair, Journal of the European Ceramic Society 32 (2012) 3637–3646

[69] Data sheets of the product: INGESSIL SS2942

[70] Data sheets of the product: Imerys M 1200 S

[71] Data sheets of the product: Ferrari Carbon RCF MF100

[72] Data sheets of the product: Lapinus Rockblade RB215 – Roxul 1000

[73] M. Bishop and A. R. Barron, Cement Hydratation Inhibition with Sucrose, Tartaric Acid, and Lignosulfonate: Analytical and Spectroscopic Study, Ind. Eng. Chem. Res., 45, 7042-7049, American Chemical Society, 2006

[74] J. Davidovits, Inorganic polymer, US patent n° 4,472,199

[75] A. Palomo, P.F.G. Ban II, A. Fernandéiz-Jiméinez, D.S. Swift, Properties of alkali-activated y ashes determined from rheological measurements, Adv.Cem. Res. 17 (2005) 143–151

[76] S. Goodyer, Measuring polymers using a rotational rheometer in oscillatorymode product manager for rheology, Telford Polym. Assoc. (2013) 1–35

[77] P. Rovnanik, Effect of curing temperature on the development of hard structure of metakaolin-based geopolymer, Construction and Building Materials 24 (2010) 1176–1183

[78] B. Jingwu, T. Zhenghong, Z. Shiyu, T. Zilong, Effect of Sand Content on Strength and Pore

Structure of Cement Mortar, Journal of Wuhan University of Technology-Mater. Sci. Ed., Apr.2017

[79] E. N. Kani, A. Allahverdi, J. L. Provis, Efflorescence control in geopolymer binders based on natural pozzolan, Cement & Concrete Composites 34 (2012) 25–33

[80] F. Skvara, L. Kopecky, L. Myskova, V. Smilauer, L. Alberovska, L. Vinsova, Aluminosilicate Polymers – Influence of Elevated Temperatures, Efflorescence, Ceramics – Silikáty 53 (4) 276-282 (2009)

[81] Z. H. Zhang, T. Yang, H. Wang, The effect of efflorescence on the mechanical properties of fly ash-based geopolymer binders, in ST Smith (ed.), 23rd Australasian Conference on the Mechanics of Structures and Materials (ACMSM23), vol. I (2014)

[82] Z. Zhang, H. Wang, J. L. Provis, A. Reid, Efflorescence: A Critical Challenge for Geopolymer Applications? (2013)

[83] M. D. M. Innocentini, R. F. Botti, P. M. Bassi, C. F. P. R. Paschoalato, D. L. Flumignan, G. Franchin, P. Colombo: Lattice-shaped geopolymer catalyst for biodiesel synthesis fabricated by additive manufacturing. Ceramics International (2019) 1443-1446

[84] W. M. Kriven, J. L. Bell, M. Gordon, Microstructure and microchemistry of fully-reacted geopolymers and geopolymer matrix composites, Ceramic Transactions vol. 153, 227-250 (2003)

[85] G. Franchin, L. Wahl, P. Colombo, Direct ink writing of ceramic matrix composite structures, J. Am. Ceram. Soc. 2017; 100:4397–4401

[86] G. Franchin, H. S. Maden, L. Wahl, A. Baliello, M. Pasetto, P. Colombo, Optimization and Characterization of Preceramic Inks for Direct Ink Writing of Ceramic Matrix Composite Structures, Materials 2018, 11, 515

[87] ASTM C1161 – 18, Standard Test Method for Flexural Strength of Advanced Ceramics at Ambient Temperature

[88] P. He, D. Jia, T. Lin, M. Wang, Yu Zhou, Effects of high-temperature heat treatment on the mechanical properties of unidirectional carbon fiber reinforced geopolymer composites, Ceramics International 36 (2010) 1447–1453

[89] T. Lin, D. Jia, P. He, M. Wang, D. Liang, Effects of fiber length on mechanical properties and fracture behavior of short carbon fiber reinforced geopolymer matrix composites, Materials Science and Engineering A 497 (2008) 181–185

[90] T. Lin, D. Jia, P. He, M. Wang, In situ crack growth observation and fracture behavior of short carbon fiber reinforced geopolymer matrix composites, Materials Science and Engineering A 527 (2010) 2404–2407

[91] F. U. A. Shaikh, Review of mechanical properties of short fibre reinforced geopolymer composites, Construction and Building Materials 43 (2013) 37–49

[92] Data sheets of the product: BASF MasterFiber 080

[93] N. Ranjbar, S. Talebian, M. Mehrali, C. Kuenzel, H. S. C. Metselaar, M. Z. Jumaat, Mechanisms of interfacial bond in steel and polypropylene fiber reinforced geopolymer composites, Composites Science and Technology 122 (2016) 73-81

[94] B. Nematollahi, P. Vijay, J. Sanjaya, A. Nazari, M. Xia, V. N. Nerella, V. Mechtcherine, Effect of Polypropylene Fibre Addition on Properties of Geopolymers Made by 3D Printing for Digital Construction, Materials 2018, 11, 2352

[95] ASTM D 2979, Standard Test Method for Pressure-Sensitive Tack of Adhesives Using an Inverted Probe Machine

[96] S.L. Yong, D.W. Feng, G.C. Lukey, J.S.J. van Deventer, Chemical characterisation of the steel–geopolymeric gel interface, Colloids and Surfaces A: Physicochem. Eng. Aspects 302 (2007) 411–423

Publications

Paper

- Franchin, G., Scanferla, P., Zeffiro, L., Elsayed, H., Baliello, A., Giacomello, G., Pasetto, M., Colombo, P. (2017). Direct ink writing of geopolymeric inks. *Journal of the European Ceramic Society*, *37*(6), 2481–2489. https://doi.org/10.1016/j.jeurceramsoc.2017.01.030

Patent

- P. Colombo, A. Conte, A. De Marzi, P. Scanferla, A. Italiano, Geopolymer based binder for the additive production of manufactured items, its use and process for manufacturing additives, date of publication 17/05/2017, EP 3168203 A1, US 20170129134 A1

Oral presentations

- P. Scanferla, G. Franchin and P. Colombo (2018); Direct ink writing of geopolymers; *young Ceramists Additive Manufacturing Forum 2018*

- P. Scanferla, G. Franchin and P. Colombo (2018); 3D-printing of geopolymers: the path to innovative ceramic composites; *Workshop for young ceramists* – Participation at the Student Speech Contest

- P. Scanferla, G. Franchin and P. Colombo (2018); 3D-printing of geopolymers: the path to innovative ceramic composites; *III European geopolymer network* – 1st prize winner of the JECS Trust Best Oral Award Competition

- P. Scanferla, G. Franchin and P. Colombo (2019); 3D-printing of geopolymers: the path to innovative ceramic composites; *43rd International Conference and Exposition on Advanced Ceramics and Composites*

- P. Scanferla, G. Franchin and P. Colombo (2019), 3D-printing of geopolymers: the path to innovative ceramic composites; *XVI Conference and Exhibition of the European Ceramic Society*

Posters

- P. Colombo, G. Franchin, H. Elsayed, P. Scanferla, A. De Marzi, A. Conte, A. Italiano (2016); Direct and indirect 3D-printing of components with geopolymers; *Giornate di studio sui geopolimeri – IX edizione: compositi geopolimerici*

- P. Scanferla, G. Franchin, L. Zeffiro, P. Colombo (2017); 3D-printed geopolymeric lattices: effect of processing parameters on the mechanical properties; *XV Conference and Exhibition of the European Ceramic Society*

- P. Scanferla, G. Franchin, P. Colombo (2018); 3D-printed geopolymeric lattices: effect of different filler materials on mechanical properties; *Engineering International Conference – Alkali Activated Materials and Geopolymers: Versatile Materials Offering High Performance and Low Emissions*